BAJECE

e-mail: editor@bajece.com

Balkan Journal of Electrical & Computer Engineering

An International Peer Reviewed, Referred, Indexed and Open Access Journal

SPECIAL ISSUE:
Recent Trends on Electrical & Computer Engineering Applications
The studies are selected from National Engineering Research Symposium, UMAS 2015 (Duzce University)

www.bajece.com

Vol : 3
No : 4
Year : 2015
ISSN : 2147 - 284X

Sponsored by the

- Istanbul Technical University
- Klaipeda University

This journal is accredited by the Istanbul Technical University subsidy purposes. It is abstracted and indexed in, Index Google Scholarship, the PSCR, DOAJ, Research Bible, Indian Open Access Journals (OAJ), Institutional Repositories (IR), J-Gate (Informatics India), Ulrich's, ResearchGate, International Society of Universal Research in Sciences, DRJI, EyeSource.

General Publication Director & Editor-in-Chief
Ş.Serhat Seker, Istanbul Technical University, Turkey

Vice Editor
Eleonora Guseinovienė, Klaipeda University, Lithuania
Tahir Cetin Akinci, Kirklareli University, Turkey
Yogeshwarsing Calleecharan, University of Mauritius, Mauritius

Editorial board
Amir Tokić, University of Tuzla, Bosnia and Herzegovina
Audrius Senulis, Klaipeda University, Lithuania

Scientific Committee
Abhishek Shukla (India)
Aleksandar Georgiev (Bulgaria)
Ahmet Hamdi Kayran (Turkey)
Arif M. Hasimov (Azerbaijan)
Arunas Lipnickas (Lithuania)
Belgin E. Turkay (Turkey)
Belle R. Upadhyaya (USA)
Brijender Kahanwal (India)
Daniela Dzhonova-Atanasova (Bulgaria)
Enver Hamiti (Kosovo)
Ferhat Sahin (USA)
Gursel Alici (Australia)
Hakan Temeltaş (Turkey)
Ibrahim Akduman (Turkey)
Jan Izykowski (Poland)
Javier Bilbao Landatxe (Spain)
Kunihiko Nabeshima (Japan)
Lambros Ekonomou (Greece)
Marcel Istrate (Romania)
Mehmet Korurek (Turkey)
Marija Eidukeviciute (Lithuania)
Milena Lazarova (Bulgaria)
Muhammad Hadi (Australia)
Muhamed Turkanović (Slovenia)
Mourad Houabes (Algerie)
Murari Mohan Saha (Sweden)
Okyay Kaynak (Turkey)
Osman Nuri Ucan (Turkey)
Ozgur E. Mustecaplioglu (Turkey)
Padmanaban Sanjeevikumar (India)
Rumen Popov (Bulgaria)
Tuiebakhova Zoya Kaimovna (Kazakhstan)
Sead Berberovic (Croatia)
Seta Bogosyan (USA)
Savvas G. Vassiliadis (Greece)
Suwarno (Indonesia)
Tahir M. Lazimov (Azerbaijan)
Tulay Adali (USA)
Vitalijus Volkovas (Lithuania)
Veselina Nedeva (Bulgaria)
YangQuan Chen (USA)
Youcef Soufi (Algeria)

Aim & Scope

The journal publishes original papers in the extensive field of Electrical-Electronics and Computer engineering. It accepts contributions which are fundamental for the development of electrical engineering, computer engineering and its applications, including overlaps to physics. Manuscripts on both theoretical and experimental work are welcome. Review articles and letters to the editors are also included.
Application areas include (but are not limited to): Electrical & Electronics Engineering, Computer Engineering, Software Engineering, Biomedical Engineering, Electrical Power Engineering, Control Engineering, Signal and Image Processing, Communications & Networking, Sensors, Actuators, Remote Sensing, Consumer Electronics, Fiber-Optics, Radar and Sonar Systems, Artificial Intelligence and its applications, Expert Systems, Medical Imaging, Biomedical Analysis and its applications, Computer Vision, Pattern Recognition, Robotics, Industrial Automation.

BAJECE

Balkan Journal of Electrical & Computer Engineering

An International Peer Reviewed, Indexed and Open Access Journal

© BAJECE

ISSN: 2147- 284X
Vol: 3
No : 4
Year: December 2015

SPECIAL ISSUE: *Recent Trends on Electrical & Computer Engineering Applications*

The studies are selected from National Engineering Research Symposium 2015 (Ulusal Mühendislik Araştırmaları Sempozyumu) UMAS 2015 (Duzce University).

CONTENTS

BALKAN
JOURNAL OF
ELECTRICAL & COMPUTER ENGINEERING
(An International Peer Reviewed, Indexed and Open Access Journal**)**

Contact
Istanbul Technical University
Department of Electrical Engineering
Ayazaga Campus, Maslak, Istanbul-Turkey

Web: https://www.bajece.com
http://dergipark.ulakbim.gov.tr/bajece/
e-mail: editor@bajece.com

Priority Based Wireless Body Area Network with Cognitive Radio

E. Seven, and A. Çalhan

***Abstract*— Wireless Body Area Networks provide to measure various physiological and biological data and monitor human body functionalities. In this study, a cognitive radio based coordinator node is designed for Wireless Body Area Networks and a data priority queue structure is constructed in the coordinator node. Cognitive Radio is capable of connecting various wireless access points with perception and adaptation features. We have developed, modeled and simulated example network scenarios by using the Riverbed Modeler simulation software for this purpose. The prominent parameters user speed, access point delay, and connection cost are taken into account when selecting the wireless access point. In this way, the coordinator node provides to deliver data to the destination with priority and ensure to send data over optimum access point with minimum delay and cost.**

Index Terms—Wireless Body Area Networks, Cognitive Radio, Data Priority

I. INTRODUCTION

WIRELESS Body Area Networks (WBAN) consist of devices which can measure and collect biological and physiological signals and send them a central unit with sensors located on wireless node.

These wireless nodes can be located in/on human body. Every year many people die from cancer, Parkinson diseases, asthma, cardiovascular diseases, obesity, diabetes and many other chronic or terminal illnesses. Researches show that early diagnosis and early response by medical units decrease death rate [1]. Also, increasing world population and expensive health services cause to increase usage of WBANs [2].

WBANs make patients to control their body functions while they're doing their daily works. As it is shown in Figure 1, data from the sensor nodes located on/in patient can be sent to health units by coordinator node such as cell phone of the patient. WBANs having different data traffics (e.g. normal and urgent) increase the importance of determining the order of data process in the queue [3].

E. Seven, Electrical-Electronic and Computer Engineering Department, Duzce University, 81620, Duzce, Turkey, (e-mail: eseven41@gmail.com).

A. Çalhan, Computer Engineering Department, Technology Faculty, Duzce University, 81620, Duzce, Turkey (e-mail: alicalhan@duzce.edu.tr).

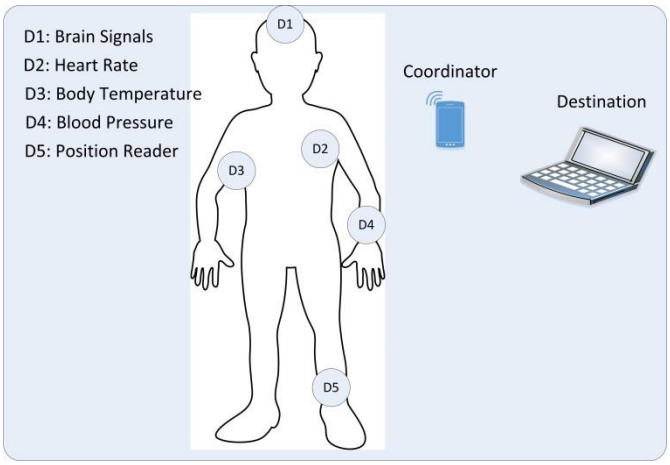

Fig.1. Wireless Body Area Network Structure

In our study, it is planned to send received data from coordinator rapidly according to order of priority. Therefore M/G/1 priority queue model is used for this purpose. With this model, when an urgent data is received it will be the first to be sent. Another part of this study is that coordinator node with M/G/1 priority queue sends data to medical center; it also has an ability to choose the most suitable access point by evaluating the parameters from all access points around. As choosing the access points coordinator node will be aware of all other access points around and will be able to send data these access points when it is requested. Because of that, our coordinator node is designed to have cognitive radio abilities in order to sense and connect the access points around [4]. In order to select the most suitable access point, the coordinator node should connect an access point by evaluating specific parameters of access points. Finally, the coordinator node will send data to a medical unit as a destination by using the chosen access point.

Using only one metric for selecting access point is not efficient since existing access points overlap with each other. Considering more performance metrics, such as delay, connection cost, user's speed etc., more realistic performance results can be achieved. For robustness of decision making in the coordinator node to connect to an optimum access point, several parameters are evaluated efficiently. Therefore, the important parameters user speed, access point delay, and connection cost are taken into account when choosing the wireless access point in this study.

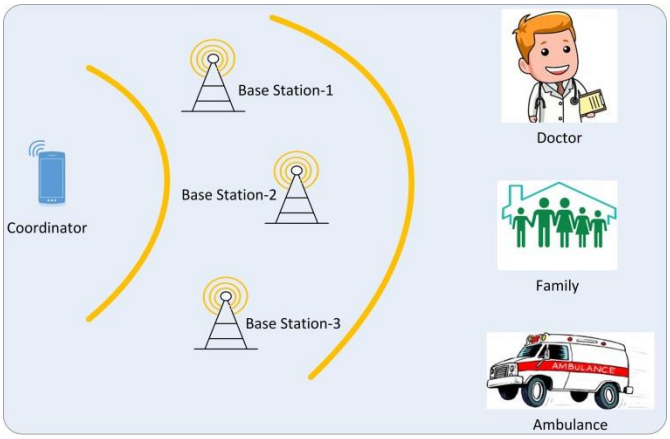

Fig.2. The designed WBAN structure

In the literature many protocols and algorithms for Wireless Sensor Networks are developed [5]. In our study Time Division Multiple Access (TDMA) protocol is used for communication of sensor nodes. Also multi-attribute decision making methods are used for choosing access points in the literature [6, 7]. In our study a data base is used in order to choose access points. Parameters coming from access points to coordinator node are evaluated by matching in the data base and the most suitable access point is chosen accordingly. By this way, as it is shown in Figure 2 the most suitable access point is chosen and patient data is sent to a medical unit.

II. Theoretical Ground

In our study, Riverbed (OPNET) Modeler software is utilized to design the structure of WBAN. Wireless sensor nodes measure the vital and biological signals (i.e. electrocardiography, electroencephalography, and electromyography) and activities, such as respiratory, heartbeat, body temperature, and glucose level in blood and send them to the coordinator node. The designed WBAN has several wireless sensor nodes with 3 different data traffic and one coordinator node. Sensor nodes collect and send first, second and third priority data to coordinator node. The coordinator node sorts the received data according to priority order. In the proposed study, first priority data are cardiac rhythm, body temperature; second priority data are position of the patient; third priority data are biological data e.g. electroencephalography (EGG), electromyography (EMG) [8].

Cognitive radio is a system which is aware of the wireless environment, can learn and can adjust itself as shown in Figure 3. It senses the wireless environment for all possible access points and changes its transmission and reception features in order to get connection to an optimum wireless access point. In our study the coordinator node has cognitive radio capabilities, and in different cases cognitive radio has to change its many parameters. Radios used in this kind of applications should have not just learning ability but also improved learning and decision making abilities. The designed coordinator node can record features of access points and when required it can connect the most suitable access point as a serving access point.

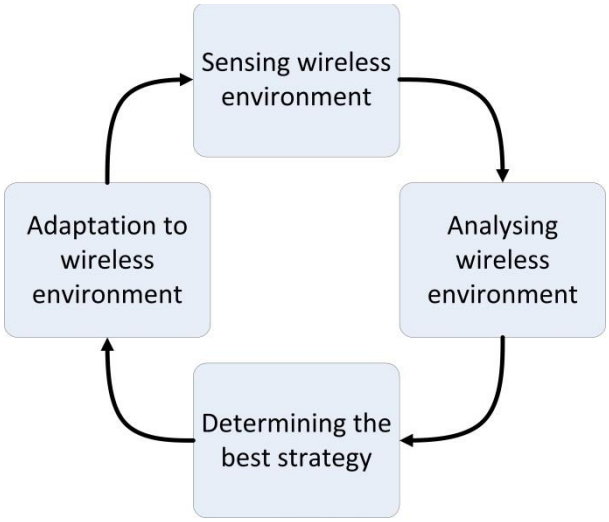

Fig.3. Cognitive radio cycle

III. Results Obtained and Discussion

In the simulation scenarios, wireless body sensor nodes are assumed to continuously collect the vital and biological signals and activities of patient, such as respiratory, body temperature, and heartbeat. Sensor nodes each have a distinct time slot in a TDMA frame, and send their packets to the coordinator node in their own time slots. The coordinator node has to organize priority queue of data from body sensor nodes as can be seen in Figure 4. By this way data which have priority can be sent to medical centers according to an order.

As data generated by sensors on the structure of WBAN increase, the data traffic on the network structure also increases. The aim of this study is to send data to medical centers with minimum delay. In order to show the performance evaluation of WBAN structure, two scenarios are executed in this study. Scenarios are designed according to frequencies of package production of sensor nodes. In the first scenario, the first node generates first priority data as 1 package/second, the second node generates second priority data as 2 packages/second, and the third node generates third priority data as 4 packages/second. End to end delay results of this scenario is shown in Figure 5. In the second scenario all nodes generate priority data as 5 packages/second. End to end delay results of the second scenario is also shown in Figure 6. As it is seen in Figure 5 and 6; when package frequencies of nodes increase, end to end delays increase as well.

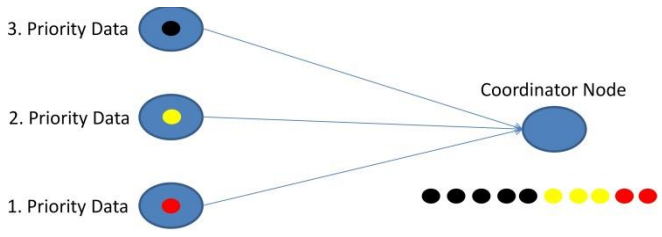

Fig.4. Data priority order in the coordinator node

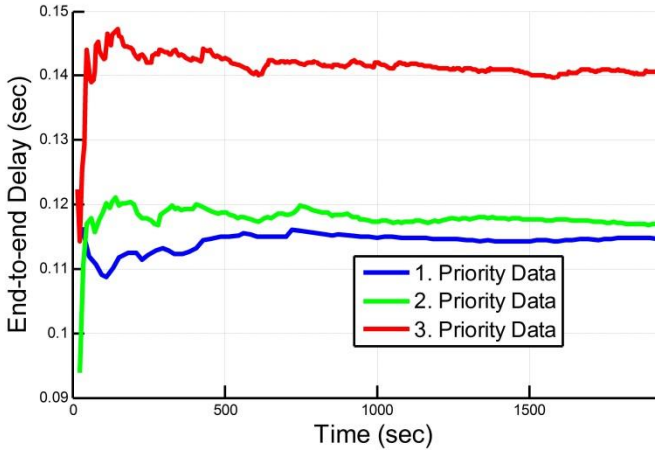

Fig.5. The end-to-end delay results of first scenario

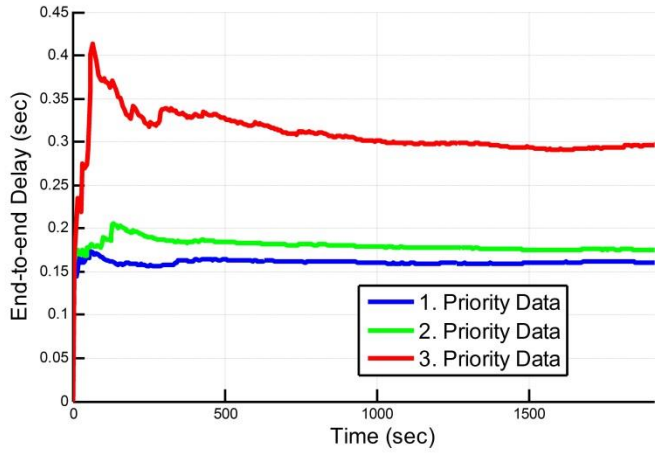

Fig.6. The end-to-end delay results of second scenario

To illustrate the performance evaluation of the proposed WBAN model, the packet generation frequencies are changed in each scenario. As can be seen in Figure 5 and Figure 6, the first priority data packets are sent to the destination with minimum delay than others. And also, the second priority data packets are sent to the destination in less time according to third priority data packets.

The coordinator node with a priority queue has been constructed on the WBAN structure and also based on cognitive radio features and can be connected to an optimum access point.

In order to make a connection to any access point, coordinator node can change some features such as working frequency, modulation technique and medium access method. The coordinator node chooses the optimum access point accordance with the features of WBAN. Some parameters are important for selecting process. In general, access point selection procedures need to consider many parameters including user profiles, application requirements and network conditions. While the optimum access point is selected as a serving access point, the coordinator node must evaluate speed of the user that has wireless body sensors, access point delay, and connection cost in this study. The coordinator node can select the preeminent access point for these three parameters.

In our study, several scenarios are evaluated under an assumption of that there are three different access points around WBAN. The features of these three access points in the scenarios are given in table 1.

TABLE I
ACCESS POINTS PARAMETERS

	Supported Speed	Access Point Delay	Connection Cost
Access P-1	0-30 km/h	2-4 sec	0.1
Access P-2	0-60 km/h	0.2-1 sec	0.8
Access P-3	0-90 km/h	0-0.2sec	1.5

TABLE II
USER PARAMETERS AND SELECTED ACCESS POINTS

	Moving speed	Delay	Selected Access Point
User-1	10 km/h	3 sec	Access P-1
User-2	50 km/h	0.5 sec	Access P-2
User-3	80 km/h	0.1 sec	Access P-3

In the scenarios, the access point selection procedure is provided for sending the data of three WBAN users. And also it is given in the table 2 that chosen access points after parameter evaluation according to the requirements of those three users. For example, speed of User-1 is 10 km/h and estimated delay is 3 seconds. Under these conditions, User-1 coordinator node will evaluate the parameters based on table 1 and choose the best access point.

As seen in the table 1, the best access point is Access P-1 under the conditions of User-1 requirements and connection price. In this way, the best access point can be chosen for three users by favor of a data base which is stored in the coordinator node structure.

IV. CONCLUSIONS

In this study, a priority based wireless body area network with cognitive radio is proposed. There are three types of priority data in the network and the developed coordinator node sorts the data in its queue and sends them to the health center with minimum end to end delay. Also, the coordinator node in the proposed WBAN is designed with cognitive radio capabilities for adopting any access point around. A WBAN needs to stay connected to a local or a wide area network by using different wireless access points. Thus, the sorted data from body sensors in the coordinator node can be sent over optimum access point to the destination. As choosing the best serving access point has critical importance to provide quality of service support and cost efficient connections for WBAN users.

It can be seen from the analysis of the results that coordinator node can sort the data and choose the best access point for sending them to the destination within the best performance. It is also aimed to have an improvement for making a decision based on artificial intelligence of coordinator node structure for the next studies.

ACKNOWLEDGMENT

The study is selected from National Engineering Research Symposium 2015 (Ulusal Mühendislik Araştırmaları Sempozyumu) UMAS 2015 (Duzce University).

REFERENCES

[1] S. Movassaghi, M. Abolhasan, J. Lipman, D. Smith, A. Jamalipour, "Wireless body area networks: a survey", IEEE Communications Surveys & Tutorials, Vol.16, No. 3, pp. 1658-1686, 2014.

[2] A. Milenkovic´, C. Otto, E. Jovanov, "Wireless sensor networks for personal health monitoring: Issues and an implementation", Computer Communications, Vol. 29 No. 13-14, pp. 2521-2533, 2006.

[3] M. Nabi, M. Blagojevic, M. Geilen, T, Basten, "Dynamic Data Prioritization for Quality-of-Service Differentiation in Heterogeneous Wireless Sensor Networks", in Sensor, Mesh and Ad Hoc Communications and Networks (SECON), 2011 8th Annual IEEE Communications Society Conference on, pp. 296-304, 2011.

[4] A. Ahmad, S. Ahmad, , H. Rehmani, N. U. Hassan, "A Survey on Radio Resource Allocation in Cognitive Radio Sensor Networks", IEEE communications surveys & tutorials. Vol. 17, No. 2, pp. 888-917, 2015.

[5] I.F. Akyildiz, W. Su, Y. Sankarasubramaniam, E. Cayirci, "Wireless sensor networks: A survey". Computer Networks Vol. 38, No. 4, pp. 393–422, 2002.

[6] S. Misra, S. Sarkar, "Priority-based time-slot allocation in wireless body area networks during medical emergency situations: An evolutionary game-theoretic perspective", IEEE Journal of Biomedical and Health Informatics, Vol. 19, No. 2, pp. 541-548. 2015.

[7] A. Çalhan, S. Atmaca, "A new network coordinator node design selecting the optimum wireless technology for wireless body area networks", KSII Transactions on Internet and Information Systems Vol. 7, No. 5, pp. 1077-1093, 2013.

[8] A. Çalhan, "Trafik duyarlı kablosuz vücut alan ağlarının başarım analizi", Pamukkale Üniversitesi Mühendislik Bilimleri Dergisi, Vol. 21, No. 5, pp. 172-177, 2015.

BIOGRAPHIES

Engin SEVEN was born in Gebze - Turkey in 1985. He received the B.Sc. degree in Electronics and Computer Education Department, Technical Education Faculty, Kocaeli University, Turkey in 2009. He studies for master degree at Duzce University. His research interests are cognitive radio, and wireless body area networks.

Ali ÇALHAN received the M.Sc. and Ph.D. degrees from University of Kocaeli, Turkey in 2006 and 2011, respectively. His research interests are cognitive radio, wireless heterogeneous networks, wireless communications, and artificial intelligence.

Characteristics of Cyber Incident Response Teams in the World and Recommendations for Turkey

Y. E. Karabulut, G. Boylu, E.U. Küçüksille and M.A. Yalçınkaya

***Abstract*— Today, in countries across the world, operations such as the digitalization of critical infrastructure and public services, through the use of computer networks, has revealed the security problems of cyber space. Used for the transferring and storing of highly critical data, any weaknesses and vulnerabilities located on these computer systems have the potential to cause tangible and intangible costs and losses on the country concerned. With the concept of cyber security growing in importance globally, countries have developed strategies, launched awareness-raising activities, and organized campaigns to have maximum information security level. In what is an ongoing process, it has been revealed that countries are finding it necessary to create computer security incident response teams, in order to protect their national cyber security. Cyber incident response teams are for the early identification of threats to national security that may occur in cyberspace, and to reduce the effects of any attack that may be encountered. In this study, we examined in detail the policies being implemented for the creation of cyber incident response teams and the qualifications team members should have. In addition, the cyber incident response teams created in developed countries around the World, and the properties and activities of these teams, are investigated. The study is concluded by examining the development of cyber incident response teams in Turkey, and presenting recommendations for Turkey.**

Index Terms— **CSIRT, Incident response teams, Information security, Strategy of national security.**

I. Introduction

The transition to digital infrastructures being conducted in various countries, with the aim of providing better and faster solutions for their organizations and institutions, as well as improved services for society, has led to the emergence of the concept of cyber-security.

Y. E. Karabulut, is with the, Computer Engineering Department, Süleyman Demirel University, Isparta, Turkey, (e-mail: emrkarabulut@gmail.com).

G. Boylu, is with the, Computer Engineering Department, Süleyman Demirel University, Isparta, Turkey, (e-mail: gulistan.boylu@gmail.com).

E. U. Küçüksille, is with the, Computer Engineering Department, Süleyman Demirel University, Isparta, Turkey, (e-mail: ecirkucuksille@sdu.edu.tr).

M. A. Yalçınkaya, is with the, Computer Engineering Department, Süleyman Demirel University, Isparta, Turkey, (e-mail: mehmetyalcinkaya@sdu.edu.tr).

Discussions on this new concept have also drawn attention to the protection of these critical infrastructures against potential threats, as well as the ability to respond to attacks. Many countries, in parallel to increasingly digitalizing their critical infrastructure, have also begun to draw and publish cyber-security strategies and action plans, taking concrete steps towards restructuring their organizations and forming cyber incident response teams - one of the most critical aspects of these strategies and plans.

Around the world, cyber intervention teams are defined either as computer security incident response teams (CSIRTs) or computer emergency response teams (CERTs). Teams at cyber incident response centers focus on identifying threats to national security within the cyber environment; on reducing the impact of potential attacks; and on responding to actual attacks. Many countries have already formulated their own national cyber-security strategy, announcing their action plans and establishing their own cyber incident response centers.

In the following sections of this study, we discuss the activities and tasks of cyber incident response centers, evaluate how cyber incident response teams are formed and what their skills should be based on examples from around the world. In this context, we will highlight what is being done and should be done in Turkey.

II. Cyber Incident Response Teams

Cyber incident response teams (CIRTs) are institutional and sectorial organizations established to rapidly identify threats and potential attacks in the cyber environment, and to develop and share measures for solving the problems caused by these attacks. The goal of these teams is thus to provide cyber response skills to institutions and organizations. CIRTs are classified into three groups: national teams, institutional teams, and sectorial teams.

National CIRTs are tasked with leading the formation of institutional response teams, and with providing support to both institutional and sectorial cyber incident response teams. Institutional CIRTs, on the other hand, are tasked with the formation of sectorial cyber incident response teams. To ensure a holistic approach to security, as well as rapid response and organization, the national, institutional and sectorial cyber incident response teams all work in coordination with one another [1].

III. THE FORMATION OF CYBER INCIDENT RESPONSE TEAMS

When forming cyber incident response teams, it is important to define the teams' parameters. From the outset, procedures should be formed and policies defined, so that the teams can readily adapt to the dynamic nature of cyberspace while also being able to respond rapidly to cyber threats.

The general organizational and operational framework of CIRTs should be fully delineated. In this context, the scope of a CIRT, the institutions and organization with which it will cooperate and communicate, its aims and objectives, and the existing risks, should all be clearly laid out. It is necessary to define the elements, methods, and infrastructure of communication, while also developing a system that will prevent loss of time in emergencies and exceptional situations.

When forming CIRTs, the existing national, institutional and sectorial communication and information networks should also be evaluated and taken into consideration. In addition to responding to cyber threats and events, CIRTs are also tasked with informing the public and raising awareness. Being newly established, CIRTs should come up with a strategy for fulfilling this requirement.

The mission statement of a CIRT should clearly outline their aims and objectives. Aspects, such as how the team will respond to emergencies and exceptional situations, as well as the areas and description of the team's reactions and reflexes, should all be clearly explained. The mission statement of a CIRT is also important for defining the scope of the team's services, and for further improving the team's quality.

In addition to the mission statement, the intra-team hierarchy and the assignment of tasks should also be determined. Clearly describing the financial resources of a CIRT will also help prevent chaos and confusion during emergencies, or when steps are being to further expand the team. The purpose, the roles assumed within the country, and the areas of activities of CIRTs should all be clearly defined and announced to the public.

IV. THE COMPETENCIES OF CYBER-SECURITY TEAMS

The operational expectation of CIRTs is for them to avert cyber-attacks, and to prevent potential attacks by reinforcing the vulnerable points where attacks may occur.

The critical service infrastructure (such as power, electronic communications, finance) of CIRTs should allow them to monitor digital systems, and to resolve cyber security-related issues and weaknesses, by predicting the possible damages that might be caused by cyber-attacks.

Thus, CIRTs should possess certain skills and competencies, and as such, consist of individuals specializing in areas such as vulnerability analysis, log management, cyber response information security management [2].

A. Vulnerability Analysis

Vulnerability analysis includes the structuring and monitoring of security activities, the execution of penetration tests, and the gathering of information on the techniques used in cyber-attacks. Within the scope of vulnerability analysis, CRTs focus on identifying major system vulnerabilities and risks before actual attacks take place, while also taking measures and coordinating activities concerning these vulnerabilities and risks.

B. Log Management

Log Management includes the ability to identify attacks and to effectively track and interpret records and trails left on a system, as well as centralized security monitoring and incident management. Enabling national and institutional CIRT personnel to track system records and raise awareness of systems and threats can also be considered, within the scope of Log Management.

C. Response to Cyber Events

This competency involves the formation of an effective institutional CIRT establishment and team member selection by national CIRT personnel, as well as a firm grasp of the details pertaining to information system forensic analyses, network forensic analyses, protection methods against Distributed Denial of Service (DDOS) attacks and information technology law. This competency provides CIRTs with the necessary management and coordination skills for dealing with cyber incidents and attacks. Furthermore, this competency also covers the proper implementation and execution of the measures and methods for preserving digital evidence.

D. Information Security Management

Information security management is an important skill for cultivating an understanding of cyber-security processes, and raising cyber-security awareness, both at an institutional and public level. Increasing the awareness of institutional and sectorial CIRT personnel, on information security management, enables them to execute rapid and coordinated incident management during negative incidents and cyber-attacks.

V. INCIDENT RESPONSE TEAMS INTERNATIONALLY

In many countries, CIRTs can be found as either Computer Emergency Response Teams (CERTs) or Computer Security Incident Response Teams (CSIRTs).

The launch of the first CIRTs in Turkey began towards the end of 2013, and was soon followed by the formation of the sub-teams (i.e. institutional and sectorial teams). The structure and organization of CIRTs tends to vary, depending on the social and governance structures of the different countries. In many countries, national CIRTs have additional teams and institutions working under them.

A. *United Kingdom*

The United Kingdom's (UK's) national CIRT began its operations in March 2014 under the name CERT-UK. Infrastructure activities for the CERT-UK began soon after the publication of the national cyber-security strategy in 2011 by the British Government, and the institution became active and operational in 2014. In the UK, the CERT has been assigned with four main tasks:

- National cyber-security incident management,
- Support to companies and institutions providing national critical infrastructure services.
- Conducting activities for promoting and raising awareness on cyber-security at an academic and sectorial level,
- Contacting the cyber incident response teams of other countries to ensure coordination and cooperation.

Furthermore, within CERT, a Cyber Security Information Sharing Partnership (CiSP) team has also been established. The purpose of this team is to ensure that all institutions and sectors are kept aware of cyber-security-related developments through a cyber-security information-sharing partnership, while also informing the participants about vulnerabilities, and raising their overall knowledge on the subject. CiSP is a joint project of the British government and industry. The CiSP project endeavors to develop a holistic cyber-security approach in the UK, and share real-time information on cyber-attack news, methods and vulnerabilities with institutions and commercial sectors by closely adhering to confidentiality [3].

B. *Germany*

The German cyber incident response team was established by the German government under the name of CERT-BUND (German abbreviation: BSI). Referred to as the Federal Office of Information Security, the BSI is tasked with promoting digital and communication security for the German government, and its areas of responsibility and specialization includes:

- Protection of critical infrastructures (energy, communications, transportation) against cyber-attacks,
- Internet security,
- Setting measures against and identifying wiretapping activities.
- Developing security standards and certifications.
- Giving accreditation to security test laboratories.

BSI currently has over 600 personnel. It was established in 1986 with the information technology security authorization. The cyber incident response team was established in 2009, and the scope of BSI's authority and tasks was significantly broadened following the enactment of the most radical regulatory changes to date concerning its tasks and responsibilities [4].

C. *Japan*

The Japanese cyber incident response team is known as Japan Computer Emergency Response Team (JPCERT). JPCERT is tasked with promoting the critical infrastructure security of national GSM operators, state institutions and organizations, and of industrial organizations against cyber attacks. In addition, JPCER also led and coordinated the establishment of the first Asia-Pacific Cyber Incident Response Team, APCERT. This team is also responsible for ensuring coordination and cooperation with other national teams.

JPCERT organizes training activities on information security within the country, and also holds events, contests, and conferences for raising awareness on cyber incidents and information security. JPCERT acquired official status in 2003, becoming a non-profit organization working for the state [5].

D. *United States of America*

The American cyber incident response team is known as US-CERT. This organization's mission statement describes it as being tasked with ensuring the cyber security of the American people, that it enjoys a proactive management, and that its aim is to become the preeminent cyber incident response center in the world.

The official website of US-CERT contains information and documents on current information security vulnerabilities and cyber-attacks being carried out across the world, by posting such information and documents online, the United States (US) aims to inform and raise the awareness of its people about information security, and to create a source and reference on cyber security. This organization, also called the National Cyber Awareness System (NCAS), relays information and updates through electronic mail, allowing subscribers to receive the latest updates on cyber-space incidents by e-mail [6].

E. *Turkey*

The Cyber Security Institution of Turkey has developed, and shared with the public, a National Cyber Security Document of its first meeting. Following this, and the publication of the relevant regulations in the Turkish Official Gazette dated November 11, 2013, the National Cyber Incident Intervention (USOM) center was established. While this organization is called USOM in Turkey, it is internationally known as TR-CERT.

Following the foundation of USOM, Turkey's strategy document also considered the establishment of both institutional and sectorial Cyber Incident Response centers. The document envisages the formation of institutional CIRTs within Ministries, and in institutions and organizations affiliated with Ministries, and also emphasizes coordination and cooperation between these teams and USOM.

Sectorial CIRTs, on the other hand, will be established to promote measures for information, data, and system security, in companies providing industrial and critical infrastructure services. Sectorial CIRTs will be directly in contact with institutional CIRTs, while also engaging in information sharing and cooperation with USOM.

VI. SUGGESTIONS FOR TURKEY

The Turkish Cyber Incident Response Team USOM has closely followed the approach implemented by other countries, and has rapidly completed its organization accordingly. However, in addition to not yet being widely known by the public, at the present time USOM is also not assuming an active role. For this reason, public awareness raising activities should first be conduct to explain to the public what cyber space is, and to emphasize its importance for personal, company and national security.

One option in this context would be to form, just as it is the case in the UK and US, an external team that will conduct public awareness raising activities, define specific actions for raising awareness, and organize activities that are compatible with Turkey social fabric. Measures could also be taken to ensure continuous communication and exchange of opinions between this team and the larger public.

VII. CONCULUSION AND DISCUSSION

By examining a number of examples and organizations from around the world, this study investigated how cyber incident response centers or teams are formed, what their competencies should be, and the main methods and mechanisms they employ. In addition, the study evaluated the cyber incident response teams of developed countries such as the UK, the US and Japan, as well as the activities of these teams, and in this context, by taking into account current developments and studies, made suggestions on what steps also need to be taken in Turkey.

ACKNOWLEDGMENT

The study is selected from National Engineering Research Symposium 2015 (Ulusal Mühendislik Araştırmaları Sempozyumu) UMAS 2015 (Duzce University).

REFERENCES

[1] A. Sawicka, J. Gonzalez and Y. Qian, “Managing CSIRT Capacity as a Renewable Resource Management Challenge. An Experimental Study”. In: Proceedings of the 23rd System Dynamics Society Conference, Boston, MA, USA, July 2005, pp. 31.

[2] P. Pavel, "Adapting the ticket request system to the needs of CSIRT teams." WSEAS Transaction on Computers 8.9, 2009, pp. 1440-1450.

[3] SANS Institute InfoSec Reading Room, Computer Incident Response Team. 2001 (Accessed June 2015) http://www.sans.org/reading-room/whitepapers/incident/computer-incident-response-team-641

[4] J. Wiik, J. J. Gonzalez, P. I. Davidsen, and K. P. Kossakowski, Preserving a balanced CSIRT constituency. In Twenty Seventh International Conference of the System Dynamics Society July, at Albuquerque, NM, USA, 2009.

[5] Cyber Emergency Response Team UK Organization, (Accessed July 2015) http://www.cert.org/resilience/research/index.cfm

[6] Listing Of Worldwide CERT Organization, (Accessed August 2015) https://scadahacker.com/resources/cert.html

[7] JPCERT Coordination Center Incident Response, (Accessed August 2015) http://www.jpcert.or.jp/.

[8] US-CERT, United States Computer Emergency Readiness Team, (Accessed August 2015) https://www.us-cert.gov/

[9] Ulusal Siber Olaylara Müdahale Merkezi, (Accessed August 2015) https://www.usom.gov.tr/

BIOGRAPHIES

Yunus Emre KARABULUT was born in Sivas in Turkey. He received the B.Sc. Degree from Süleyman Demirel University, Turkey. Since 2015, he is currently M.Sc. student in Computer Engineering Department at Süleyman Demirel University. His current research interests are information security and search engine algorithms.

Gülistan BOYLU was born in Denizli in Turkey. He received the B.Sc. Degree from Süleyman Demirel University, Turkey. Since 2014, he is currently M.Sc. Student in Computer Engineering Department at Süleyman Demirel University. His current research interests are software engineering and software development.

Ecir Uğur KÜÇÜKSİLLE was born in Isparta, Turkey in 1976. He received the B.Sc. degree in Computer Systems Education form Gazi University, Turkey and M.Sc. degree in Department of Mechanical Education from Suleyman Demirel University. He obtained the Ph.D. degree in Numerical Methods in 2007 from Suleyman Demirel University, Turkey. His current research interests are information security and penetration tests.

Mehmet Ali YALÇINKAYA was born in Isparta in Turkey. He received the B.Sc. and M.Sc. Degrees from Süleyman Demirel University, Turkey. Since 2013, he has been with the Department of Computer Engineering at Süleyman Demirel University, Turkey as a Research Assistant. His current research interests are information security and penetration tests.

Thermal Change for Photovoltaic Panels and Energy Effects

N. Imal, S. Hasar, H. Çınar and E. Sener

***Abstract*—Photovoltaic panels (solar cells), they receive photon energy from sunlight, convert them to electrical energy by the semiconductor structural features. Photovoltaic panels produce a voltage, depending on the change of functional sunlight exposure. Produced voltage and determining of provided electrical power, must be dealt with the physical parameters that uses the concepts of light and temperature. In this study, usage of monocrystalline and polycrystalline structured photovoltaic panels electrical energy conversion for different atmospheric temperature and different sunlight intensity are studied. With the realization of the applications, photovoltaic panels' thermal change effects upon the energy production is discussed. With the conclusions obtained from the research applications and analyses, for heat exchange in photovoltaic panels to effects upon energy production, the obtained principles of functional changes are interpreted.**

***Index Terms*—Photovoltaic panel, solar energy, power**

I. INTRODUCTION

AS working structure, photovoltaic panels are to interact with sunlight. Sun, as a result of events occurring as core fusion, inherently spread light energy to its surrounding. Because, our world is a part of the solar system, it is continuously exposed to this interaction of light. For that reason, solar energy does not require any resources for the production according to other energy production sources. As a result of above, they are intensely preferred [1].

Crystalline and thin-film silicon solar cells are the state of art technology and they have a great potential for future energy production. They have many structure types [16]. This work includes monocrystalline and polycrystalline comparison within.

In this study, samples of monocrystalline and polycrystalline photovoltaic panels, according to previous studies, positioned in a certain direction and angle; afterwards, applications were performed [2].

N. Imal, Electrical Electronic Engineering Department, University of Bilecik Seyh Edebali, Bilecik, Turkey, (e-mail: nazim.imal@bilecik.edu.tr).

S. Hasar, Osmaneli Vocational High School, University of Bilecik Seyh Edebali, Bilecik, Turkey, (e-mail: sahabettin.hasar@bilecik.edu.tr).

H. Çınar, University of Bilecik Seyh Edebali. Bilecik, Turkey, (e-mail: harun.cinar@bilecik.edu.tr).

E. Sener, Electrical Electronic Engineering Department, University of Bilecik Seyh Edebali. Bilecik, Turkey, (e-mail: eralp.sener@bilecik.edu.tr).

With the panels used in the applications;

- For fixed temperature conditions, effects of energy conversion related to the changes in light parameters,
- For the fixed light intensity, effects to energy conversion of the changes in temperature parameters,

were studied [3-4].

In this study, for electrical energy generation in photovoltaic panels; depending the light intensity, by direct exposure of sun and absorption of the photon are considered to be effectively to what extent. Of which monocrystalline and polycrystalline panels is to have more electrical power generation capacity upon the parameters effecting the efficiency, investigations were carried out. In figure 1, it is seen photovoltaic panels used in the studies.

Fig.1. Monocrystalline and polycrystalline PV panels

In literature, a yearlong test has shown that the monocrystalline cells have higher efficiency than polycrystalline cells. It is shown that average module efficiency of 11.8% for monocrystalline and 11.5% for polycrystalline cells [14]. Also effects of irradiance and temperature can be calculated by formulas and using dark current values [15-16].

II. PHOTOVOLTAIC PANELS

Photovoltaic energy production by light excitation to electronic semiconductor components are provided with a potential difference occurring in the electrical energy levels. In a photovoltaic panel that contains silicon crystal, the substrate is covered with the P-type material, the upper layer is covered with N-type material that emitting chemical alloys of free-electron such as phosphorus, antimony or arsenic. The gaps between the photovoltaic cells, coated with a material as aluminum, gallium, indium; formation of traces between cells is provided. Thus, with light exposure of them, the passing of

electrons to the substrate of the *"P"* is provided. These electrons have the ability to move on serial and parallel roads obtained in photovoltaic panels. So, creating "I" current by *"E"* emf in photovoltaic panel, electrical energy production can be achieved. Although there are many photovoltaic panels that improved and being developed is present, here are the most widely known and used types are discussed. Moreover in figure 2, visual images of which belong to these products are shared [5-6].

- *Monocrystalline silicon photovoltaic panels:* High purity parts of the silicon structure by means of subjecting "Czochralski pulling" and "floating zone" process, Mono crystalline silicon photovoltaic cells are made from very efficient, yield values can reach 18%.
- *Polycrystalline silicon photovoltaic panels:* Despite the high efficiency of the monocrystalline silicon solar panels, due to the difficulties and high costs of production, simple structure than single crystal silicon of "Czochralski", polycrystalline silicon structures have been developed. Although energy production efficiency of "Polycrystalline Silicon Structure" is low (8-10%), due to advantages of easier and lower cost of production they are preferred.
- *Amorphous - silicon photovoltaics panels:* They are produced by placing the amorphous silicon vapor and window films on to the stainless steel that few micrometers thick. When compared to the mono and poly crystalline structures, much less silicon structure (as 1%) is required. Although, yields are low (as 4-5%), because of have much lower cost per watt compared to other structures, it makes them advantageous.

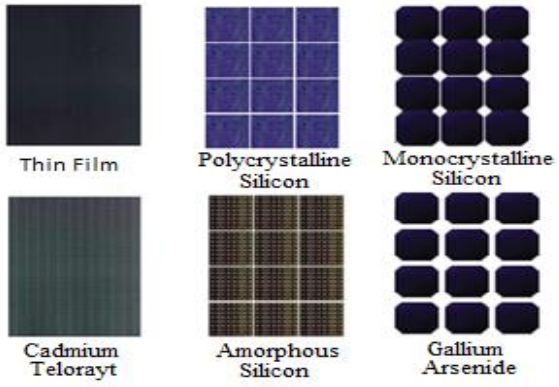

Fig.2. Photovoltaic panel types

- *Gallium arsenide photovoltaic panels:* The highest yield (22%) owner of photovoltaic structures includes single-crystal gallium arsenide. Despite the high efficiency, also high costs lead to less preference.
- *Thin film photovoltaic panels:* It can be produced on cross section of very thin, such as cadmium sulfide, amorphous silicon, copper-indium-diselenide and e.t.c are polycrystalline structures in large surface areas. Although it has approximately 10% efficiency, it has low cost, and if it can be developed in many buildings exposed to sunlight, they can be used as roofing materials. They are the major advantages.
- *Cadmium telluride photovoltaic panels:* They are crystal structures that compound form of cadmium and tellurium. They are semiconductor structures that produced with layered superpose of cadmium sulfide and their efficiency approaches to 19%.

III. APPLICATION ANALYSIS OF ELECTRICITY GENERATION IN MONOCRYSTALLINE AND POLYCRYSTALLINE PANELS

In this performed study, according to the many operating conditions, the most preferred monocrystalline and polycrystalline photovoltaic panels are placed in order to more sun seeing places , fixed in most suitable position and electric power generation analyzes were performed. Prior to the application, reviewing of the literature on the subject in preparation, work planning had been done [7-8-9-10-11-12-13].

In the study, using one polycrystalline panels and two monocrystalline panels which connected in series, applications were made. Specifications of used materials in practice in table 1 and table 2. For applications, the image of the products used in construction is shown in figure 3.

TABLE I
CHARACTERISTICS OF MONOCRYSTALLINE PHOTOVOLTAIC PANELS

Panel Model	ANALES OKDA - 18
Maximum Power (Pmpp)	66,65W
Tolerance of Power	+/-5%
Rated Voltage (Vmpp)	8,63V
Rated Current (Impp)	7,72A
Open Circuit Voltage (VOC)	11,23V
Short Circuit Current (ISC)	8,31A
Max. System Voltage	1000V

TABLE II
CHARACTERISTICS OF POLYCRYSTALLINE PHOTOVOLTAIC PANELS

Panel Model	Conergy Q 30PA
Maximum Power (Pmpp)	30W
Tolerance of Power	+/-5%
Rated Voltage (Vmpp)	16,5V
Rated Current (Impp)	1,83A
Open Circuit Voltage (VOC)	20,0V
Short Circuit Current (ISC)	2,0A
Max. System Voltage	600V

Fig. 3. Application equipments

At the graphics below between figure 4 and figure 15, for monocrystalline and polycrystalline photovoltaic panels, variance graphics of electrical energy production application analysis is shown. The nonlinearity seen in these measurements are caused by color spectrum of the light and momentarily deviation in photon distribution.

A. ANALYSIS OF ELECTRICAL ENERGY GENERATION IN MONOCRYSTALLINE PANELS

In figure 4, figure 5 and figure 6, for monocrystalline panel, power changes seen for fixed illumination and different temperature conditions. In this variation graphics, it emerges that power decreases as long as temperature increases. This is caused by increasing resistance values of the semiconductor structure and resistance value of connection path according to temperature.

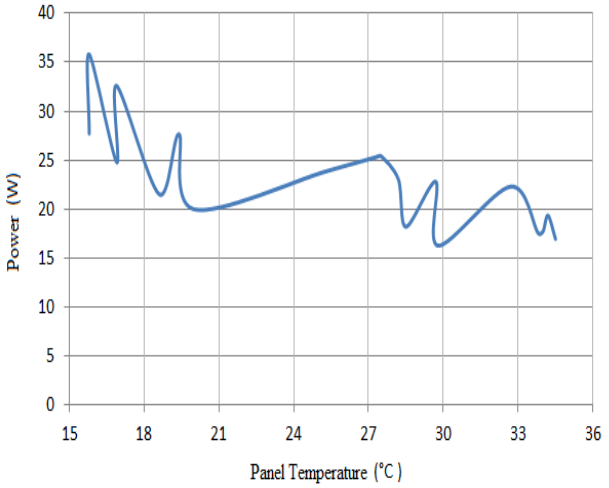

Fig. 4. For mono crystalline panel: while Icd≅30.000 Cd, P=f (Tp) graph)

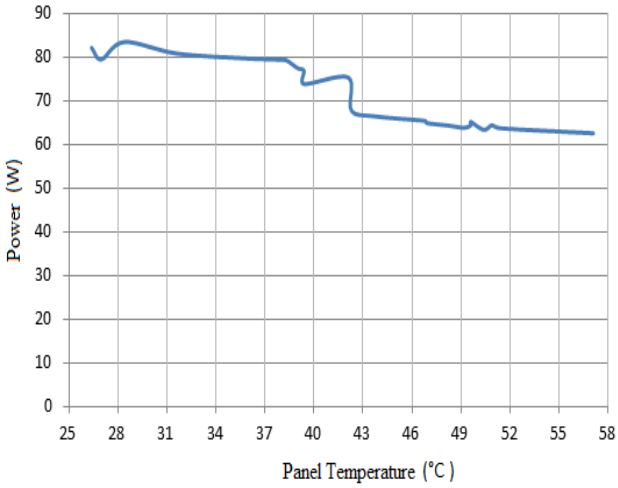

Fig. 5. For monocrystalline panel: while Icd≅90.000 Cd, P=f (Tp) graph

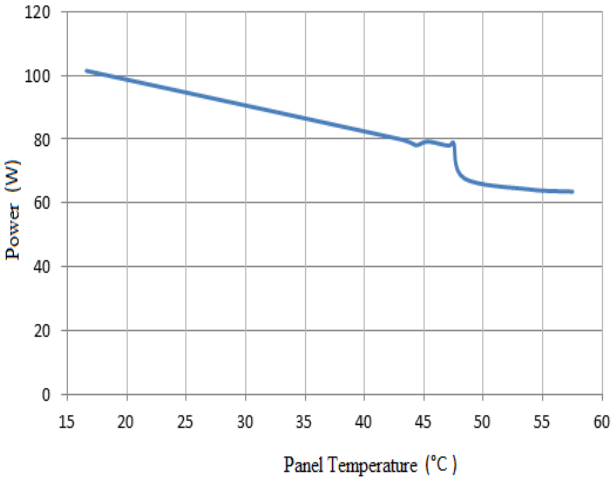

Fig. 6. For monocrystalline panel: while Icd≅130.000 Cd, P=f (Tp) graph

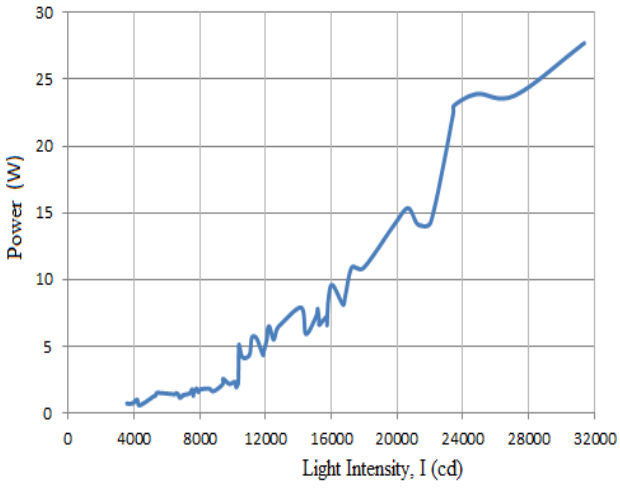

Fig. 7. For monocrystalline panel: while Tp≅ 15 °C, P=f (I_{CD}) graph

In figure 7, figure 8 and figure 9, for monocrystalline panel, power changes seen for fixed temperature and different illumination conditions. In this variation graphics, it emerges that power increases as long as temperature increases. This is caused by fixed resistance values of the semiconductor structure and resistance value of connection path according to fixed temperature and also increasing illumination provides more photons for energy conversion. In figure 7, the lesser energy production for low panel temperature is caused by lack of photons at the time of measurement.

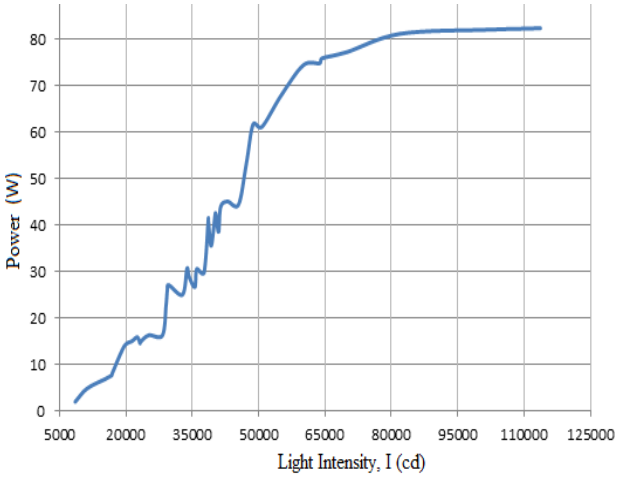

Fig. 8. For monocrystalline panel: while Tp≅ 30 °C, P=f (I_{CD}) graph

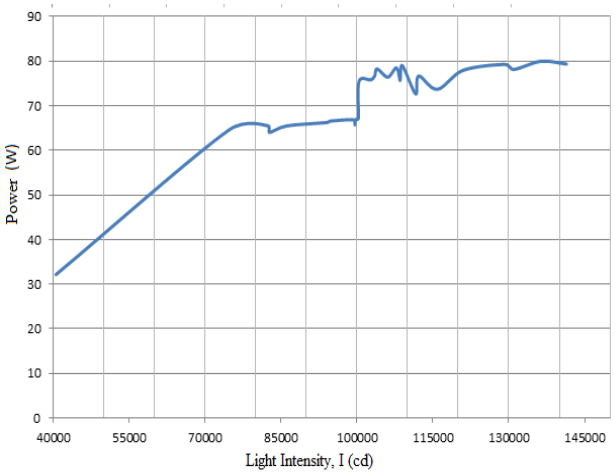

Fig. 9. For monocrystalline panel: while Tp≅ 45 °C, P=f (I_{CD}) graph

B. ANALYSIS OF ELECTRICAL ENERGY GENERATION IN POLYCRYSTALLINE PANEL

In figure 10, figure 11 and figure 12, for polycrystalline panel, power changes seen for fixed illumination and different temperature conditions. In this variation graphics, it emerges that power decreases as long as temperature increases. This is caused by increasing resistance values of the semiconductor structure and resistance value of connection path according to temperature.

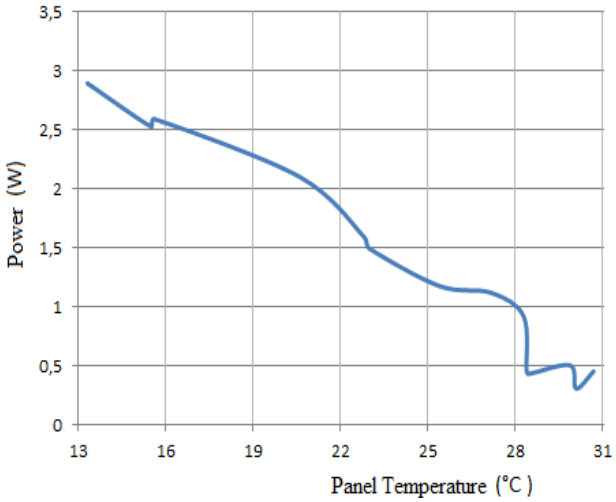

Fig. 10. For polycrystalline panel: while Icd≅30.000 Cd, P=f (Tp) graph

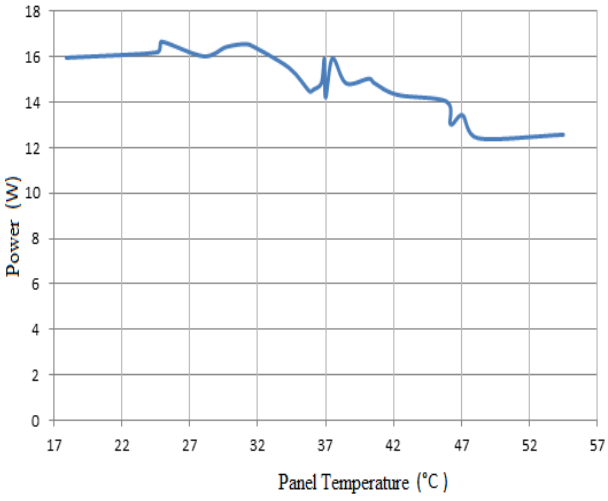

Fig. 11. For polycrystalline panel: while Icd≅90.000 Cd, P=f (Tp) graph

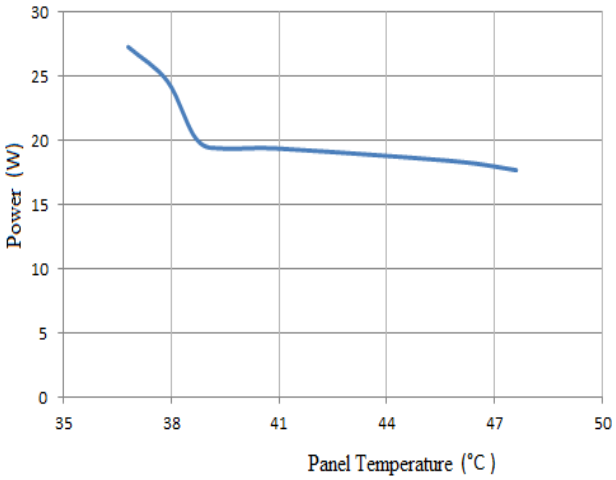

Fig. 12. For polycrystalline panel: while Icd≅130.000 Cd, P=f (Tp) graph

In figure 13, figure 14 and figure 15, for polycrystalline panel, power changes seen for fixed temperature and different illumination conditions. In this variation graphics, it emerges that power increases as long as temperature increases. This is caused by fixed resistance values of the semiconductor structure and resistance value of connection path according to fixed temperature and also increasing illumination provides more photons for energy conversion. In figure 13, the lesser energy production for low panel temperature is caused by lack of photons at the time of measurement.

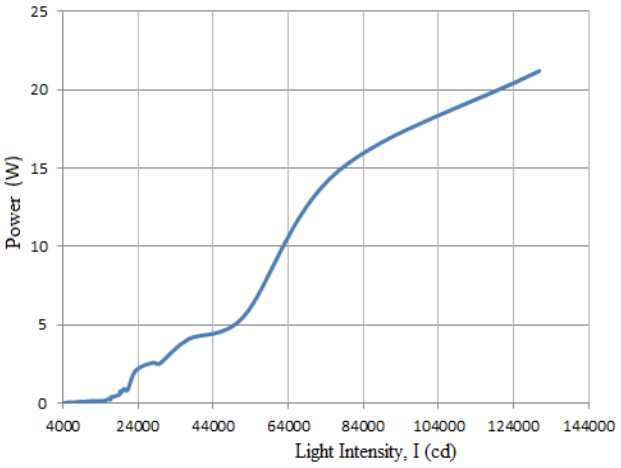

Fig. 13. For polycrystalline panel: while Tp≅15 °C, P=f (I_{CD}) graph

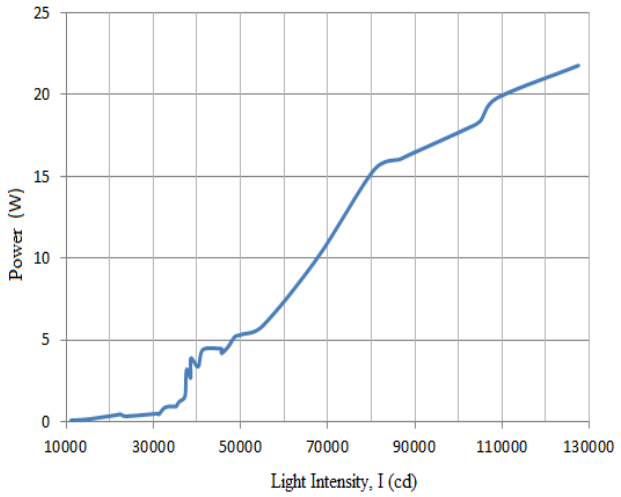

Fig. 14. For polycrystalline panel: while Tp≅ 30 °C, P=f (I_{CD}) graph

Mathematical variance tables of the acquired data from the applications are shown in Table 3. The power values of the panels which are not tested for irradiation and temperature changes can be calculated using those functions.

For example; for a monocrystalline panel, for fixed light intensity at 30000 Cd, using the power function related to temperature shown in table 3 the value of power at 30 degrees ($P=0{,}0116*Tp^2-1{,}143*Tp+44{,}333$) can be calculated as 20,48 watts, and at 60 degrees as 17,51 watts.

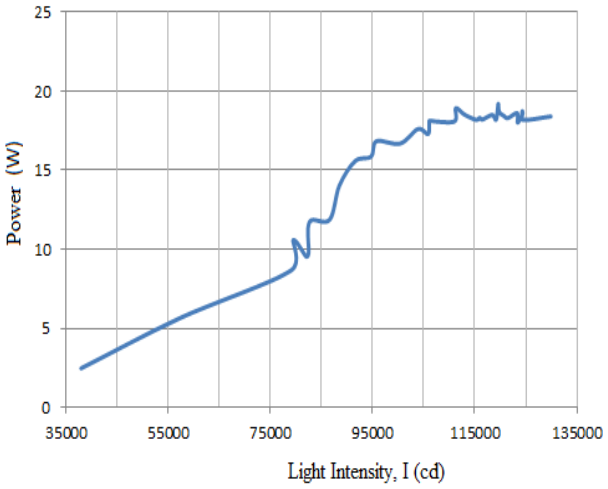

Şekil 15. For poly cristalline panel: while Tp≅45 °C, P=f (I_{CD}) graph

TABLE III
MATHEMATICAL EXPRESSION OF THE APPLICATION DATA

Panel Type	Sabit ve y=f(X)	Değişim Fonksiyonu
MONOCRYSTALLINE PANEL	Icd≅30.000 Cd => P=f (Tp)	$P=0{,}0116*Tp^2-143*Tp+44{,}333$
	Icd≅90.000 Cd => P=f (Tp)	$P= -0{,}0074*Tp^2-0{,}2292*Tp +94{,}878$
	Icd≅130.000 Cd => P=f (Tp)	$P= -0{,}0119*Tp^2-0{,}0955 *Tp+106{,}39$
	Tp≅ 15 °C => P=f (I_{CD})	$P=0{,}00000003*I_{CD}^2+0{,}0002*I_{CD} -0{,}9733$
	Tp≅ 30 °C => P=f (I_{CD})	$P= -0{,}00000001*I_{CD}^2+ 0{,}0021 *I_{CD}-26{,}099$
	Tp≅ 45 °C => P=f (I_{CD})	$P= -0{,}000000005*I_{CD}^2+ 0{,}0013 *I_{CD}-12{,}317$
POLYCRYSTALLINE PANEL	Icd≅30.000 Cd => P=f (Tp)	$P= -0{,}002*Tp^2-0{,}061*Tp +4{,}0271$
	Icd≅90.000 Cd => P=f (Tp)	$P= -0{,}0034*Tp^2+0{,}1163*Tp +15{,}491$
	Icd≅130.000 Cd => P=f (Tp)	$P= 0{,}185*Tp^2-16{,}342*Tp +377{,}29$
	Tp≅ 15 °C => P=f (I_{CD})	$P= 5*10^{-10}*I_{CD}^2+0{,}0001 *I_{CD} -1{,}1442$
	Tp≅ 30 °C => P=f (I_{CD})	$P= 3*10^{-10}*I_{CD}^2+0{,}0002*I_{CD} -4{,}5996$
	Tp≅ 45 °C => P=f (I_{CD})	$P= -10^{-9}*I_{CD}2+0{,}0004*I_{CD} -12{,}914$

IV. CONCLUSIONS

As the result of the examination, about the electrical energy obtained from the photovoltaic panels;

- Monocrystalline panels provide more electrical energy conversion than polycrystalline panels.
- Fixed I_{cd} values as shown above, as seen in *P=f(Tp)* graphics, increased temperature causes power to decrease according to the semiconductor structure and resistance increment at the connection lines.

- Fixed *Tp* values as shown above, as seen in $P=f(I_{CD})$ graphics, increased irradiance causes power to increase.
- As shown in Table 3, using $P=f(Tp)$ function, for monocrystalline and polycrystalline panels, pre-measured power values depending on temperature can be guessed.
- As shown in Table 3, using $P=f(I_{CD})$ function, for monocrystalline and polycrystalline panels, pre-measured power values depending on illumination can be guessed.
- Harvesting solar power is direcly related to photon absorbtion,
- Indirect illuminated placement causes low electrical harvesting due to lack of photon.
- In spite of photon absorptions positive effect on energy harvesting, increasing temperature of solar panel can effect the transformation efficiency negatively due to the semiconductor structure and resistance increment at the connection lines.
- Providing natural heat transfer from the solar panel at the mounting process will increase the photovoltaic panel's efficiency.
- In architectural applications, increasing heat of the solar panels may cause high temperature, so that situation must be considered for fire safety.
- Solar power plant establishments must be settled for the most vertical irradiated positions and not high temperature places.

ACKNOWLEDGMENT

The study is selected from National Engineering Research Symposium 2015 (Ulusal Mühendislik Araştırmaları Sempozyumu) UMAS 2015 (Duzce University).

REFERENCES

[1] Güçlü, S., (2009). Dumlupınar Üniversitesi Merkez Kampus çevre aydınlatma elektrik enerjisinin güneş enerjisi ile sağlanması, Dumlupınar Ünv. Fen Bil. Ens. Elk-Elkt. Müh., Kütahya.
[2] Turhan, K., (2011). Fotovoltaik modüller için bir gerçek saha performans ölçüm platformunun tasarımı, kurulumu ve testleri, Enerji Enstitüsü, İTÜ, İstanbul.
[3] Öztürk, E., (2014). Fotovoltaik panellerin verimine modül sıcaklığının etkisinin deneysel olarak araştırılması, Karabük Ünv. Fen Bil. Ens. Elk-Elkt. Müh., Karabük.
[4] Aslan, C.O., (2011). Isı etkisinin solar panel verimliliğine etkisinin incelenmesi, Marmara Ünv. Fen Bil. Ens. Mekatronik ABD, İstanbul.
[5] Muhtaroğlu, T. K., (2012). Güneş enerjisini elektrik enerjisine çeviren çevre dostu sistemin tasarlanması, Gazi Ünv. Fen Bil. Ens. Elk-Elkt. Müh., Ankara.
[6] Yusufoğlu, G., (2013). Şebeke elektriğinin bulunmadığı tarımsal alanlarda güneş enerjisiyle sulamanın yapılması, Marmara Ünv. Fen Bil. Ens. Makine Eğitimi ABD, İstanbul.
[7] Keçel, S., (2008). Türkiye'deki bölgesel sıcaklık değişimlerinin güneş panellerinin verimliliğine etkisi, Gazi Üniversitesi Endüstriyel Sanatlar Eğitim Fakültesi Dergisi, Sayı: 22, s.12-20.
[8] Sahri, A.,Toumi S., (2013). Temperature effects on the power production based Photovoltaic cells, University of Badji-Mokhtar, Annaba, Algeria.
[9] Werner, L., (1969). Temperature Cycling Effects on Solar Panels, TRW Systems, Redondo Beach, California.
[10] Balázs, P., (2014). Characterization of solar cells by thermal transient testing, Budapest University of Technology and Economics (BME), Department of Electron Devices, Budapest, Hungary.
[11] Temaneh-Nyah, C., (2015). An investigation on the effect of operating temperature on power out put of the Photovoltaic System, Department of Electronics and Computer Engineering, University of Namibia Faulty of Engineering and IT Ongwediva, Namibia.
[12] Işıker, Y., (2006). Fotovoltaik Panel Gücüne Etki Eden Çalışma Parametrelerinin Araştırılması, Makine Mühendisliği Bölümü, Harran Üniversitesi, Şanlıurfa.
[13] Altaş, İ., (1998), Foto voltaj Güneş Pilleri :Eşdeğer Devre Modelleri ve Günışığı ile Sıcaklığın Etkileri, Elektrik-Elektronik Mühendisliği Bölümü ,Karadeniz Teknik Üniversitesi, Trabzon.
[14] Zain, Z.M., (2013), Grid Connected Monocrytalline and Polycrystalline Photovoltaic System: A Comparative Study on Performance
[15] Stutenbaeumer, Ulrich, (1999)"Equivalent model of monocrystalline, polycrystalline and amorphous silicon solar cells." Renewable Energy 18.4: 501-512.
[16] Green, Martin A. (2003)"Crystalline and thin-film silicon solar cells: state of the art and future potential." Solar energy 74.3 181-192.

BIOGRAPHIES

Nazım İMAL was born in Samsun, Turkey, in 1970. He received the professional qualification in electrical department from the Gazi University, Ankara, in 1992. Ms.Sc. degree in Dumlupinar University, department of electronics and computer, completed in 1996, Ph.D. degree in electrical and electronics engineering, completed in Sakarya University. He has been Assistance Professor in Bilecik Seyh Edebali University since 2008.

Şahabettin HASAR was born in Mardin, Turkey in 1978. He received the professional qualification in electrical department from the Gazi University, Ankara, in 2002. He has been a lecturer in Bilecik Seyh Edebali University since 2009 (Osmaneli Vocational High School).

Harun ÇINAR was born in Bolu, Türkiye in 1984. He received the engineer qualification in electrical and electronics engineering from the Karaelmas University, Zonguldak, in 2006, Ms.Sc. degree in Energy Systems Engineering is ongoing in Bilecik S.E University. Working as an engineer in Bilecik S.E University.

Eralp ŞENER was born in Eskişehir, Turkey in 1987. He received the engineer qualification in electrical and electronics engineering from the Anadolu University, Eskişehir, in 2011, Ms.Sc. degree in Energy Systems Engineering is ongoing in Bilecik S.E University. Working as a Teaching Assistant in Bilecik S.E University.

DETERMINATION of GENERAL PARAMETERS of WSNs DESIGNED for 3-D CLOSED ENVIRONMENTS

E. Gunduzalp, G. Yildirim and Y. Tatar

***Abstract*—Use of Wireless Sensor Networks (WSNs) has become widespread in many critical environments. For example, this technology has come into use in tunnels, mines and so on. In this kind of environments, a WSN system design must be far away from randomness and be done systematically. Therefore simulators play a significant role in a WSN system design. Success of a simulator affects directly success of the system. In this paper, we preferred Castalia simulator which is a successful WSN simulator based on OMNET. Many parameters such as different data size, indoor environment features, and various transmission power levels etc., which have an effect on packet reception ratio (PRR), were examined by Castalia. Finally, we explain how to design a WSN system, and what should be considered in a WSN simulation.**

***Index Terms*— Wireless Sensor Networks, Path loss model, simulator, Castalia**

I. INTRODUCTION

WIRELESS Sensor Networks (WSNs) are network technologies used for measuring various physical phenomenon such as humidity, temperature, pressure etc. They communicate generally through radio frequency (RF). In RF propagation, some factors such as distance, reflection, absorption, scattering and other RF signals lead to three important effects; path loss, shadowing and multi-path effects. The three effects have to be taken into consideration in a wireless channel modelling.

Today, we have seen many WSN systems that are deployed in closed critical environments like tunnels, mines. Technical features, locations of sensor nodes and environmental parameters of the area directly affect the performance of the system. Therefore simulations are of paramount importance to detect unanticipated results in a system design. There are some significant features in applications in which environment modelling is important. Some of these features are wireless channel model, radio model, MAC support, adoption and scalability. Naturally, a WSN simulator is supposed to have these models.

In this paper, we show some general steps to be considered in design of a WSN system, which is especially deployed in closed environments. For this, we used OMNET++ based Castalia simulator and different scenarios.

E. Gündüzalp is with DSI, Elazig, Turkey (e-mail: emrullahg@dsi.gov.tr)

G. Yildirim are with DSI, Elazig, Turkey (e-mail: gyildirim@dsi.gov.tr)

Y. Tatar is with the Department of Computer Engineering, Firat University, Elazig, Turkey (e-mail: ytatar@firat.edu.tr)

II. RELATED WORK

Castalia is an effective simulator for analysis of various layers of WSNs. For example, the method presented in [1] hides location privacy of resources, and its effect on energy efficiency is observed by Castalia. In [2], a design of Collection Tree Protocol – CTP- and its performance are evaluated with the help of Castalia. In another study, [3], the energy performance of an algorithm that keeps track of mobile nodes is analyzed by it. On the other hand, analyses of various routing algorithms can be done by using the simulator. To give an example, in [4], the success of the RBR (Resource Biased Routing) algorithm is shown by Castalia. In another study, [6], the RPL algorithm, which has gotten famous through IPv6, and the LOADng algorithm are compared on Castalia simulations. A framework called PASES, which is designed to evaluate energy performances in WSNs, is run on Castalia in [7]. Castalia also claims to be successful in WBAN applications. A study [8] does a performance test for evaluating various WBAN MAC protocols. A comprehensive survey about some WSN simulators and their general features can be found in [5].

III. CASTALIA

OMNET++ is a discrete event network simulator, which is based on object oriented and modular as well. Many communication networks can be modeled by it. The C/C++ support provides programmers with a flexible design platform [9]. Castalia is based on OMNET++, and enable to make detailed simulations of WSNs, WBANs and networks consisting of embedded device with low-energy consumption. Researchers are able to test their own protocols and algorithms with a real-like wireless channel, radio unit and node models in it [10]. A network in Castalia is composed of various sub-modules.

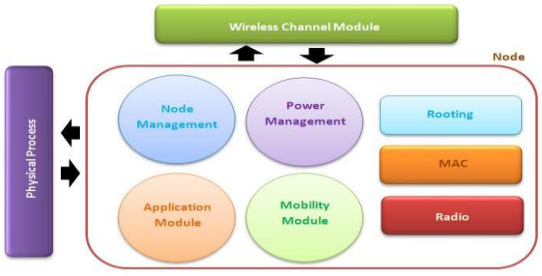

Figure1. The modules in Castalia

The main modules are wireless channel module, node module and physical operation modules. The node module is a composite module and consists of different sub-modules shown in Fig.1.

The radio propagation model of Castalia is modelled in the wireless channel module. As known, in a radio propagation,

distance, reflection, absorption, scattering and other radio signals give rise to three important effects; path-loss, shadowing and multi-path effect. Since the effects have direct influence on radio signals, communication quality will be directly affected by them. There are many approaches concerning modelling of radio propagation in literature. Therefore, success of simulators rests on the choice of an appropriate and real-like propagation model. Castalia, which uses the log-normal shadowing model as default, provides a successful wireless channel model. As known, absorption, scattering and multi-path effects make signal estimation quite difficult in a radio propagation model. In this field, the log-normal shadowing model has proven itself to be successful [13]. The model computes possible random losses of a signal according to Eq.1 [12]. In the equation, PL(d) is total reduction of the signal power at distance "d", expressed as dBm. While PL(d0) represents "reference path loss" for a known distance "d0", the second term represents "path loss" depending on the distance. The third terms is a Gaussian random variable modelling shadowing effect,the modelling of which is difficult.

$$PL(d) = PL(d_0) + 10\eta log_{10}\left(\frac{d}{d_0}\right) + X_\sigma \quad (1)$$

Xσ is computed according to the Gaussian function in Eq.2 [12-13].

$$X_\sigma = \frac{1}{\sqrt{2\pi\sigma^2}}\, e^{-\frac{(X-\mu)^2}{2\sigma^2}} \quad (2)$$

Where, μ is zero, and standard deviation - σ and coefficient – η depend on environment conditions, which are calculated experimentally in many studies in literature [11].

Castalia includes many features to provide the radio model with low-energy consumption. In addition, Castalia allows users to define their own radio file in a standard format.

A MAC layer is an important part of a WSN, which explains accesses of nodes to a communication media. Four well-known MAC modules are can be used in Castalia [10]. Those are;

- *Tunable MAC*
- *TMAC and SMAC*
- *IEEE 802.15.4 MAC*
- *IEEE 802.15.6 MAC (Baseline BAN MAC)*

In comparison to the MAC and the physical modules, the routing module of Castalia is weaker [10]. On the other hand, Castalia allows users to design their own routing modules just like the other modules.

IV. IMPLEMENTATION

In the study, a 3D closed area whose dimension is (60, 16, 8) m was modelled for the simulations. Depending on scenarios selected, seven nodes whose interactions would be observed were placed in various coordinates in the area. Since the aim of the study was to show general steps of a WSN simulation, the environment conditions were considered ideal, and non-interference model was used. In the scenarios, the nodes were placed in the area as shown Fig.2 a, and b. In the scenarios, the "Node 0", broadcasting packet every second, sent totally 500 packets to the others.

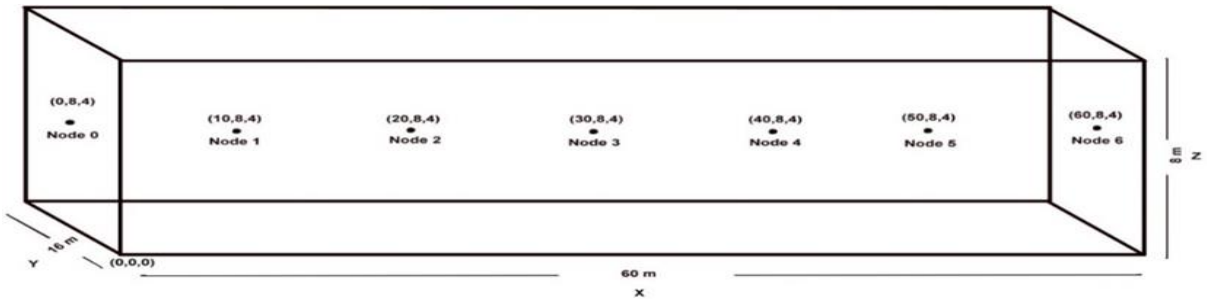

a) Horizontal

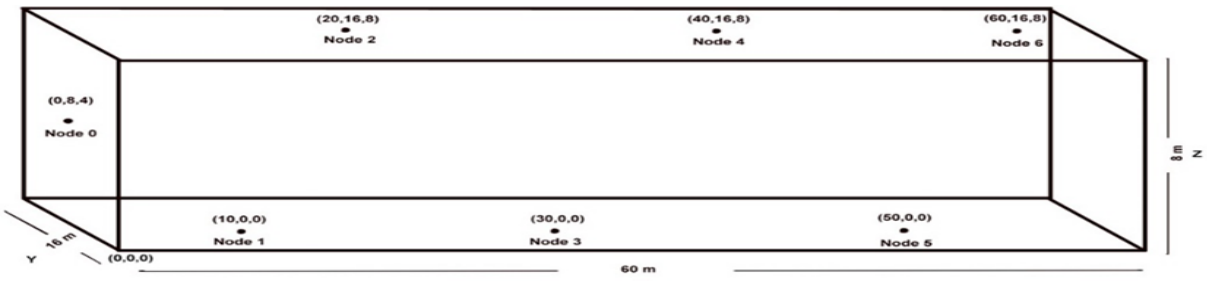

b) Random Positioning

Figure 2. The deployment of the sensor nodes according to the scenarios

In the scenarios that used the CC2420 radio and the byPassMAC, PRR variations were observed for different Tx output powers, radio sensitivities, data payload sizes and log-normal shadowing model parameters. At first, η, the environment parameter, was selected as 2.4, representing default value for a closed area, but then the system was tried again for the other η values shown in [11] to check the validation of the WSN. A collision-free model was preferred in the experiments. In addition, the Link Quality Indicators - LQIs - of the sensor were achieved and used as comparison values. The parameters of the CC2420 radio used in the simulations are given in Table I.

TABLE I. THE PARAMETERS OF CC2420

Data Rate (kbps)	*Modulation Type*	*Bits Per Symbol*	*Band width (MHz)*	*Noise Bandwidth (MHz)*	*Noise Floor (dBm)*	*sensitivity (dBm)*	*Power Consumed (mW)*
250	*PSK*	*4*	*20*	*194*	*-100*	*-95*	*62*

A. PRR Variation for various Tx power levels

The aim in this experiment is to find the optimum Tx power and an average node distance (d_av). For this, the sender Node 0 broadcasted periodically with powers of 0 dBm, -3 dBm and -7 dBm respectively. The PRR variation of the nodes for the Tx powers were obtained as in the Fig 3 a-f.

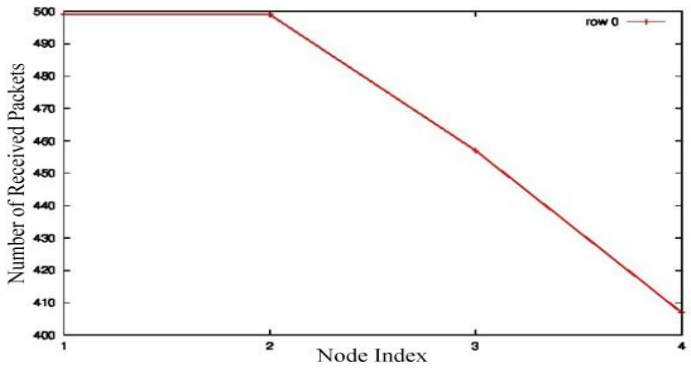

a) Horizontal, Tx = 0 dBm

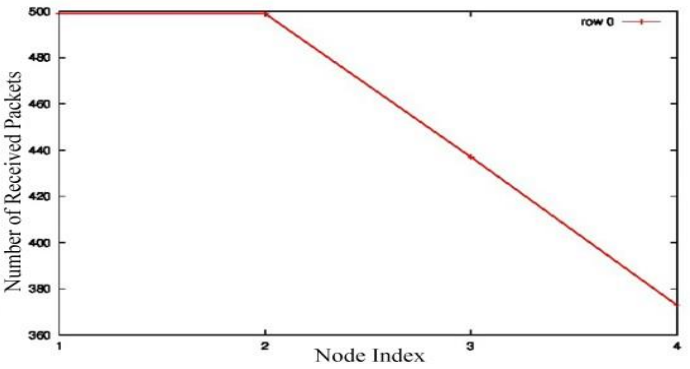

b) Random, Tx = 0 dBm

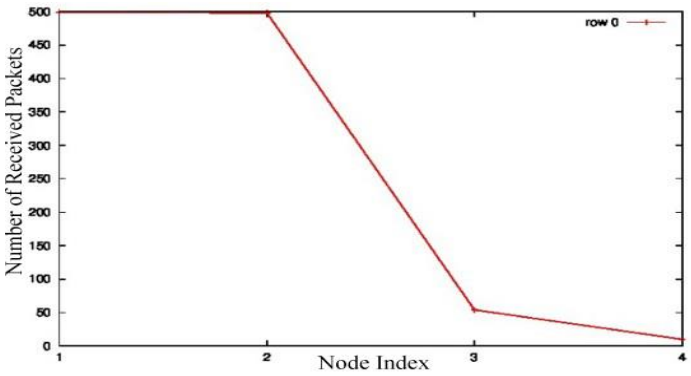

c) Horizontal, Tx = -3 dBm

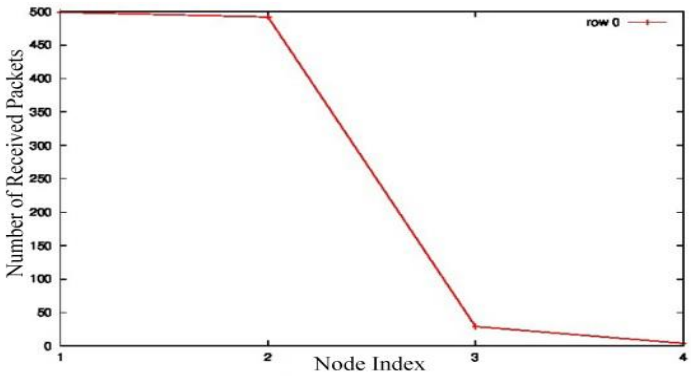

d) Random, Tx = -3 dBm

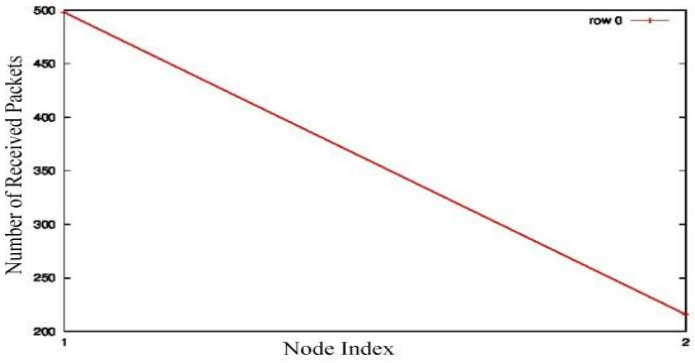

e) Horizontal, Tx = -7 dBm

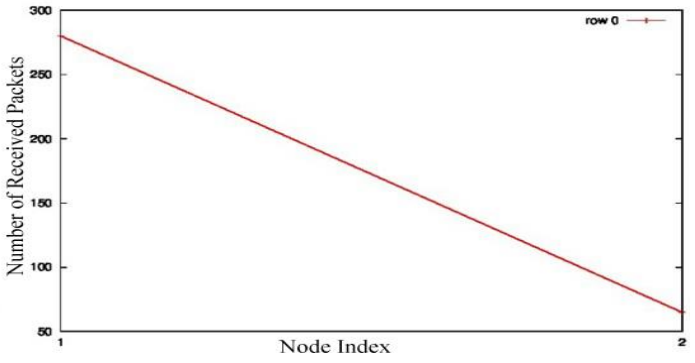

f) Random, Tx = -7 dBm

Figure 3. The PRR Variations for various Tx power levels

Since WSNs are generally multi-hop applications, distance between sensors nodes is important. This will affect directly the energy efficiency and performance of the system. As it is understood from the figures above, Tx= -3 dBm output power seems suitable for a distance of 20 m in both the horizontal and the random scenarios. Thus a gain of 3 dBm can be achieved compared to Tx=0 dBm, which provide an energy saving.

B. PRR Variation for various radio sensitivities

Radios with receiver sensitivity of between -95 dBm and -110 dBm have been frequently used in practical applications. In the experiments, the PRR variations were observed for the two sensitivity values in the both scenarios. The Tx powers used are 0 dBm, -3dBm and -7 dBm. The PRR values of the experiments are shown in Fig.4 a-m.

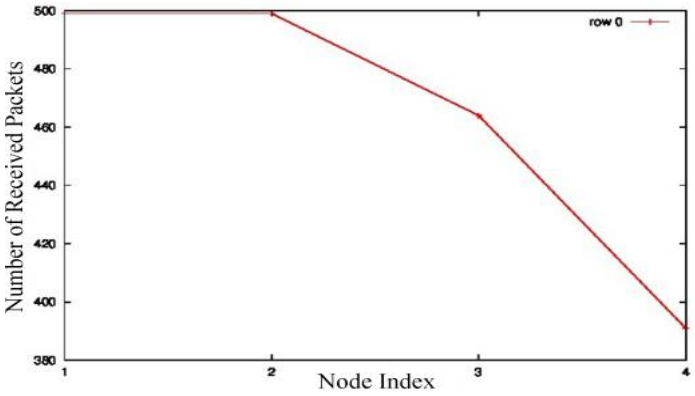

a) Horizontal, Tx = 0 dBm, sensitivity= -95 dBm

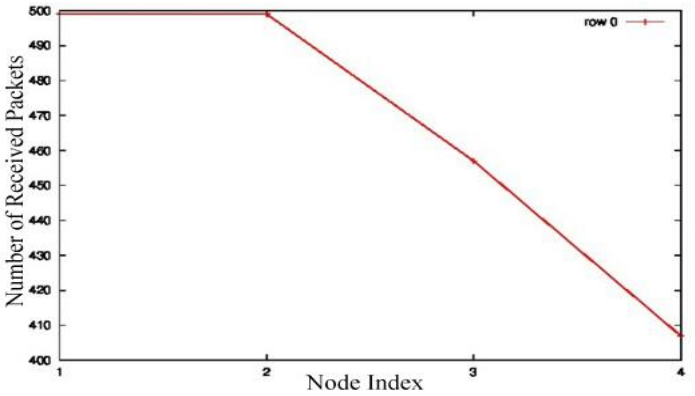

b) Horizontal, Tx = 0 dBm, sensitivity= -110 dBm

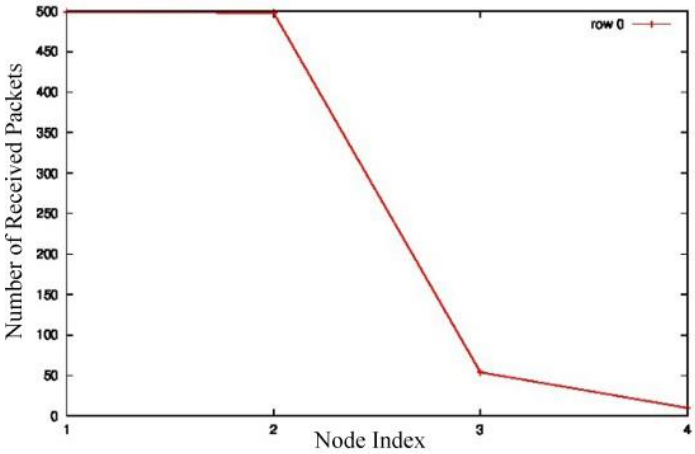

c) Horizontal, Tx = -3 dBm, sensitivity= -95 dBm

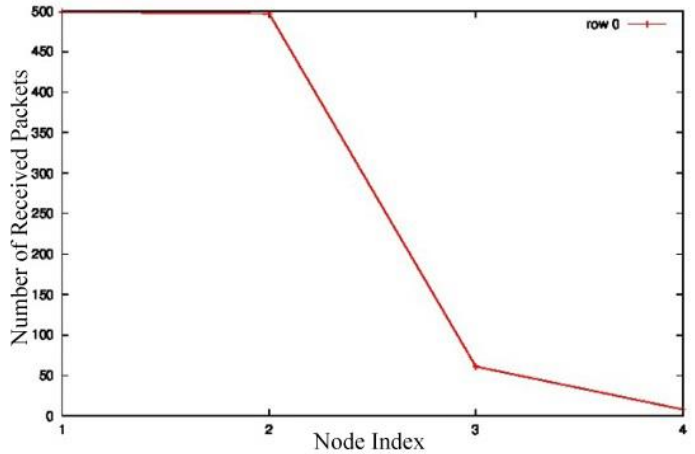

d) Horizontal, Tx = -3 dBm, sensitivity= -110 dBm

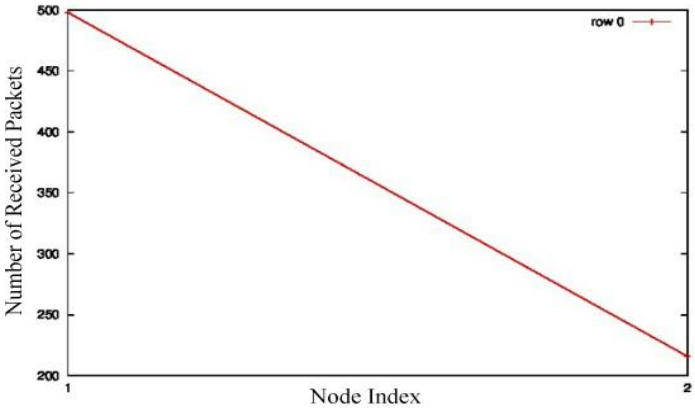

e) Horizontal, Tx = -7 dBm, sensitivity= -95 dBm

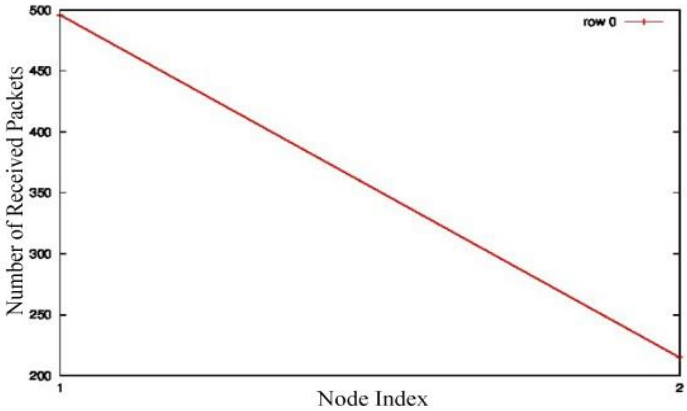

f) Horizontal, Tx = -7 dBm, sensitivity= -110 dBm

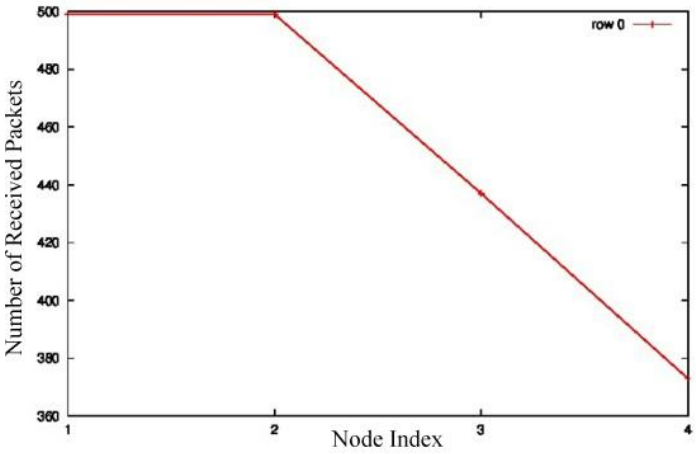

g) Random, Tx = 0 dBm, sensitivity= -95 dBm

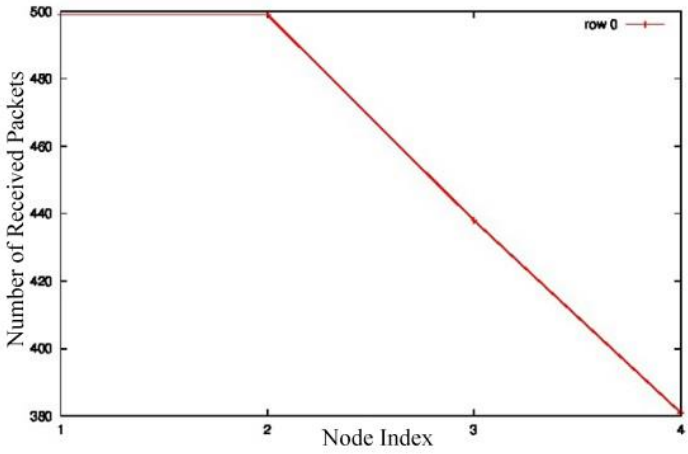

h) Random, Tx = 0 dBm, sensitivity= -110 dBm

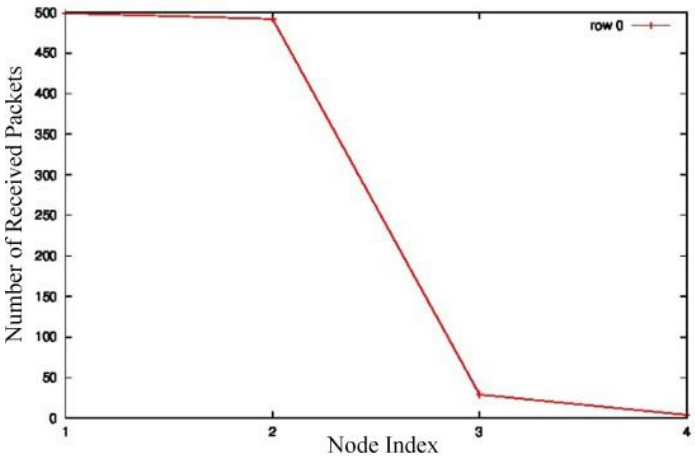

j) Random, Tx = -3 dBm, sensitivity= -95 dBm

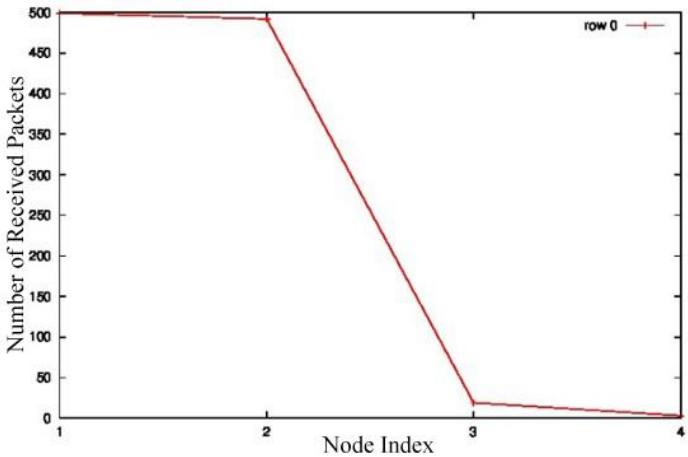

k) Random, Tx = -3 dBm, sensitivity= -110 dBm

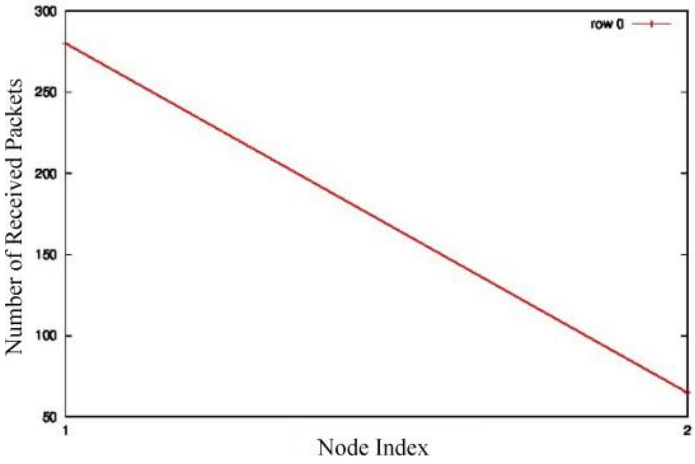

l) Random, Tx = -7 dBm, sensitivity= -95 dBm

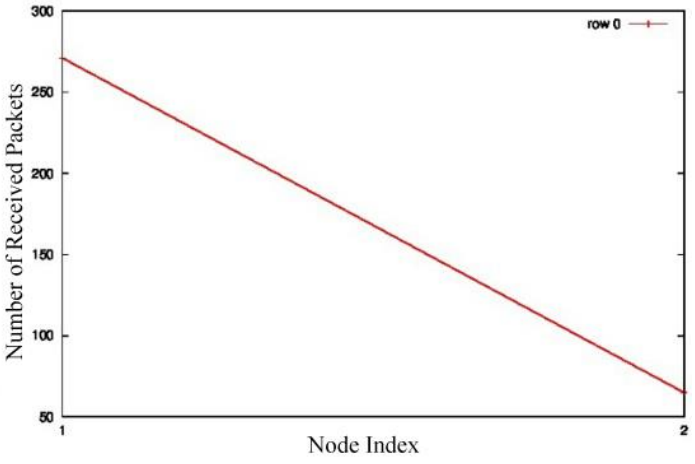

m) Random, Tx = -7 dBm, sensitivity= -110 dBm

Figure 4. The PRR Variation for radios with various sensitivities

As it is seen in the Figures, there is not important difference in the PRR variations for the both receive sensitivities. Accordingly, a radio with sensitivity of -95 dBm is adequate for a WSN system, which has nodes with -3 dBm Tx power and a d_av of about 20 m. Thus, when it is considered that more sensitive radios are expensive, there is no need additional cost for the selected values aforementioned.

C. PRR Variation for various data payload

Payload size is a performance criterion in a WSN system. For example, the 802.15.4 standard states that 1% PRR must be achieved in -85 dBm receiver sensitivity and 20 byte payload [10]. In the experiment, different payload (20, 50 and 80 byte) was used for the given Tx, d_av values. The results obtained are given in the Fig.5 a-f. As it is seen from the Figures, increase in the payload doesn't affect the performance a lot for the multi-hop system running with the given parameters.

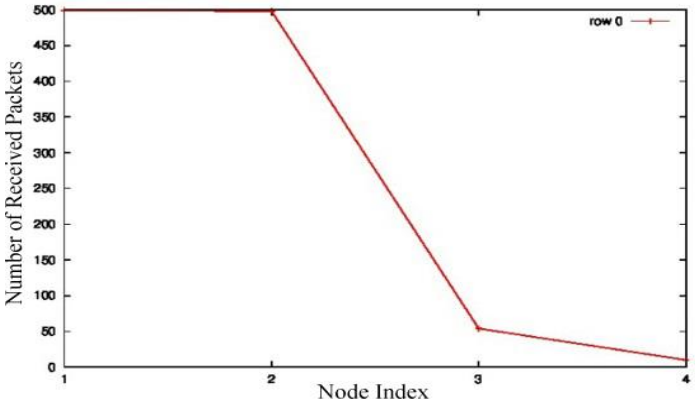

a) Horizontal, Tx = -3 dBm, payload = 20 byte

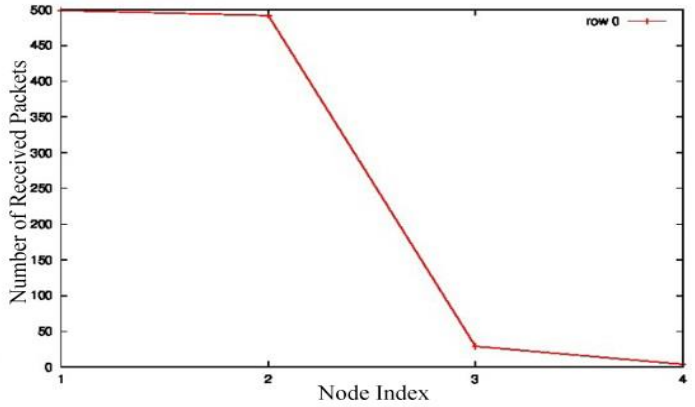

b) Horizontal, Tx = -3 dBm, payload = 20 byte

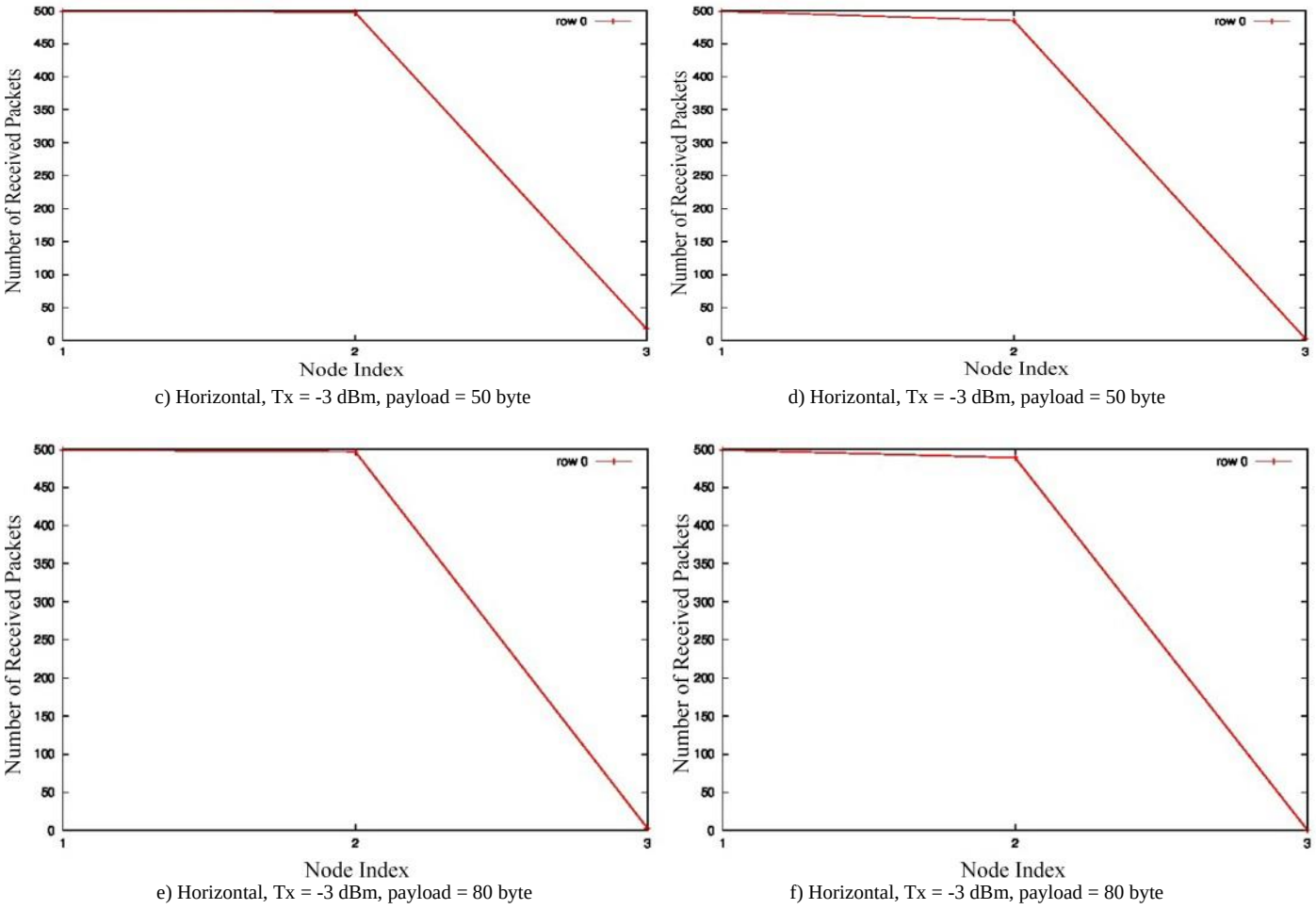

c) Horizontal, Tx = -3 dBm, payload = 50 byte

d) Horizontal, Tx = -3 dBm, payload = 50 byte

e) Horizontal, Tx = -3 dBm, payload = 80 byte

f) Horizontal, Tx = -3 dBm, payload = 80 byte

Figure 5. PRR Variation for various data payload

D. PRR Variation for various η values

The parameters *η and σ in* Eq.2 are coefficients, and varies by environmental conditions. In literature, the *η* parameter is between 1.6 (LoS) and 2.4 in free-space building. Since the environment was considered ideal and free space, the selected parameters were tried for *η=1.6, 2 and 2.4.* The *σ* was selected between 0 and 13. The results are shown Fig.6 a-n. But it shouldn't be forgotten that a system must be tested in a real-like parameters, so the environmental features must be known in advance. As seen in the Figures, the system can run seamlessly for Tx=-3dBm, d_av=20 m and the *η – the σ* values.

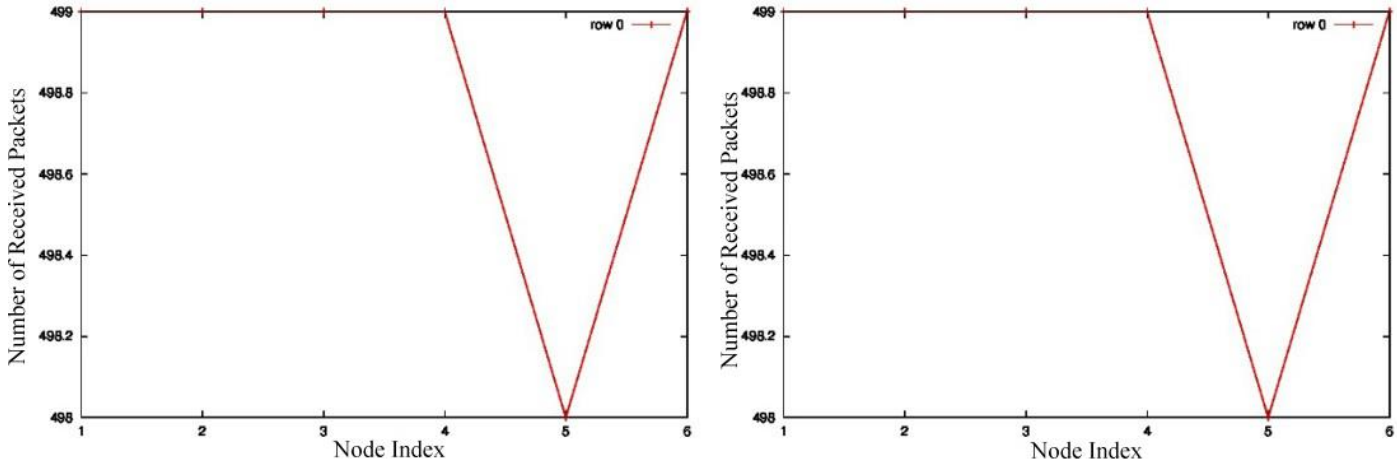

a) Horizontal, Tx = -3 dBm, η = 1.6, sigma(σ) = 4

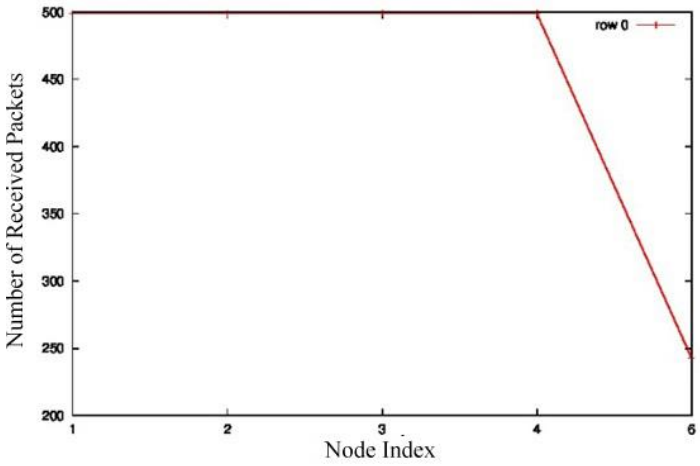

b) Random, Tx = -3 dBm, η = 1.6, sigma(σ) = 4

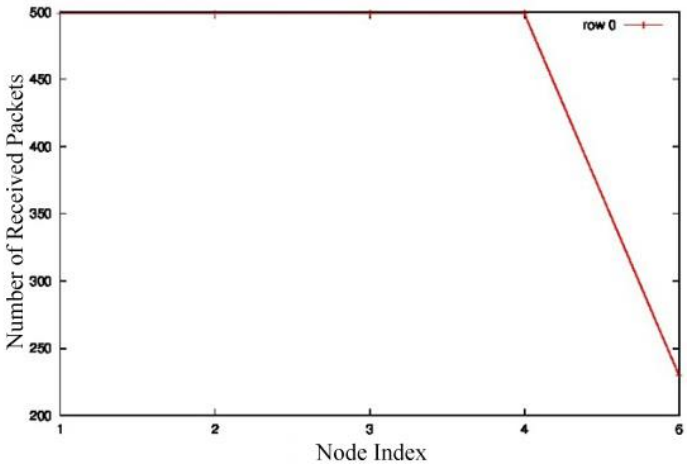

c) Horizontal, Tx = -3 dBm, η = 2, sigma(σ) = 4

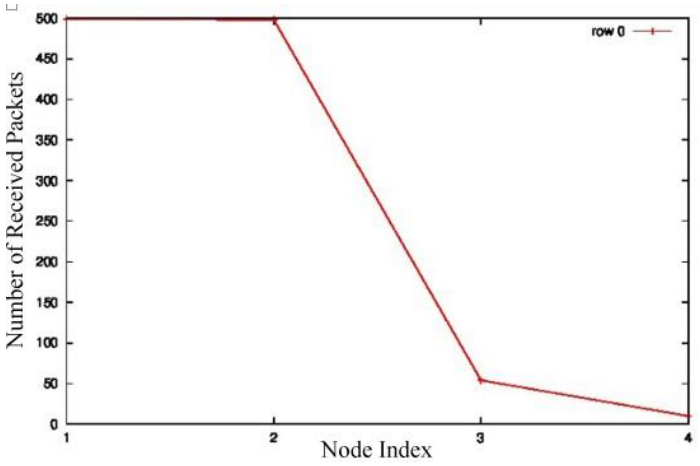

d) Random, Tx = -3 dBm, η = 2, sigma(σ) = 7

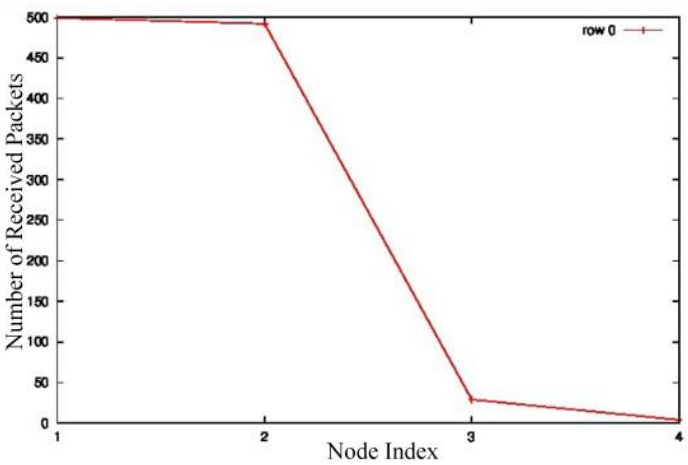

e) Horizontal, Tx = -3 dBm, η = 2.4, sigma(σ) = 7

f) Random, Tx = -3 dBm, η = 2.4, sigma(σ) = 10

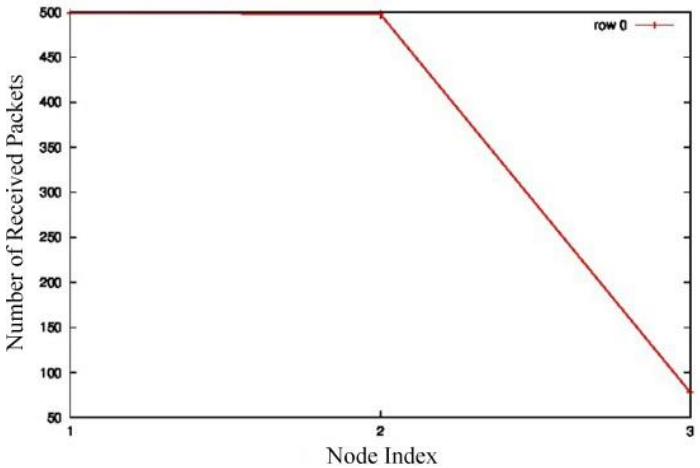

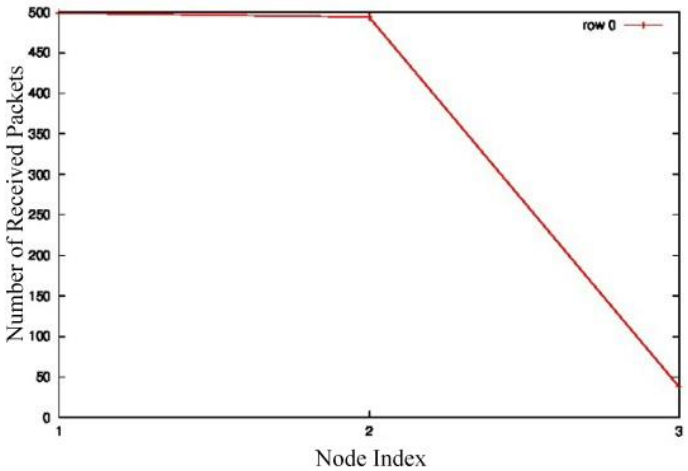

g) Horizontal, Tx = -3 dBm, η = 1.6, sigma(σ) = 0

h) Random, Tx = -3 dBm, η =1.6, sigma(σ) = 0

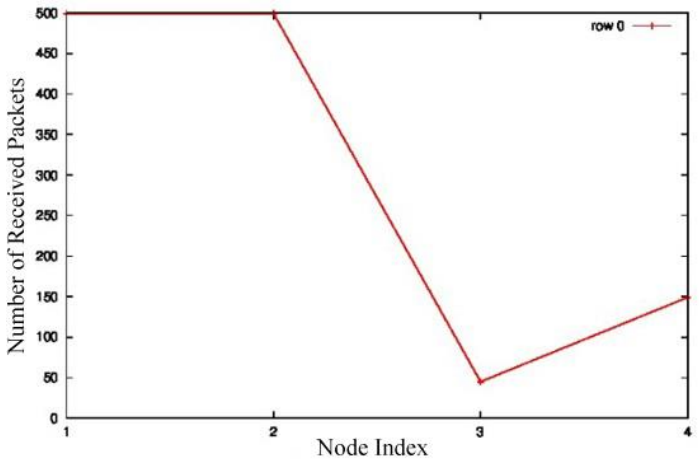

i) Horizontal, Tx = -3 dBm, η = 1.6, sigma(σ) = 7

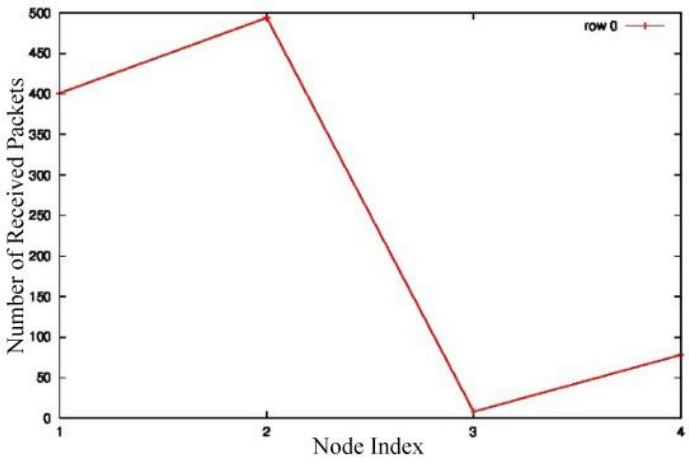

j) Random, Tx = -3 dBm, η =1.6, sigma(σ) = 7

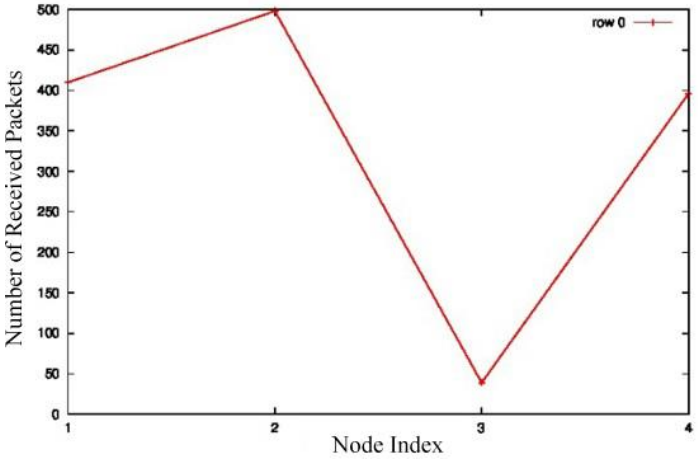

k) Horizontal, Tx = -3 dBm, η = 1.6, sigma(σ) = 10

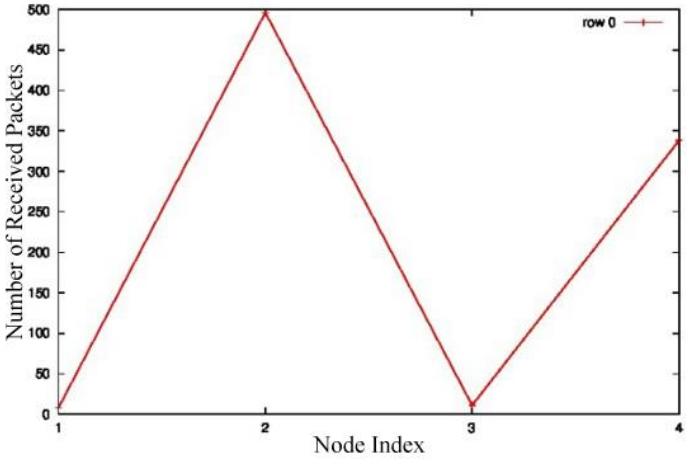

l) Random, Tx = -3 dBm, η =1.6, sigma(σ) = 10

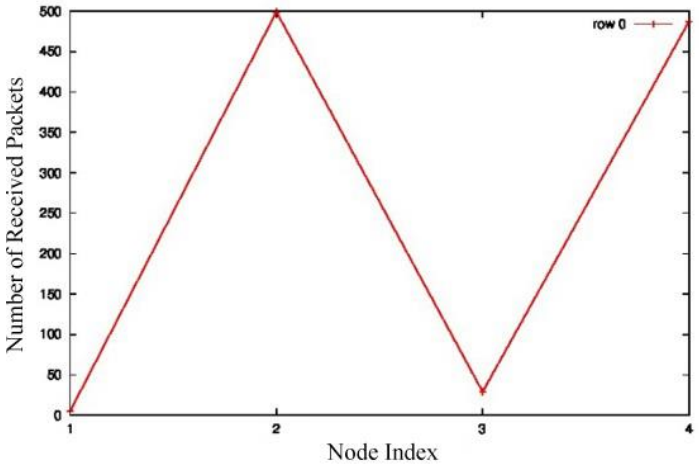

m) Horizontal, Tx = -3 dBm, η = 1.6, sigma(σ) = 13

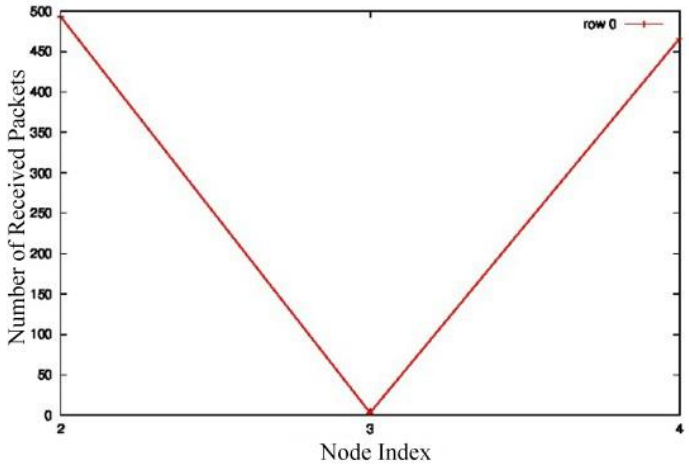

n) Random, Tx = -3 dBm, η =1.6, sigma(σ) = 13

Figure 6. PRR Variation for various n and sigma(σ) values

TABLE II. THE LQI TABLE

Receiver / Transmitter	***node=0*** *Sen1/Sen2*	***node=1*** *Sen1/Sen2*	***node=2*** *Sen1/Sen2*	***node=3*** *Sen1/Sen2*	***node=4*** *Sen1/Sen2*	***node=5*** *Sen1/Sen2*	***node=6*** *Sen1/Sen2*
index=0	*0/0*	*100/100*	*99/99*	*99/99*	*100/100*	*69/64*	*100/100*
index=1	*100/100*	*0/0*	*100/100*	*100/100*	*100/100*	*100/100*	*100/100*
index=2	*100/100*	*100/100*	*0/0*	*100/100*	*100/100*	*100/100*	*100/100*
index=3	*100/100*	*100/100*	*100/100*	*0/0*	*100/100*	*100/100*	*100/100*
index=4	*100/100*	*100/100*	*100/100*	*100/100*	*0/0*	*100/100*	*100/100*
index=5	*89/87*	*100/100*	*100/100*	*100/100*	*100/100*	*0/0*	*100/100*
index=6	*100/100*	*100/100*	*100/100*	*100/100*	*100/100*	*100/100*	*0/0*

E. LQI Values

LQI tables can provide supplementary information about the performance evaluation. Accordingly, their analysis may be useful from technical point of view. In the scenarios, each node, positioned horizontal and random as in Fig2, sent 100 packets. In Castalia, each node has a table for recording LQI values. When a node receives a packet, the sender of which is known, it increases the counter of the sender. In the study, the LQI table obtained from the experiments is given in Table 2. As seen in the table, the LQI values validated the PRR values obtained according to the values chosen.

V. CONCULUSION AND DISCUSSION

For a good performance pre-assessment, some main parameters of a WSN system designed must be chosen well. The parameters affect directly the life time of the WSN, the energy consumption, the network traffic, data loss and so on. Some of the parameters are the transmission power, the receiver sensitivity and the environments parameters. In the paper, simulation of a WSN system deployed in a 3D closed area and the selection of its parameters were carried out. For this, Castalia simulator and two different scenarios were used. In the study, the PRR variations were observed for different Tx powers, different payloads, different receiver sensitivities and various environment parameters. In addition, the LQI table of the experiment was presented for comparison. As a result, the optimum parameters of the WSN and the closed area were specified. Thus, a design model approach, far from randomness, and its steps were presented shortly. Also the effect of the main parameters on the result was shown. Although the used features are not all parameters to be considered for a WSN design, they must be always taken into account. With various combinations and interference models, these experiments can be diversified.

ACKNOWLEDGMENT

The study is selected from National Engineering Research Symposium 2015 (Ulusal Mühendislik Araştırmaları Sempozyumu) UMAS 2015 (Duzce University).

REFERENCES

[1] Tangil G. S., Palomar E., Ramos B., Ribagorda A., 2010, An Experimental Comparison of Source Location Privacy Methods for Power Optimization in WSNs,ADVANCES in SENSORS, SIGNALS and MATERIALS, 79-84.

[2] Colesanti U., Santini S., (2010), A Performance Evaluation Of The Collection Tree Protocol Based On Its Implementation For The Castalia Wireless Sensor Networks Simulator, Technical Report, Department of Computer Science, ETH Zurih.

[3] Elbishti M., Elleithy K., Almazaydeh L., 2014, An Energy Efficient Algorithm for Object - Tracking Wireless Sensor Networks, ICAT'14 International Conference on Advanced Technology & Science, DOI: 10.13140/2.1.1639.3609.

[4] Saraswat L. K., Kumar S., 2013, Extending the Network Lifetime in Wireless Sensor Networks using RBR Algorithm, Advance in Electronic and Electric Engineering, 3(3) 287-294.

[5] Jevtic M. Zogovic N., Dimic G., 2009, Evaluation of Wireless Sensor Network Simulators, 17th Telecommunications forum TELFOR, 1303-1306.

[6] Tripathi J., Oliveira J.C., Vasseur J.P., 2014,Proactive versus reactive routing in low power and lossy networks: Performance analysis and scalability improvements, Ad Hoc Networks, 23 121-144, http://dx.doi.org/10.1016/j.adhoc.2014.06.007

[7] Minakov I., passerone R., 2013, PASES: An energy-aware design space exploration framework for wireless sensor networks, Journal of Systems Architecture, 59 626-642, http://dx.doi.org/10.1016/j.sysarc.2013.05.020

[8] Bradai N., Fourati L. C., Kamoun L., 2014, Investigation and performance analysis of MAC protocols for WBAN networks, Journal of Network and Computer Applications, 46 362-373, http://dx.doi.org/10.1016/j.jnca.2014.09.012

[9] https://omnetpp.org/doc/omnetpp/manual/usman.html, OMNeT++ User Manual Version 4.5,

[10] https://forge.nicta.com.au/projects/castalia/, Castalia User Manual Version 3.2

[11] Cebula S.L., Ahmad A., Graham J.M, Hinds C.V., Wahsheh L.A, (2011), Empirical Channel Model for 2.4GHz IEEE 802.11 WLAN, Proceedings of the 2011 International Conference on Wireless Networks.

[12] Akyildiz, I.F, Vuran,M.C., 2010. Wireless Sensor Networks, WILEY, ISBN 978-0-470- 03601-3.

[13] Goldsmith A., 2005, Wireless Communications, Stanford University, ISBN: 9780521837163

BIOGRAPHIES

Emrullah GÜNDÜZLAP received the B.S. degree in computer engineering from Firat University, and is currently doing his M.S. in the same department. He is also working as an IT engineer in the General Directorate of State Hydraulic Works, DSI. His current research interest are in the area of wireless sensor networks, computer networks.

Güngör YILDIRIM received the B.S. degree in Electrical and Electronic Engineering, the M.S. degree in Computer Engineering from Firat University. He is currently a Phd student in the computer engineering at the same university. He is also working as a project engineer in the General Directorate of State Hydraulic Works, DSI. His main research areas are wireless sensor networks, programing language.

Yetkin TATAR is a Professor in the Department of Computer Engineering, Firat University, Turkey. He received the B.Sc. in EDMMA in 1974, and M.Sc and D.Sc degrees in Electrical and Electronic Engineering from Firat University, in 1984 and 1994, respectively. His research areas are wireless sensor networks, computer networks, network security, and power electronic.

Direction and Position Reconstruction on Mobile Robots

E. Şimşek, G. Tümüklü Ozyer and B. Özyer

***Abstract*— The control of autonomous mobile robot motion are still a big challenge due to the uncertainties of the complex environment, noisy sensor signals on robot and failure of mechanical design. Mobile robot needs to determine its location accurately for performing different task such as trajectory tracking and mapping. In this paper, we propose two different rule-based methods for reconstructing robot position and the direction during the motion. We initially introduce the four wheel mobile robot that we have developed for this study by giving the detail information about mechanical, electronic and software design steps and components. The proposed methods are used to estimate position and direction error and then reconstruct its motion while moving in the forward direction. The proposed methods are tested on a real mobile robot.**

***Index Terms*— Localization, Robot Path Planning, Mobile Robots.**

I. INTRODUCTION

THERE have been so many types of mobile robots designed for achieving complex task such as search and rescue, mine dragging, shipping and mapping during the last decades [1,2]. While wheel based structured mobile robot are designed to move on a flat surface, leg based mobile robot are developed to demonstrate locomotion in non-deterministic environment. These robots are all equipped with some sensors such as sonar, infrared, laser, camera or Wifi. By the help of these sensors, robots can able to contact with an environment such that they can measure distance of any object or determine its location in a space and so on. Moreover, these mobile robot can be remotely controlled by computer via wireless communication protocols to perform autonomous movement.

In the literature, 3D mapping in complex environment, distributed multi agent system and autonomous swarm robotics have been studied mostly in the mobile robotics in the last decades [3-6]. To achieve autonomous movement of mobile robot, the initial step is to determine the location of robots accurately by using sensors mounted on robots. However, sensory data coming from the different sensor are so noisy. For instance, the encoder that measure the displacement of motor shaft reads unreliable data due to unexpected changes on the ground and wheel rotation. Kalman filter and particle filter are well known algorithm to filter the noisy data that decreases error in controlling the motion [7]. The sensitive and precise component that are used in the while developing a robot is another important issue to decrease the noisy data, however in that case production cost increases. In addition to the sensor mounted on the mobile robot, the communication protocols between the controller and robots is another important issue that should be considered to design a mobile robot [8]. In spite of Bluetooth, infrared and RF that are commonly used to control mobile robots for indoor application, UDP and TCP protocols is more preferable that is because they are more safe and stable in short distance range applications [9], [13]. By the increasing the technological sophistication of the internet, cloud robotics are become popular in robotic research area [14]. The cloud system allows user to communicate with robots from all over the world. This approach is a new generation of robots that provide wireless networking, big data, artificial intelligence algorithms and wide range applications such as surgery, driving and shipping [10]-[12]. Despite these developments, in order to achieve autonomously control the mobile robot, there is still need to estimate the noisy data coming from the sensor to determine the direction and location of the robot accurately.

In this study, we propose rule-based method to estimate and fix the error while moving in a forward direction, which leads to autonomous motion. The rest of the paper is organized as follows. In Section II, we represent the designing steps including mechanical, electronics, communication and software design. The problem definition is given in Section III. The detail information about the proposed method to estimate the direction and position deviation are given in Section IV. The real time experimental results are represented in Section V. We conclude and give the future direction of our research in the last section.

II. MOBILE ROBOT DESIGN

Our major goal to design such a 4 wheeled mobile robot is to achieve autonomous motion indoor area by fixing the positional and directional error. In this section, we represent three design stages consisting of mechanical, electronics and software design.

A. Mechanical Design

As shown from the Figure-1a, we initially manufactured the body of the robot using transparent board. The size of the body of the robot is about 15x25 cm that is enough to mount 4 dc

E. Simsek, Computer Engineering, Atatürk University, 25240, Erzurum, Turkey, (e-mail: emrah.simsek@atauni.edu.tr).

G. T. Özyer, Computer Engineering, Atatürk University, 25240, Erzurum, Turkey, (e-mail: gulsah.ozyer@atauni.edu.tr).

B. Ozyer, Computer Engineering, Atatürk University, 25240, Erzurum, Turkey, (e-mail: baris.ozyer@atauni.edu.tr).

motors, electronic cards, sensors, wires and microcontroller. As shown on the right hand side of the Fig.1-a, there are screw holes on chassis to stabilize electronic modules, sensors and other components. Wheels are only allowed to move in a forward direction. The left and right rotational motion of robot is realized by adjusting the velocity of the wheels. The final version of the robot at the end of the design process is shown in Fig.1-b.

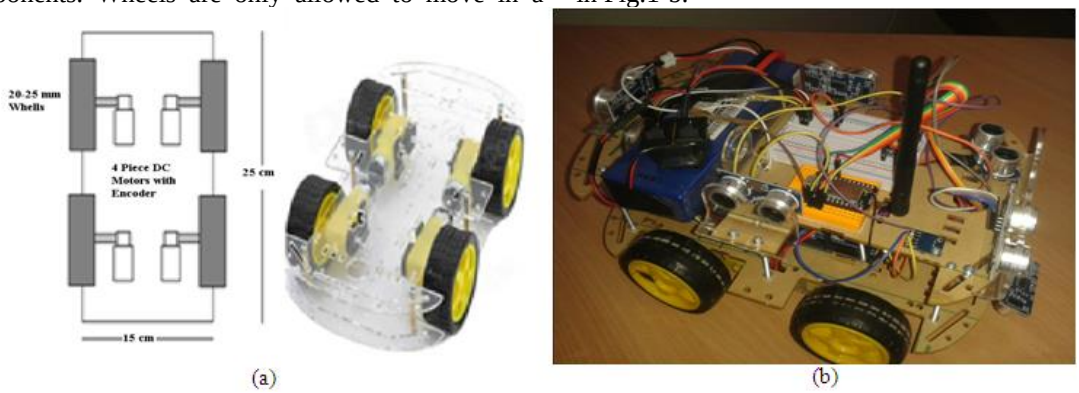

Fig.1. Mobile robot design (a) The basic chassis of mobile robot (b) Mobile robot design after assembling electronic and mechanical components on the robot

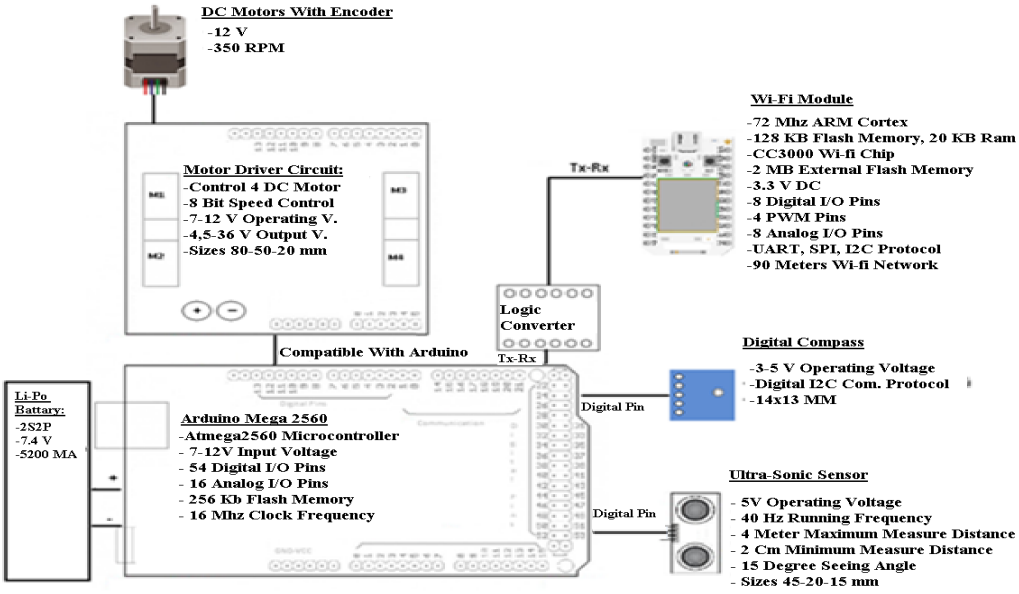

Fig.2. Block Diagram of Electronic Circuit Design

B. Electronic Design

In this section, we describe the electronic design process to gather the electronic components. The schematic view of the electronic components including sensor, microcontroller digital compass, Wifi Module and motors are shown in Figure-2. In order to measure the direction of the motor, we use HMC588L3 type 3 axis digital compass. Hc-SR04 type ultra-sonic sensor is used to measure the distance of the obstacle while moving in direction. Spark Core Wi-Fi module is used to communicate the robot with PC. Arduino Mega 2560 microcontroller is used to interface with the hardware component and implement PWM functions to control the motors. The robot is remotely controlled by PC via Wifi Network.

We use serial communication protocols with 2 digital pins in same clock frequency as shown Figure-3. This protocol allow us to data transfer in 2Mbps.

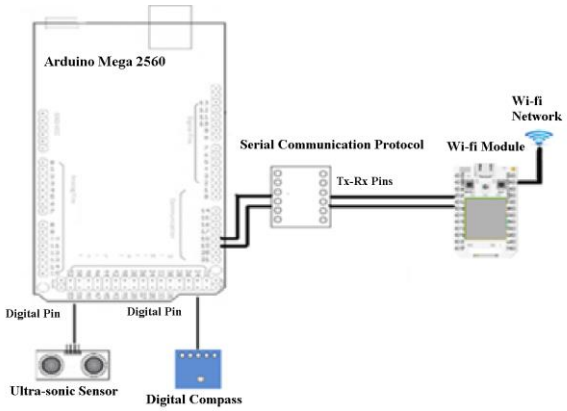

Fig.3. Serial communication protocols

C. Software Design

Software design process consists of three main stages. The first one is applied on microcontroller using C programming

language to control the motors and read the sensor signals. The second one is used for communication protocols between Arduino microcontroller and PC. The last one is designing interface to allow the user to control the motors and illustrating the sensor data. The Arduino IDE, which very simple and useful in designing and programming electronic circuit, is used to program the microcontroller. Wifi modules are used to communicate the PC and microcontroller. We developed communication techniques using serial ports that enable to control the motor in real time. The user interface is designed in MATLAB as shown Figure-4. The user can set velocity and direction of the motors by sending commands on the interface. The position of the motor obtained from the encoder and direction of the motor obtained from the digital compass are also monitored on the interface.

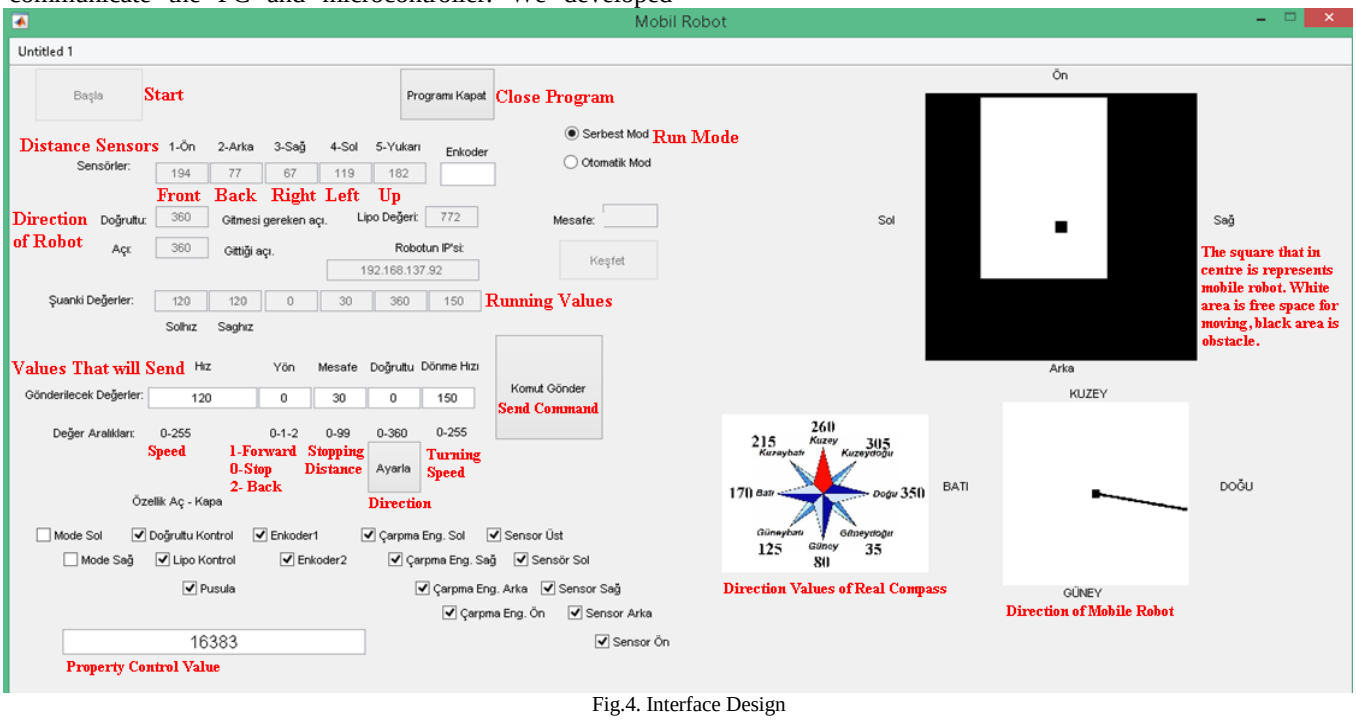

Fig.4. Interface Design

III. PROBLEM DEFINITION

In this section, we descried the problem definition by giving an example at first. Then, we will present details of the methods that we proposed for this study in the following sections. While the mobile robot autonomously moves through the environment, there would be some error measurement caused by the floor, wheel encoders and sensors. These error leads to directional and positional deviations of the robot. In this study, our goal is to estimate these errors at first and then develop a method to fix these undesirable errors. In order to clarify the problem, we consider the scenario shown in Figure 5. As shown from the figure, robot starts its movement at the instant of t_0 and intends to move through the line. After a while robot moving in a forward direction, there is a directional deviation from the path at the instant of t_1 due to the external errors. Our first goal is to estimate the directional deviation and fix it as fast as possible. Then, at time t_2, although the directional deviation is fixed, the position of the deviation cannot be fixed as shown from the Figure 5. This is because the sensors and encoders is not enough to compensate the velocity of the motors. On the other hand, it is important to protect robots direction and position for achieving autonomous motion.

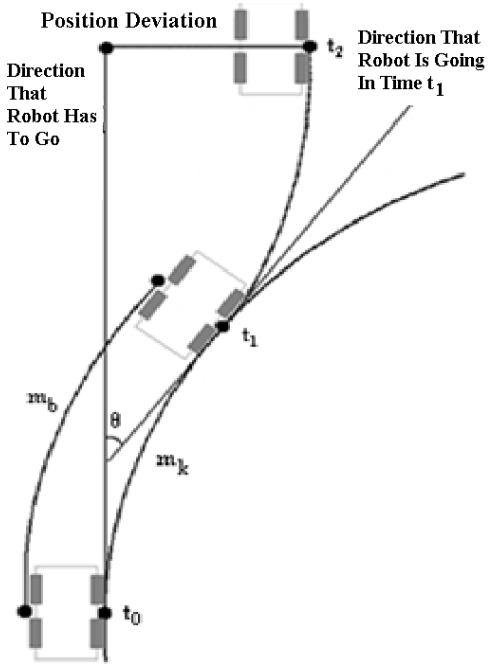

Fig.5. Direction and Position Deviation

IV. METHOD

We propose two different methods to fix the directional and positional deviations while the robots move autonomously

in the indoor environment. Before representing the algorithms to fix these deviations, we first describe how to estimate the error caused by the sensors, mechanical components and environment factors.

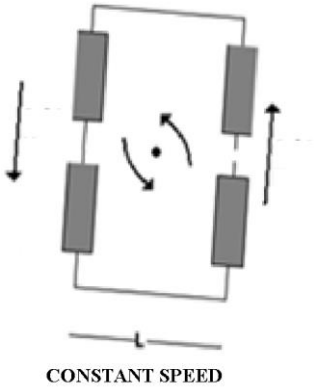

Fig.6. Mobile Robot's initial state without moving

We assume that robot moves at a constant speed to the line in forward direction as shown in Figure-6. The rotational angle of the motors on the robot obtained from the encoder is vertically placed behind to each motors. The rotational angle is theoretically calculated by the following equation

$$\theta = \frac{m \times 360}{\pi \times L} \quad (1)$$

where m is the distance of wheel's movement, L is the width of mobile robot, θ is rotation degree around the z axis.

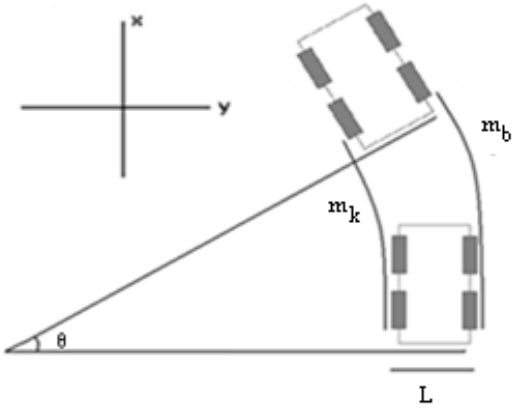

Fig.7. Rotation while the robot is moving in the forward direction

After the robot just starts to move in a trajectory shown in Figure -7, the rotational angle of the motor on the wheel is calculate by,

$$\theta = \frac{(m_b - m_k) \times 180}{\pi \times L} \quad (2)$$

where m_b and m_k is the distance of the inner and outer of the front wheel respectively. The equation (2) is recalculated as follows,

$$(m_b - m_k) = \frac{\theta \times \pi \times L}{180} \quad (3)$$

The positional deviation along x-y axis is estimated by the following equation,

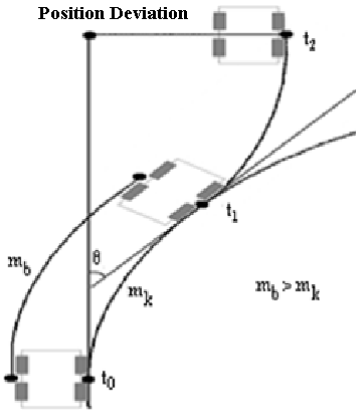

Fig.8. Fixing the deviation of direction

$$KF_y = \frac{[(m_k \times 360) + (L \times \pi \times A)]}{2 \times \pi \times \theta} \times (1 - \cos\theta) \quad (4)$$

$$KF_x = \frac{[(m_k \times 360) + (L \times \pi \times \theta)]}{2 \times \pi \times \theta} \times \sin\theta \quad (5)$$

where KF_x and KF_y is the amount of positional deviation along x- axis and y- axis respectively.

The first method that we propose is aimed to detect and estimate the directional deviation. Digital compass is used to measure the directional deviations of robots while moving in forward directions. Figure-8 shows the directional deviations robot at the instant of time t_1. The velocity of the motors on the wheels at different time step is calculated by the following equations,

$$\begin{matrix} V_k = V_k & t = t_0 \\ V_k = V_k + V_{fark} & t = t_1, t_2 \end{matrix} \quad (6)$$

$$\begin{matrix} V_b = V_b & t = t_0, t_2 \\ V_b = V_b - V_{fark} & t = t_1 \end{matrix} \quad (7)$$

where V_k and V_b is the velocity of the left and right of the wheel. V_{fark} is the difference velocity that is calculated by the equation represented as,

$$V_{fark} = V_k * (\frac{m_b}{m_k} - 1) \quad (8)$$

The second method that we propose is to fix the positional deviation. We assume that positional deviation consist of four stages at different time step shown in Figure-9. The directional deviation initially is estimated and fixed at t_1 and t_2. The velocity of the wheels at all-time step is calculated by the following equation,

$$\begin{matrix} V_k = V_k & t = t_0, t_3 \\ V_k = V_k + V_{fark} & t = t_1, t_2, t_4 \end{matrix} \quad (9)$$

$$\begin{matrix} V_b = V_b & t = t_0, t_3, t_4 \\ V_b = V_b - V_{fark} & t = t_1, t_2 \end{matrix} \quad (10)$$

The positional deviation is fixed by setting the inversion velocity of the both left and right front wheels at t_3 and t_4 time. Algorithm-1 represents how to protect the positional deviations.

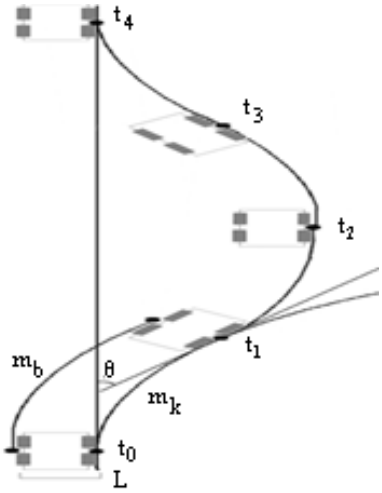

Fig.9. Fixing the Direction and Location Deviation

Algoritm-1: Protection of Position Deviation

```
WHILE (true)
   speed=readcommand("speed");
   rightspeed= speed;
   leftspeed= speed;
   k_ direction = readcommand ("direction");
   g_ direction = control_direction();
   IF(k_ direction!= g_ direction & section == 0)
      section =1;
   END IF
   IF (section!= 0)
      rightspeed =calculate_ rightspeed (section);
      leftspeed = calculate_ leftspeed (section);
   END IF
   move(leftspeed, rightspeed);
END WHILE
```

V. EXPERIMENTAL RESULTS

The proposed methods are tested on real mobile robot which has four motors, digital compass, sonar sensors. Our major goal is to test the proposed algorithms with real data. We observe that even if the robot moves to line at constant speed on the flat surface, the directional deviation is increasing over time. The reason is for this deviation is caused by the mechanical and electronic components on the robot. For instance, we put some weight on the robot to investigate how positional deviation will change during the motion. We observe that robot moves more stably under the heavy weights.

In order to show the performance of the algorithms, firstly the directional deviation is measured about 5 degree by using digital compass. The data is read every 0.6 seconds from the digital compass represented in Algorithm-1. When the mobile robot get out of the line, equation (9) and (10) is used to calculate the velocity of the motor that is being applied on motors for protecting the directions at t_1 shown in Figure-9. If there is not any direction deviation, the velocities of the motor will not be changed. Table -1 shows the values of the velocity of motors, directions of the motion and compass sensor information during the motions. The first column represents the time, second column KD represents command direction value, GD represents running direction value of mobile robot. Left and right are the motor's velocity, DH is angular velocity. The velocity of the right and left front wheel are set to 120 cm/s and 136 cm/s at the instant of t_4. Figure-10 shows the angular velocity values at different time step. Figure-11 illustrates the total trajectory of robot from t_0 to t_4.

TABLE I

Directions and Velocity Logs

Time	KD	GD		Left (cm/sn)	Right (cm/sn)	DH
12:41:21.238	174	174	t_0	120	120	150
12:41:21.563	174	174		120	120	150
12:41:21.874	174	174		120	120	150
12:41:22.186	174	178	t_1	104	136	150
12:41:22.488	174	174	t_2	104	136	150
12:41:22.813	174	174		104	136	150
12:41:23.749	174	170	t_3	120	120	150
12:41:24.055	174	170		120	120	150
12:41:24.365	174	174	t_4	120	136	150
12:41:24.680	174	174		120	136	150
12:41:24.994	174	174		120	136	150

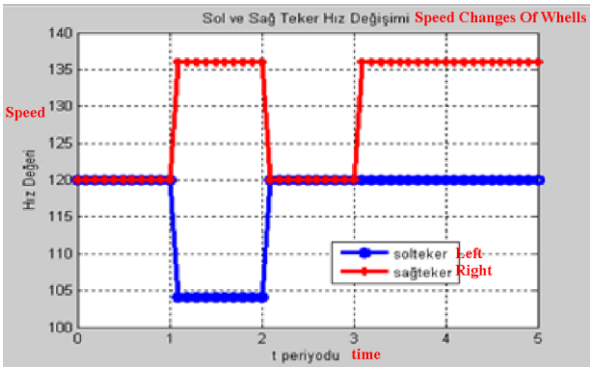

Fig.10. Velocity change of right (red) and left (blue) front wheels at different time step

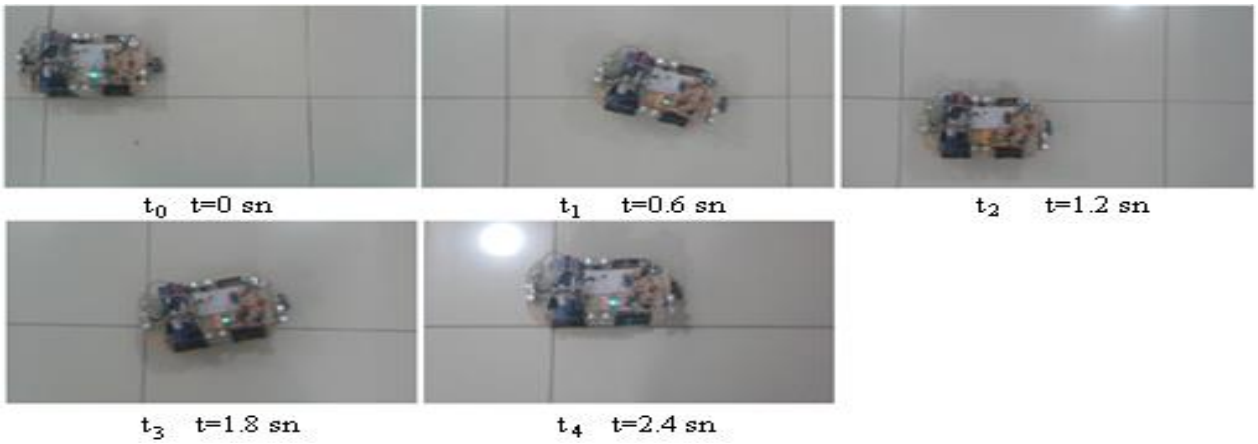

Fig.11. The figure shows the forward direction of the robot's movement at different time step. The deviation in the direction is formed at t=0.6 seconds, then robot fixed its direction at t=1.2 seconds. Robot starts to move to fix its the location about t=1.8 seconds and achieve to fix both location and direction at t=2.4 seconds.

VI. CONCLUSION AND DISCUSSION

In this study, we present a ruled based method to estimate and fix the positional and directional deviations of mobile robot while moving autonomously indoor environment. At first, we described the mechanical and electronic design process of the mobile robot. Digital compass is used to measure the directional deviations. We observe that digital compass is not enough to accurately measure the directional deviation in real time application. There is another important result of the experiment is that robots cannot achieve simple task due to error caused by the mechanical and electronic components. The proposed ruled based method is sufficient in some cases when the floor is flat and the velocity of the motors should be low enough to measure the sensor values. As a future work, we are planning to implement the mapping algorithms on the robot while it's moving in the environment autonomously.

VII. THANKS

This study is supported by TUBITAK 2209-A Supporting Program for Country-House Research Projects.

ACKNOWLEDGMENT

The study is selected from National Engineering Research Symposium 2015 (Ulusal Mühendislik Araştırmaları Sempozyumu) UMAS 2015 (Duzce University).

REFERENCES

[1] Brooks, Rodney A. "A robust layered control system for a mobile robot."Robotics and Automation, IEEE Journal of 2.1 (1986): 14-23.
[2] Nagatani, Keiji, et al. "Redesign of rescue mobile robot Quince." Safety, 2011 IEEE International Symposium on. I Security, and Rescue Robotics (SSRR), 2011.
[3] Dulimart, Hansye S., and Anil K. Jain. "Mobile robot localization in indoor environment." Pattern Recognition 30.1 (1997): 99-111.
[4] Durrant-Whyte, Hugh, and Tim Bailey. "Simultaneous localization and mapping: part I." Robotics & Automation Magazine, IEEE 13.2 (2006): 99-110.
[5] Turgut, Ali E., et al. "Kobot: A mobile robot designed specifically for swarm robotics research." Middle East Technical University, Ankara, Turkey, Metu-Ceng-Tr Tech. Rep 5 (2007): 2007.
[6] Özen, Seçil, Ekin Yıldız, And Tuncay Uzun. "Bilgisayar Kontrollü Gezgin Robot Uygulaması." 2000.
[7] Thrun, Sebastian, et al. "Robust Monte Carlo localization for mobile robots."Artificial intelligence 128.1 (2001): 99-141.
[8] Allard, James R. "Method and system for remote control of mobile robot." U.S. Patent No. 6,535,793. 18 Mar. 2003.
[9] Winfield, Alan FT, and O. E. Holland. "The application of wireless local area network technology to the control of mobile robots." Microprocessors and Microsystems 23.10 (2000): 597-607.
[10] J.E.F. Baruch and M.J. Cox, Remote control and robots: an Internet solution, Computing & Control Engineering Journal, Volume 7, Issue 1, 1996, pp.39 – 45
[11] T. Mirfakhrai and S. Payandeh, "A delay prediction approach for teleoperation over the Internet," Proc. IEEE Int. Conf. Robotics and Automation, vol. 2, 2002, pp.2178–2183.
[12] Peter Xiaoping Liu, Meng, M.Q.-H., Yang, S.X., Chao Hu, Jie Sheng, Internet-based remote control by using adaline neural networks, IEEE International Symposium on Intelligent Control, 2003, pp.252 – 257
[13] E. Bekiroglu and N. Daldal, "Remote control of an ultrasonic motor by using a GSM mobile phone," Elsevier, Sensors Actuators A Phys., vol. 120, no. 2, pp. 536–542, May 2005.
[14] Kehoe, Ben, et al. "A survey of research on cloud robotics and automation." Automation Science and Engineering, IEEE Transactions on 12.2 (2015): 398-409.

BIOGRAPHIES

Emrah ŞİMŞEK received B.Sc degree in Computer Engineering from Ataturk University in 2015. He is now M.Sc student in the same department of Ataturk University. His research area includes mobile robotic and machine learning.

Gulsah TUMUKLU OZYER received the B.Sc. degree in Computer Engineering at Erciyes University in 2001. She obtained Integrated M.Sc & Ph.D degree in Computer Engineering at Middle East Technical University in 2012. In 2007, she was a visitor researcher at Penn State University under supervised by Prof. Dr. James Wang for one year. She is now working as an Assistant Professor in Computer Engineering Department at Ataturk University. Her research interests are broadly in computer vision, pattern recognition and machine learning.

Baris OZYER He received the B.Sc. and Integrated M.Sc & Ph.D degrees in all Electrical and Electronics Department at Erciyes University in 2002 and Middle East Technical University in 2012, respectively. He spent one year as an intern in Computational Neuroscience Laboratory (CNS) under Advanced Telecommunication Research Institute (ATR) in Japan. He is currently Assistant Professor in Computer Engineering Department at Ataturk University. His research interest includes robotics, grasping, biologically inspired robotics and control theory.

Tire-Road Friction Coefficient Estimation and Experimental Setup Design of Electric Vehicle

C.Elmas, U.Güvenç, and M.U.Doğan

***Abstract*—Nowadays, electric vehicles have become an important area because of air pollution, increasing use of renewable energy sources and being exhausted of oil fuels. In our country even the usage of electrical vehicles is not widespread nowadays, but also very popular and it is thought that it will increase. In this area, new studies and projects appear continuously Real systems are moving systems and it is difficult and expensive to evaluate by electrical vehicles; therefore an experiment mechanism has been created. In this study two fixed magnet synchronous hub motors have been used as wheels and the other one as load. In order to find the speed of the wheel, load value and coefficient of friction related to sliding, Burckhardt model has been used and the results obtained with different speed and road conditions have been presented here.**

***Index Terms*— HUB Motor, Electric vehicles, Burckhardt model, Slip Ratio, Friction Coefficient**

I. INTRODUCTION

NOWADAYS, productivity and saving of energy subjects have become very important because of pollution, decreasing amount of petroleum and energy problems. Natural gas, water and oil are very important energy resources. If we consider our lands geographically, water is our most important energy resources. However, it is a fact that the earth is balance has been damaged because of global warming and if precautions have not been take earth will face to face with drought [1]. The most important problem is that oil is not an external energy resource and it will be exhausted in a short time [2]. The idea of moving reliable, effective and environment-friendly electrical energy vehicles with electrical motors can be thought as the starting point of electrical vehicles [3].

In the history, Improving first electrical vehicles have started in 1835 and electrical railway has been produced in 1835 and electrical railway has been produced in 1835. Lead acid batteries have been improved in 1859 and then their usage at the electrical vehicles have been become an important transition point [4].

C. Elmas, Electrical-Electronic Engineering Department, Technology Faculty, Gazi University, P.O. Box 06200, Ankara, Turkey, (e-mail: cetinelmas@hotmail.com).

U. Güvenç, Electrical-Electronic Engineering Department Chair, Technology Faculty, Düzce University, P.O. Box 81000, Düzce, Turkey, (e-mail: ugurguvenc@duzce.edu.tr).

M.U. Doğan, Electronic and Automation Department, Bolu Vocational High School, Abant İzzet Baysal. University P.O. Box 14200, Bolu, Turkey, (e-mail: muhdogan@yahoo.com)

Worries about pollution and oil prices have caused the automotive industry is improving electrical vehicles rapidly.

The structure of electrical vehicle is composed of inverter circuit which has been made up for power switching components, batteries group as energy storage part, control systems and mechanic power transmission system. Electrical vehicles have made advantages than classical cars, with internal-combustion engines because of not producing waste gases and not using motor oils, being environment friendly, not needing gearbox, winning back the energy at the time of braking and running silently. However, electrical vehicle cannot take place of a gasoline car because of having heavy, bulky car batteries, limited capacities, long time of filling and having bad proportions of power-weight and power/volume of electrical motors. Also control of electrical vehicles is a very important point of security. A complete modelling should be made for a wide control. Possible conditions should be taken into consideration. In this study, an experiment mechanism consisting by two hub motors has been designed in order to model electrical vehicles. One of the hub motors used at the mechanism has been chosen a wheel of the vehicle and the other one as the load. Because the road load, which has been applied according to the road conditions, has changed, in order to find wheel speed and load value, Burckhardt Model [5] has been used for using the motors at the experimental mechanism, results reference values of the different speed and road condition have been shown.

II. HUB MOTORS

Hub motors are electrical motors assembled at the central of wheel of the vehicle and they can revolve the wheel directly. These motors have took place at the electrical bicycles, ATV's and electrical vehicles mostly. Four wheels driving by an electrical motor is a widely used method at the hybrid vehicles. However, four wheels driving by an electrical motor has caused some advantages and disadvantages. The most important advantage is increasing of energy productivity. There should be a lot of power train in order to transfer kinetic energy to the wheels by a central motor, on the other hand, wheel motors provides to avoid losses created by this power train. Because it is not necessary to have differential gear, drive shafts, provides decreasing of vehicle weight. Also having control of each motors independently provides the usage of algorithms easily as traction control system. On the other hand, because of motors fitted in the wheel causes increasing of weight of wheel, convenience of driving can be decreased. In such motors, wheel shaft is directly linked to the motor.

Because of there is not a physical mediator at the time of power transfer, productivity is high at this motors. The stable windings in the motor create a specific electromagnetic field. Wheel shaft starts to turn with the effect of this electromagnetic field [6]. Electric motors have their greatest torque at startup, making them ideal for vehicles as they need the most torque at startup too.

Hub motor electromagnetic fields are supplied to the stationary windings of the motor. The outer part of the motor follows, or tries to follow, those fields, turning the attached wheel. In a brushed motor, energy is transferred by brushes contacting the rotating shaft of the motor. Energy is transferred in a brushless motor electronically, eliminating physical contact between stationary and moving parts. Although brushless motor technology is more expensive, most are more efficient and longer-lasting than brushed motor systems.

Hub motor are typically brushless motors (sometimes called brushless direct current motors or BLDC), which replace the commutator and brushes with half-a-dozen or more separate coils and an electronic circuit. The circuit switches the power on and off in the coils in turn creating forces in each one that make the motor spin. Since the brushes press against the axle of a normal motor, they introduce friction, slow it down, make a certain amount of noise, and waste energy. That's why brushless motors are often more efficient, especially at low speeds

The outer-rotation hub motor systems are type of motors that have capacity of producing high torque at the low speed space. Because the machine torque changed directly proportional according to the machine's diameter's square, need of high moment can be overcome by using high diameter. Permanent- magnet synchronous hub motor that we used at the system has 48V and the motors can produce 1kW of power.

III. TRACTION CONTROL OF ELECTRICAL VEHICLES

The most important and disadvantageous side of mechanic differential gear which take part at the cars using daily life is surely that when one of the wheels cannot hold the road and a result skidding and cannot transfer power to the other wheel. At the two motor vehicles, subject of this study, one of the wheel can produce power independently from the other one. So, one of the wheels has been on the ice or snow surface, doesn't obstruct the vehicle's moving. At the motors which are used, torque control can be done by current control [7].

Antislip control and slip ratio control in an electric vehicle have the benefit of improving the driving stability of a vehicle on a low road. However, problems arise in coordination with the accelerator, including difficulty in switching between traction control and torque control with the accelerator without creating abrupt changes in the driving force, and the inability to obtain an arbitrary driving torque even though a large driving force can be obtained by slip ratio control [8,9].

Maximum value of torque applied on the wheels at the low friction surfaces is not related to the power of motor but related to holding of the wheel to the surface. The main two factors are total vehicle weight of each wheel and friction coefficient of between the surface and the wheel [10, 11, 12, 13].

In order to create a force of wheel at the surface of the road and the moving direction, it should a bit slip. According to this, a wheel transferor and drive effort, it turns more than the needs of the road that go through. Similarly, it will turn less than the needs of the road that go through. Friction torque is connected to the condition of the wheel and the road as well as the load amount and drive force. In order to move of the vehicle, the power produced by motor should overcome the amount of road load. In a vehicle, Slip ratio is the proportion of the difference between the velocity of wheel and the actual velocity of vehicle to the velocity of wheel [14, 15].

The wheel slip ratio, which is defined as

$$s = \frac{\omega . r - V_X}{\omega . r}, \qquad \text{for driving} \tag{1}$$

$$s = \frac{V_X - \omega . r}{V_X}, \qquad \text{for braking} \tag{2}$$

where r is the wheel radius, ω is the wheel angular velocity, V_X is the actual velocity of vehicle.

As shown in Figure 1, a tire-road longitudinal friction coefficient μ is defined through the ratio between the traction force and the normal force.

$$\mu = \frac{F_x}{F_n} \tag{3}$$

$$F_x = \mu F_n \tag{4}$$

where F_x is the traction force and F_n is the the normal force as shown in figure 1, wheel model of a vehicle has been shown. This friction coefficient depends on various factors, including the type of tire, the tire air pressure, the road condition, the normal forces [16]. In several works, the friction coefficient is modeled through semi-empirical formulas, which reproduce the steady-state wheel behavior. Usually, vehicles travel through variable road conditions; therefore, the results of empirical formulas may not represent the physical model with sufficient fidelity [16,17].

In traction control, it is necessary to consider the dynamic behavior of the friction coefficient to control the traction forces with a dynamic response that is fast enough to avoid the loss of traction (skidding). Wheel model of a vehicle is shown in Figure 2.

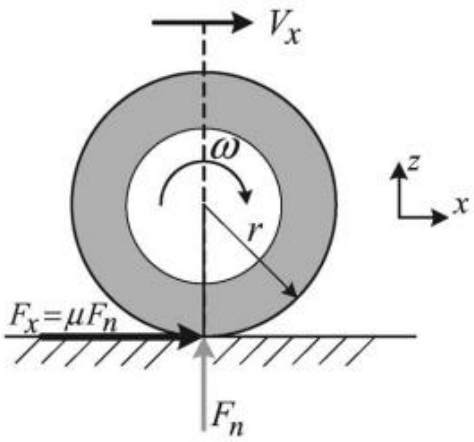

Fig.1. One wheel model of a vehicle

This friction coefficient depends on various factors, including the type of tire, the tire air pressure, the road condition, the normal forces.

In order to calculate the force of the wheel transferred at the road, a tire model has been used. At the input of this model, normal force of the tire, torque of the axle shaft and vehicle speed have been found, at the output, angular speed of the tire, torque and force applied on the road can be found. In order to calculate the force of the tires applied on the road, tires model is being used. Mostly used type models Magic Formula [18], Burckhardt models are used at modelling of tires. In this paper the Burckhardt model [5,19] will be used, as it is particularly suitable for analytical purpose while retaining a good degree of accuracy in the description of the friction coefficient.

Based on Burckhardt model, the velocity dependent braking effort coefficient between the tire and the road has the following form

$$\mu\,(s,v) = \left[C_1\,\left(1 - e^{-C_2 s}\right) - C_3\,s\right]e^{-C_4 s v} \qquad (4)$$

Where C_1 is the maximum value of friction curve; C_2 is the friction curve shape; C_3 is the friction curve difference between the maximum value and the value at $\lambda = 1$; and C_4 is wetness characteristic value. By changing the values of parameters C_1–C_4, many different tire-road friction conditions can be modeled. The parameters for different road surfaces are listed in Table 1

TABLE I
TIRE-ROAD FRICTION PARAMETERS.

Surface Conditions	C_1	C_2	C_3	C_4
Dry asphalt	1.029	17.16	0.523	0.03
Dry concrete	1.197	25.168	0.5373	0.03
Snow	0.1946	94.129	0.0646	0.03
Ice	0.05	306.39	0	0.03

IV. EXPERIMENTAL SETUP DESIGN AND RESULTS

In the systems, as the main metal is low carbonic structure steel at the quality of St 37.2, strap and two hub motors have been used. An experiment mechanism has been completed in order to transfer simulation works done at the computer environment to the practice. Longitudinal force of the tire applied on the road has been accepted as load. There are two hub motors at the experiment mechanism. Secondary hub motor will be used for load. Driving system of hub motor has been formed by inverter, digital signal processing and position sensor. According to the information of rotor position knowledge of location position, digital signal processing determines the phase for giving energy and switching are done. For stable torque production, these processes should be completed at the same time with the rotor position. Because real systems are moving systems and it is difficult and expensive to complete measurements at the electrical vehicles, experiment mechanism has been created for modelling electrical vehicles. Experimental setup is illustrated in Figure 2.

Fig 2. Experimental Setup

In this study, graphics of the friction coefficient and slip ratio as depend on vehicle speed is shown following. When speed increases friction coefficient connected with slip ratio decreases. This simulation was conducted on four road surface states dry asphalt (green), dry concrete (blue), snow (red), ice (turquois). In Figure 3, the shapes of slip ratio-friction coefficient for four different road conditions with a vehicle speed of 10 m/s are illustrated.

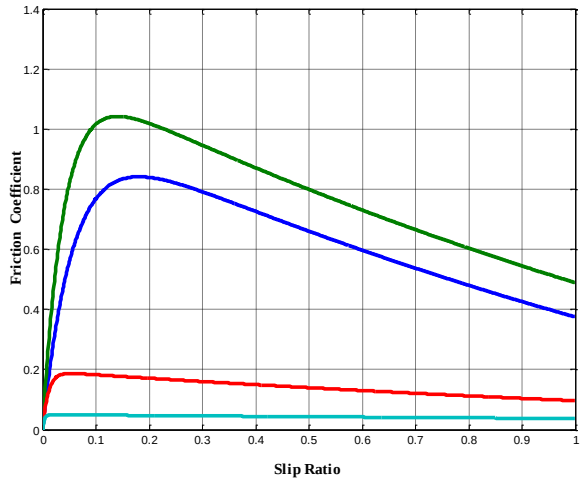

Fig 3. Slip ratio -friction coefficient graphics for different road conditions with a vehicle speed of 10 m/s

In Figure 4, the shapes of slip ratio-friction coefficient for four different road conditions with a vehicle velocity of 30 m/s are illustrated.

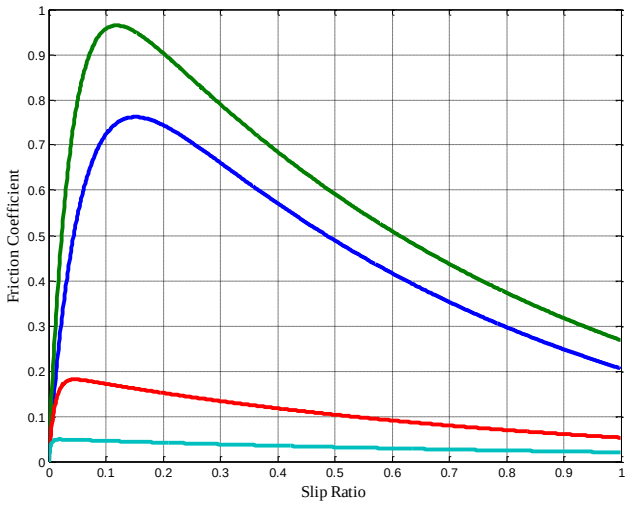

Fig 4. Slip ratio-friction coefficient graphics for different road conditions with a vehicle velocity of 30 m/s

At the Figure 3 and Figure 4, Slip ratio-friction coefficients for different road conditions, at the speed of 10 m/s and 30 m/s, by using Burckhardt model have been displayed. As speed and slip ratio increases, friction coefficient decreases. When a tire is locked, the braking effort coefficient falls to its sliding value. As a result, the vehicle will lose directional control and stability.

Slip ratio has been given as the shape of trapeze and change of wheel speed has been illustrated in Figure 5.

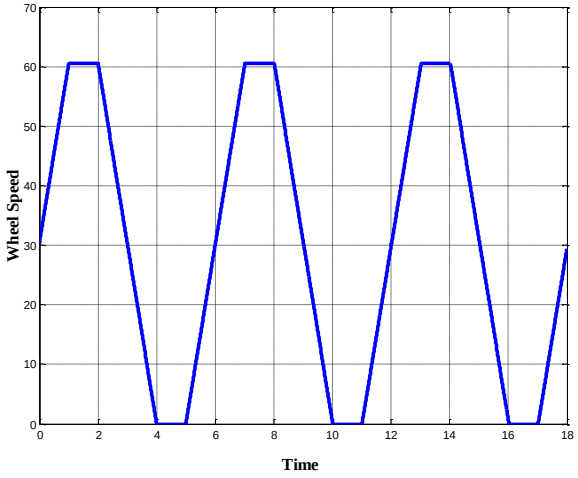

Fig 5 Angular speed of the wheel graphics when slip in the shape of trapeze with vehicle speed of 10 m/s

Slip ratio has been given as the shape of trapeze and change of wheel speed has been illustrated in Figure 6.

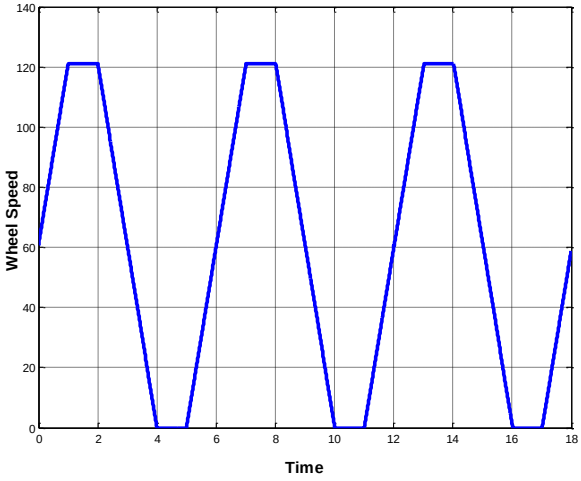

Fig 6. Angular speed of the wheel graphics when slip in the shape of trapeze with vehicle speed of 20 m/s

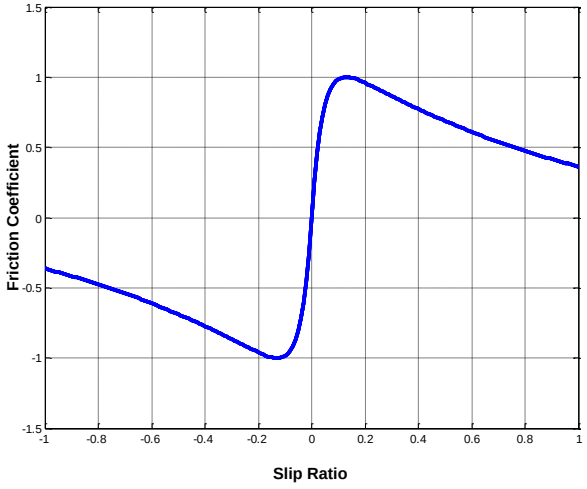

Fig 7. Friction coefficient- Slip Ratio Curve of vehicle speed 10 m/s

The model between the friction coefficient μ and slip ratio at the vehicle speed of 10 m/s is shown in Figure 7.

At figure 8 and figure 9, Slip has been given in the shape of trapeze and connected to the vehicle speed, wheel speed curves have been shown. Wheel speed was estimated using the slip chances between -1 to 1.

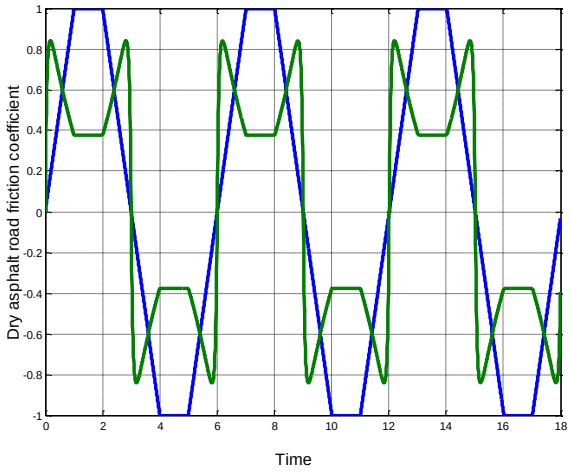

Fig 8. Dry asphalt road's coefficient of friction graphics when slip in the shape of trapeze at vehicle velocity of 10 m/s

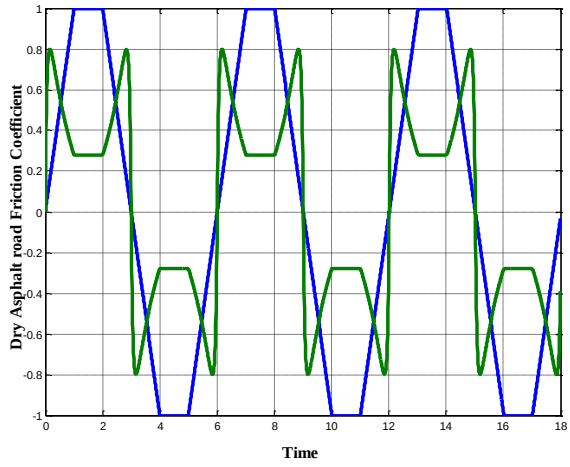

Fig 9. Dry asphalt road's coefficient of friction graphics when slip in the shape of trapeze at vehicle velocity of 20 m/s

At figure 8 and figure 9, when slip changes between -1 and 1, in the shape of trapeze, at the dry asphalt road, speed of 10 m/s and 20 m/s, friction coefficients have been shown. This effects longitudinal force of wheel and as a result it effects load force.

At the figure 10, when slip ratio changes in the shape of trapeze under different road conditions (dry asphalt, dry concrete, snow and ice).

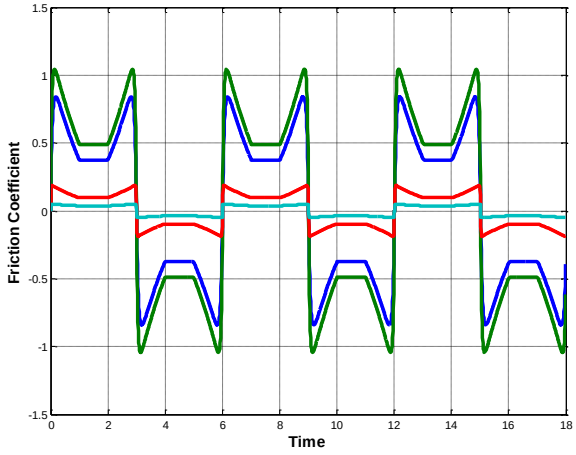

Fig 10. Friction coefficient graphics for different road conditions of vehicle velocity of 10 m/s

Simulation study of friction coefficients has been shown. The highest and the best result friction coefficient is dry asphalt and the lowest one is icy road.

V. CONCLUSIONS AND DISCUSSION

Because the real systems are moving systems and it is difficult and expensive to complete measurements, an experiment mechanism has been created. Speed of hub motor used at the electrical vehicles, connected to slip has been calculated using simulation study with *C* language.

There are also different vehicle traction systems; it is thought that directly tire drive systems will be used widespread in the future. By controlling each tire hub motors independently, breakdown of any motor can be prevented, so reliability of the vehicle's drive systems increases.

Because of increasing amount of pollution and decreasing amount of oil reserves, study of electrical vehicles should be speed up. In order to produce cheaper driving systems of electrical vehicles, control systems, projects should be started about equipment's of electrical vehicles. By modelling the precious studies, more productive, lighter, more intelligent and cheaper components should be produced. Technical staff should be raised about power electronics and design of electronics circuit. It is not impossible to produce this technology be encouragement of the state, progress of the industrials and common projects groups of the universities.

VI. ACKNOWLEDGMENTS

This paper was supported by Abant İzzet Baysal University Engineering Faculty Research and Development Laboratory and Duzce University Scientific Resarch Project Coordination.

The study is selected from National Engineering Research Symposium 2015 (Ulusal Mühendislik Araştırmaları Sempozyumu) UMAS 2015 (Duzce University).

REFERENCES

[1] Emadi, M. Ehsani, and J. M. Miller, Vehicular Electric Power Systems: Land, Sea, Air, and Space Vehicles, New York: Marcel Dekker, December, 2000.

[2] A. Emadi, S.S. Williamson, A. Khaligh, "Power electronics intensive solutions for advanced electric, hybrid electric, and fuelcell vehicular power systems", IEEE Transaction on PowerElectronics ,Vol. 21, Issue 3, May Page(s):567- 577 2006.

[3] Koca, Özmen, G., and Akpolat. Z. H., "Bulanık Mantık ve Erişim Kuralı Yaklaşımını Kullanarak Bir Elektrikli Aracın Dayanıklı Hız Denetimi." Gazi Üniversitesi Politeknik Dergisi, 9(2): 93-103, 2006.

[4] Kerem, A., "Elektrikli Araç Teknolojisinin Gelişimi ve Gelecek Beklentileri." Mehmet Akif Ersoy Üniversitesi Fen Bilimleri Enstitüsü Dergisi ,5 (1): 1-13, 2014.

[5] Burckhardt, M., Fahrwerktechnik: Radschlupf - Regelsystmeme Würzburg: Vegel Verlog, 1993.

[6] Bulgu A.E., " Tekerlek motorlu seri hibrit elektrikli araçlar için kontrol algoritmalarının geliştirilmesi" Yüksek Lisans Tezi, İTÜ Fen Bilimleri Enstitüsü, İstanbul, Türkiye, 2010.

[7] D.Azmi.,"Elektrikli Otomobiller ve Patinaj Engellenmiş bir doğrudan sürüşlü elektrikli otomobil tahrik sistemi." İstanbul Üniversitesi Mühendislik Fakültesi Journal of Elektrical & Electronics, Volume 2, Number 1-383-393, 2002.

[8] M. Yoshımura, H.Fujımoto, "Driving Torque Control Method for Electric Vehicle with In-Wheel Motors", Electrical Engineering in Japan, Vol. 181, No. 3, 2012.

[9] D.O.S.Yin, Y.Hori "A novel traction control for EV based on maximum transmissible torque estimation", IEEE Trans Industrial Electronics n;56(6), 2009.

[10] Z. Rahman., K.L.Butler, M.Ehsani "Effect of Extended-Speed, Constant- Power Operation of Electric Drives on the Design and Performance of EV-HEV Propulsion System", SAE,2000-01-1557, (2000).

[11] Rahman Z., Ehsani M., Butler K.L., (2000) "An Investigation of Electric Motor Drive Characteristics for EV and HEV Propulsion Systems" SAE 2000-01-3062.

[12] Husaın I., Islam M.S., (1999) "Design, Modeling and Simulation of an Electric Vehicle System", SAE 1999-01-1149.

[13] Çınar M.A., Gündoğan Ç., Erfan Kuyumcu F., "Elektrik Tahrikli Taşıtlar için Çekiş Kontrol Sistemi Simülasyonu", ELECO'2004 Elektrik-Elektronik-Bilgisayar Mühendisliği Kongresi, 296-300,2004.

[14] T. Gillespie, Fundamentals of Vehicle Dynamics. SAE – Society of Automotive Engineers, 1992.

[15] Sakai, S.; Sado, H.; Hori, Y. Anti-skid control with motor in electric vehicle. In Proceedings of the 6th International Workshop on Advanced Motion Control, Nagoya, Japan, 30 March–1 April pp. 317–322,2000.

[16] G. A. Magallan, C. H. De Angelo, and G. O. Garcia, "Maximization of the traction forces in a 2WD electric vehicle," IEEE Transactions on Vehicular Technology, vol. 60, no. 2, pp. 369–380, 2011.

[17] C. Canudas-de Wit, P. Tsiotras, E. Velenis, M. Basset, and G. Gissinger, "Dynamic friction models for road/tire longitudinal interaction,"Veh. Syst. Dyn., vol. 39, no. 3, pp. 189–226, Mar. 2003.

[18] Pacejka, H.B.; Bakker, E. The magic formula tyre model. Vehicle. Syst. Dyn. Int. J. Veh. Mech. Mobil. 1993, 21, 1–18.

[19] Oudghiri, M.; Chadli, M.; Hajjaji, A.E. Robust fuzzy sliding mode control for antilock braking system. Int. J. Sci. Tech. Autm. Control, 1, 13–28,2007.

BIOGRAPHIES

Cetin ELMAS was born in Bursa in Turkey. He received the B.S. degree in electrical and electronics education and the M.Sc. degree in electrical education from Gazi University, Ankara, Turkey, in 1986 and 1989, respectively, and the Ph.D. degree in electronic and electrical engineering from the University of Birmingham, U.K., in1993. From 1987 to 1989, he was a research assistant with Gazi University, Faculty of Technical Education Assistant with Gazi University, From 1994 to 1995, he was an assistant professor. He is currently a full professor and the head of the department of electrical machinery. His research interests include power electronics, electrical machines and drivers intelligent control, digital signal processing, and engineering technology education.

Ugur GUVENC was born in Zile in Turkey. He received the B.Sc. degree in electrical education from Abant İzzet Baysal University, Bolu, Turkey in 2002, M.Sc. degree from Gazi University, Turkey in 2005 and the Ph.D. degree from Gazi University, Turkey in 2008. He is currently an Assistance Professor in the Department of Electrical Education, Faculty of Technical Education, Düzce University, Turkey. His main interests are in artificial intelligent, power system and image processing.

Muhsin Uğur DOĞAN was born in Bolu, Turkey . He received his B.Sc. degree in Electronic Engineering from the Erciyes University in Kayseri, in 2002. He received his Master Degree in Electrical-Electronical engineering from the Zonguldak Karaeelmas University. He works at Abant Izzet Baysal University, Vocational High School, Department of Electronics and Automation. His main interests are in control systems, electric vehicle, electrical machines and driver.

Importance of Solar Lighting Systems in Terms of Environmental Pollution

Y. Oğuz, M. Şahin, E. Şahin and Y. Güven

***Abstract*—One of the alternatives to fossil fuels is the solar energy to produce electricity parallel with today's rapidly advancing technology. Solar energy is the most important and the cleanest energy source that it can be used in almost every field. Lighting systems come at the first of these areas. Almost %25 of produced electricity is being consumed for lighting in all over the world. Therefore, using alternative energy for lighting systems has become inevitable. For example, usage of alternative energy for lighting in the local parks, gardens and streets, long-distance highways and roads have become widespread quickly. Despite there is a transmission cost in addition to production cost in power plants, solar power systems have no transmission cost so usage of them are growing rapidly. However, it should be considered more seriously that component of solar power system must be chosen recyclable from production throughout operation. It is obvious that the usage of solar power system is inevitable when environmental effects of thermal power plant are being considered. Therefore usage of the solar energy should be expanded, especially in street, highway, park and garden lighting, traffic signals and remote area lighting system. Examples of these applications around the world should be encouraged to use in our country.**

In this sense, this study has provided information about solar lighting systems and their new technology. Furthermore, an example of the integration the solar energy within a city lighting system has been investigated.

***Index Terms*—Solar Energy, Solar Lighting, Environmental Pollution, Renewable Energy**

I. INTRODUCTION

IN recent years, renewable energy sources draw attention because of environmental impact of fossil fuels and their ongoing depletion day by day [1]. Sun is the most important energy source for our planet. Solar energy is an alternative to fossil fuels due to its clean and environmental friendly characteristic.

Y. Oğuz, Afyon Kocatepe University, Electrical and Electronics and Engineering, Afyon, Turkey, (e-mail: yukseloguz@aku.edu.tr).

M. Şahin, Erzincan University, Electrical and Electronics and Engineering, Erzincan, Turkey, (e-mail: mustafasahin@erzincan.edu.tr).

Y. Guven, Kirklareli University, Technical Science Vocational School, Kirklareli, Turkey, (e-mail: yilmaz.guven@klu.edu.tr).

The solar radiation energy falling on earth in a year is about 160 times more than the earth's fossil fuels potential determined so far [2]. In addition, it is 15000 times more than fossil, nuclear and hydroelectric energy combined which are being produced on earth every year. From this point of view, maintaining of the solar energy is not a problem. The real problem is to convert the solar energy into an energy type that can be used for human activities in most effective way [3]. Production of electrical energy is mostly utilising the burning of fossil fuels like coal. However, the burning of fossil fuels emerges carbon dioxide, ash and some other waste. These wastes have several adverse impacts for the environment. Photovoltaic cells are leading alternative energy production method with no polluting effect [4-5].

It is necessary to extend the usage of solar energy as an alternative energy source to meet the growing energy demand all over the world [6-7]. Turkey is fortunate in the sense of solar energy potential with its geographical location compared to many other countries. According to a study conducted by EIE, based on measurements of State Meteorology Affairs General Directorate between 1966 and 1982, it has been found that annual sunshine duration of Turkey is 2640 hours (7,2 hours daily) and average total radiation intensity is 1311 kWh per square meter in a year. [8]. Electrical energy derived from solar energy can run all systems which are being powered by main grid with the help of appropriate hardware. The aim of this study is to emphasize the importance of solar energy as an alternative to fossil fuels for lighting systems in terms of environmental pollution.

A. Integration of Lighting System and Solar Energy

The most important method to obtain electricity from solar energy is solar cells; they are also known as photovoltaic systems. It requires higher technology and more money to obtain electricity from solar energy. However, increasing environmental awareness has intensified efforts to use this method. Many studies have been occurred to produce electricity more efficiently with the invention of photovoltaic cells in 1959. Photovoltaic technology has made great progress in the past 50 years [9]. Systems that can provide electricity for 15000 homes were produced in 1990.

Photovoltaic cells are formed by combining two different semiconductor materials. These materials are usually made of silicone and they can generate electricity in each case of sun. So they can continue to generate electricity by emitting the radiation of sun in even cloudy weather. The most important features and advantages of photovoltaic cells are that they are reliable and they need little maintenance. They consist of four main parts as listed below.

Parts of the Photovoltaic system:

- Solar Panel: Consist of Mono-crystalline cells and it produces the electricity.
- Battery: The unit that stores the energy.
- Invertors: The part allows home appliances to use the electricity produced by solar panels.
- Regulator: The part that secures the system [9].

LED (Light Emitting Diode) is a semi-conductor, light emitting electronic circuit element. LEDs have low energy consumption, long life, durability, small size, quick response and many other advantage compare to traditional light sources. Cost of LED units is dwindling in parallel to the technological development so they can be used in lighting applications widely. It is observed that they are being used in tunnels, facades, sport area, industry as much as traditional street illumination. Integration of LEDs within new application in European countries has reached 50%-70% beyond the optimistic estimations [10].

According to the data provided by Ministry of Energy and Natural Resources in 2014, there are about 17 million street lamps in Turkey. This number has a 2.5% share of total consumed electricity and cost an annual amount of 288 million U.S. dollar. Again according to ministry's statistics, if these street lights replaced with LEDs, 75% saving would be achieve [11]. LEDs produce more light flux per watt than standard incandescent lamps produce. As we know the vast majority of energy used by standard bulbs is used as thermal effect. However, the thermal effect of the LEDs is greatly reduced and they have long uptime. Today, 3W power LEDs can produce 231 lm per watt theoretically. Different lamps used in photovoltaic lighting application are given in Table 1. The value of light in lumen per consumed watt shows the superiority of LEDs [10].

TABLE I
THE LAMPS USED IN PHOTOVOLTAIC LIGHTING APPLICATIONS

Lamp Types	Light per-watt (Lumen/Watt)
Tungsten lamps	6-10
Halogen lamps	16-22
Compact fluorescent lamps	30-60
Fluorescent lamps	46-95
Gas discharge lamps	55-125
LED lamps	60-132

Along with the raising environmental awareness, usage of solar powered for outdoor lighting systems is increasing while lighting systems are moving away from traditional methods. Solar lighting systems perform outstanding results for required parameters. They are also economic and efficient [12]. Solar panels are being used for these systems to produce individual electrical energy.

Solar street lighting systems have a wide range of application area. They are not only used in the street but also airports, harbours, docks, parks, gardens, road and highways. They are both environmental friendly and cost-effective. A solar street illumination system is composed of a solar panel, a group of batteries, a charge controller, sensors and lighting units (LED lamps). There might be a wind turbine additionally.

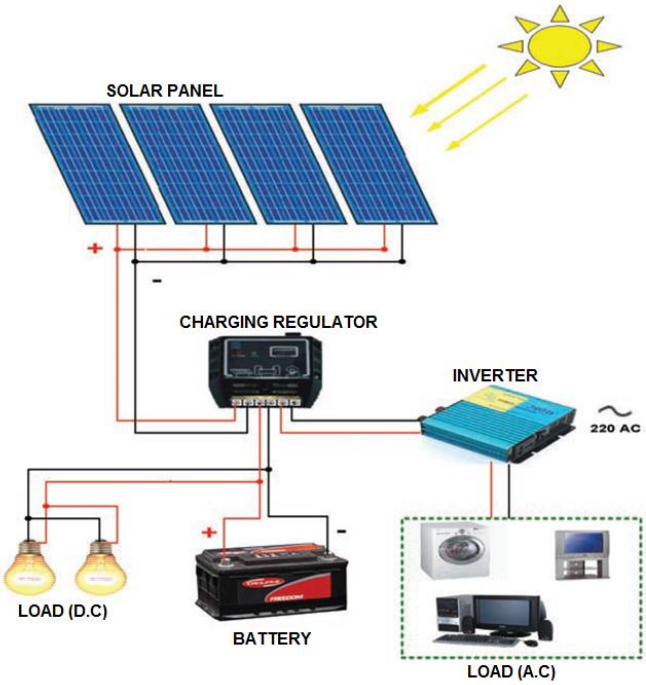

Fig 1. Basic parts of a solar street illumination system [13].

LED lighting armatures are optimized for thermal and photometric performance to achieve different illumination level. Thereby, the systems can be integrated to an automation system for different application and illumination levels. This can reduce the energy consumption between 50% and 80% [14]. All of these are the first and the most important step towards the concept of smart cities [15].

Typical applications that use Solar Lighting System are follows:

- Park and gardens,
- Urban streets and roads,
- Intercity highway and roads,
- Hotels, resorts and harbors,
- Ambient lighting of homes that is away from residential areas,
- Earthquakes and weather observation stations,
- Warning Systems and the traffic lamps,

can be listed as application area of the solar lighting systems [16]. The followings specify the advantages of solar lighting system with power-LED:

- It is environmental friendly, it has low heat and light pollution.
- It has long lifetime and low cost.
- It does not strain eyes with high density, brightness and contrast.
- Consumes 10 times less energy than standard lighting systems.
- It gets instant access to the actual brightness and it is efficient.
- It is maintenance-free and it has a plug-and-play capability.
- There is no need to wiring.
- It has zero carbon dioxide emissions.
- It has resistant to shocks and physical impacts.
- It does not generate electromagnetic waves or interference signals and it does not contain heavy metal within [17].

II. THEORETICAL GROUND

The aim of this study is to provide 1072 watts electrical energy for two laboratories from solar-wind hybrid power generation system in the climate condition of Afyonkarahisar. To achieve this, a hybrid power generation system, consisting of three 190W 24V mono-crystalline solar panels and 600W 3 phase permanent magnet synchronous generator (PMSG) that can rotate 360º according to the direction of the wind, have been established. At the same time, six of 100Ah 12V deep cycle gel batteries have been installed to store unused electric energy for continuity of renewable energy system. The general view of the solar-wind hybrid power generation system with battery support is shown in Figure 2. The charge control unit is regulating the produced electrical energy to recharge the batteries. The amount of generated energy is being recoded through charging control unit with the help of a computer in every 10 second. The stored energy is being converted to A.C. by 3kW sine wave inverter for supplying our loads [18].

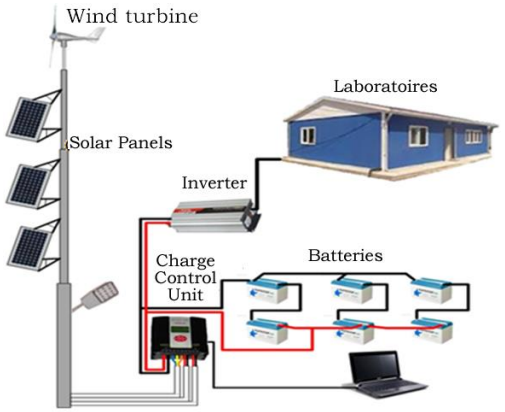

Fig 2. General view of the installed wind-solar hybrid power generation system [18]

Another important part of a hybrid power generation system is the charge controller. The low-voltage feature is enabled at 4V. That means, the systems goes on production when the wind turbine reaches the speed that can generate 4V if the batteries are below 28.2V. This feature allows the turbine to produce energy even at low wind speed. The charge control unit has two D.C. outputs. The first output enables or disables D.C. depending on the light intensity over solar panels. The second one does the same thing but it can be set up to be disabling at any desire time. These features prevent unnecessary energy consumption related to LED fixture on outdoor lighting.

This is necessary to know the general consumption of illumination system in these two laboratories based on their weakly course schedule to analyze the efficiency of hybrid power generation system. Then it can be found how much of the electrical energy that is being produced by the hybrid power generation system. According to the obtained data, energy saving rate can be determined when the hybrid power generation system is in use. When we look at the entire months' production and consumption data as shown in Figure 3, it has been seen that production of power is greater than the consumption except June. Due to failures that have occurred in the system, data could not be obtained within 15 days of June [18].

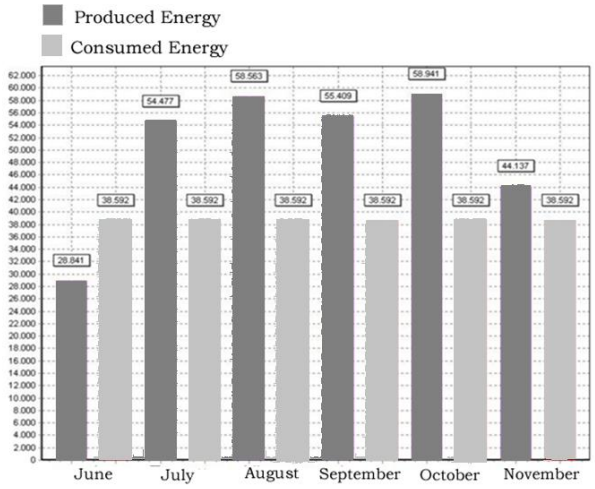

Fig 3. The total energy productions and consumptions by the months [18]

The difference between production and consumption can be determined by this comparison. The comparison in unit price which is $0.145 can be seen in Table 2. Calculations shows that the amount of consumed electricity for general illumination of laboratory was $33,42 for six months and the amount of produced electrical energy was $43,38. As it can be seen on Table 3, the production of the hybrid power generation system has met the electrical energy consumed by the general illumination system with $9,94 surplus.

TABLE II
THE AMOUNT OF ENERGY SAVING BY THE USE OF HYBRID POWER GENERATION SYSTEM [18]

Data / Months	Produced (kWh)	Consumed (kWh)	P-C (kWh)	Cost of Produced Energy ($)	Cost of Consumed Energy ($)	Production Cost ($)
June	28.84	38.592	- 9.75	4.16	5.57	- 1.40
July	54.47	38.592	15.88	7.87	5.57	2.29
August	58.56	38.592	19.97	8.45	5.57	2.88
September	55.40	38.592	16.81	8.02	5.57	2.43
October	58.94	38.592	20.34	8.51	5.57	2.94
November	44.13	38.592	5.545	6.37	5.57	0.8
Total	300.3	231.55	68.81	43.3	33.42	9.94

The result of 6 months data shows that the solar-wind hybrid power generation system can produce more than enough electrical energy to illuminate entire two electrical laboratories. The numerical data express it clearly that this contributes in providing alternative energy source for consumers and also provides economical contribution to the country. By all accounts, it is also estimated that the system will amortize its cost within 7 or 8 years.

III. Conclusions

The usage of fossil fuel-based energy is not promising method because of environmental pollution, greenhouse effect, adverse effects on human health and natural vegetation. In parallel with the technological development, usage of renewable energy sources which are environmental friendly and inexpensive will be widespread. Particularly, it is accepted that solar and wind power will provide opportunity for individual energy production to use in both cities and rural areas within high potential. In modern cities, it is possible that individual energy production based on solar and wind will change urban architecture and energy policy radically.

In this context, solar and wind energy should be considered under subheading, researches and projects should be supported while environmental strategies are being determined. Primarily, streets and roads, parks and gardens, highways, traffic lamps, remote areas lighting systems should be expanded to use renewable alternative energies. It should be encouraged to use these systems in our country which have many examples all over the world.

References

[1] D. Cristian D. Bica, "Photovoltaic Laboratory for Study of Renewable Solar Energy". *In International 43th Universities Power Engineering Conference* 2008, p 1-5, 2008.

[2] M. Bojic, 'Will Renewable Energy Save Our Planet?' In 3rh Global Conference, Power Control And Optimization, p 12-21, 2010.

[3] K.B. Varinca, M.T. Gonullu, "Solar Energy Potential in Turkey and Degree of use of this potential, A Survey on Prevalence and management", First National Solar and Hydrogen Energy Congress, Turkey, 2006.

[4] M.A. Batman, "A new method to increase the operational efficiency of solar cells for generating electricity". *İstanbul technical University, Doctorate thesis*, Turkey, 2001.

[5] V. Altın, "Electric production with solar system". *Journal of Architects and Engineers,* Vol. 33. pp. 28-31, 2004.

[6] S. Iscan, R. Karayel, Z.O. Ozcan, S. Gurleyen, "Solar Trackıng System (2-Way)". MKT2012, *Project-Based Mechatronics Training Workshop*, Çankırı, Turkey, 2012.

[7] S. Abdallah, OO. Badran, "Sun tracking system for productivity enhancement of solar stil". *Elsevier, Desalination* Vol. 220, pp. 669–676, 2008.

[8] Why Solar and Wind Energy?, http://www.yesaenerji.com/, Date of access: 05.08.2014

[9] Renewable energy sources, megep.meb.gov.tr/, Date of access: 04.08.2014

[10] S. Oktik, "Solar Energy Generating Electricity from direct (photovoltaic) industry and LED", Lighting applications, Solar Energy Industries Association and Industry, 2013.

[11] E.M. Yegin, M.Z. Bilgin, Energy Efficiency of LED Street Lighting Fixtures for Use in Kocaeli region and Impact on Costs, Kocaeli University, Department of Electrical Engineering.

[12] G. Held, "Introduction to Light Emitting Diode Technology and Applications". ISBN 9781420076622 , CRC Pres, 2008.

[13] Grounding and Lightning Protection Solar Panels, http://www.guneshaber.net/, Date of access: 22.07.2015

[14] J.W. Twidell and A.D. Weir, "Renewable Energy Resources", E.& F.N. Spon Ltd., London, New York, 1986.

[15] Y. Chen, Z. Liu, 'Distributed Intelligent City Street Lamp Monitoring and Control System Based on Wireless Communication chip nRF401', 2009 International Conference on Networks Security, Wireless Communications and Trusted Computing, DOI 10.1109/NSWCTC.2009.69, 2009.

[16] New Trends in Road and Street Lighting, http://www.elektrikport.com/, Date of access: 06.08.2014

[17] Solar sokak aydınlatma sistemleri, http://www.na-me.com.tr/ , Date of access: 06.09.2014

[18] H.H. Oguz, "Installation of wind-photovoltaic power generation system and control of general illumination system with PIC 16F877 controller for efficient use of energy", Afyon Kocatepe University, Graduate School of Natural and Applied Sciences , Master Thesis, 2012.

Biographies

Yüksel OĞUZ, He was born in Afyon, Turkey, in 1971. He has received his B.Sc degree from the Marmara University, Faculty of Technical Education, Department of Electrical Education, Istanbul. After that, he has received his M.Sc and Ph.D. degrees in Electrical Education from the Marmara University, Institute for Graduate Studies in Pure and Applied Sciences, between 2000 and 2007, respectively. He is working as Associate Professor in the Electronic and Electronic Engineering Department at Afyon Kocatepe University. He mainly teaches and studies in education of control systems, automatic control applications, electrical machines, power generation systems and control, renewable energy, and intelligent control systems.

Mustafa ŞAHİN, He was born in Bursa, Turkey, in 1981. He has received his B.Sc degree from the Marmara University, Faculty of Technical Education, Department of Electrical Education. After that, he received the M.Sc. degree in 2010 and Ph.D. degree in 2014 respectively from Institute for Graduate Studies in Pure and Applied Sciences at Marmara University, TURKEY. He is currently working as Assistant Professor in Department of Electrical & Electronics Engineering at Erzincan University. His research interests are artificial neural networks, illumination systems and renewable energy.

Elif ŞAHİN She was born in Istanbul, Turkey, in 1985. She has received B.Sc degree from the Sakarya University, Faculty of Arts and Science s, Department of Physics. Then she has received the B. Eng. in Medical Physics (Industrial Physi cs) from Istanbul Commerce University betwee n 2010 and 2012 respectively. Her research interests are nuclear physics, medical physics, lase rs and renewable energy.

Yılmaz GÜVEN, He was born in Gaziantep, in 1981. He has received B.Sc degree from the Marmara University, Faculty of Technical Education, Department of Electrical Education. Then he received the M.Sc. degree in 2010 from the Institute for Graduate Studies in Pure and Applied Sciences at Marmara University, TURKEY. He is continuing his education for Ph.D. degree at the same institute. He is currently working as a lecturer in Vocational School at Kırklareli University. His research interests are automation systems, microcontrollers and electrical machinery.

Structural Optimization of Payload Fairing Used for Space Launch Vehicles

H. Atar, and E. Acar

***Abstract*— Space Launch Vehicle (SLV) is a system to transport and place the Payloads (PL) such as satellites, experimental tools, and observation robots into desired orbit. PL are transported in Payload Fairing (PLF) that is a part of SLV and protects PL from environmental effects exposed during SLV's flight. PL capacity is the major criteria in design of SLVs. One option to increase PL capacity of SLV is to minimize PLF weight while protecting the volume allocated for PL. In this study, an Optimization System (OS) is developed to minimize PLF weight while maintaining the PLF structural design strong enough to protect PL from effects such as aerodynamic and inertial loads that emerged from flight conditions. Tabu Search is integrated to the OS to perform optimization. Structural analysis program is integrated to the OS to evaluate the structural strength. It is found that an optimized and structurally appropriate PLF configuration can be selected with Tabu Search integrated OS.**

***Index Terms*—Structural optimization, payload fairing, Tabu Search, heuristic methods.**

I. INTRODUCTION

Space Launch Vehicle (SLV) is a system that is used to transport Payloads (PL) like satellites, experimental vehicles, and observation robots to outside of atmosphere and place them to the desired orbit. SLV is composed of stages which has propulsion generators and Head Module (HM) which transport PL inside it. When the propellants inside of stages run out of, the stages are separated from SLV. After the stages separated from SLV, next stage starts to operate and generates the propulsion needed to transport PL to the target orbit. PL is transported inside PLF which protects PL from environmental effects exposed during flight.

Existing PLF design is given in **Hata! Başvuru kaynağı bulunamadı.**. Diameter of present design is 2500 mm. PLF is composed of cylindrical and conic section. PLF consists of longitudinal and transverse beams in it.

H. Atar, System Engineering and Technology Management Engineer in Space Systems Company, Ankara, Turkey, (e-mail: hakan.atar@roketsan.com.tr).

E. Acar, TOBB University of Economics and Technology, Söğütözü 06560 Ankara, Turkey, (e-mail: acar@etu.edu.tr).

PLF consists of 20 pieces of longitudinal beam and 10 pieces of transverse beam in cylindrical section and 20 pieces of longitudinal and 4 pieces of transverse beam in conic section. PLF nose is conic shaped. PLF material is aluminum. The shell thickness of PLF is 2 mm. The beams inside the PLF are I-beam.

There exists various studies in literature on structural optimization of PLF. In the prior examples of PLF optimization, Analytical Hierarchy Process method was used. Different design and production criteria were considered while realizing this method. Best PLF composite material was chosen by scoring PLFs that produced from different composite materials according to the criteria [2]. Another method that used was hybrid heuristic method. Both Genetic Algorithm and Sequential Quadratic Programming were used in optimization system [11]. Also, HyperSizer program and finite element model were used to optimize Minotaur Launch Vehicle PLF design in relevant study [1]. MATLAB Genetic Algorithm Tool was used another study subjected structural optimization. In this study ANSYS analysis program was used to get structural analysis results [5, 8]. 2-D roof and tower cage systems were optimized using this method.

In this study, the weight of a PLF is minimized while maintaining the PLF structural design strong enough under aerodynamic and inertial loads. Tabu Search is used to perform optimization, and a structural analysis program is integrated to optimization to evaluate the structural strength.

II. THEORETICAL GROUND

Firstly, mathematical model is constructed inside the PLF structural optimization study. Criteria which should be considered for optimization system is determined during this phase of study. Information related to mathematical model is given in Section A.

Optimization System (OS) is established by using inputs gathered from mathematical model. PL structural design is optimized by using OS. Detailed information related OS is given in Section B.

A. Mathematical Model

Decision variables and parameters of the mathematical model used for the PLF structural design optimization is given in TABLE I and TABLE II, respectively. The upper and lower bounds of the design variables are provided in TABLE IV.

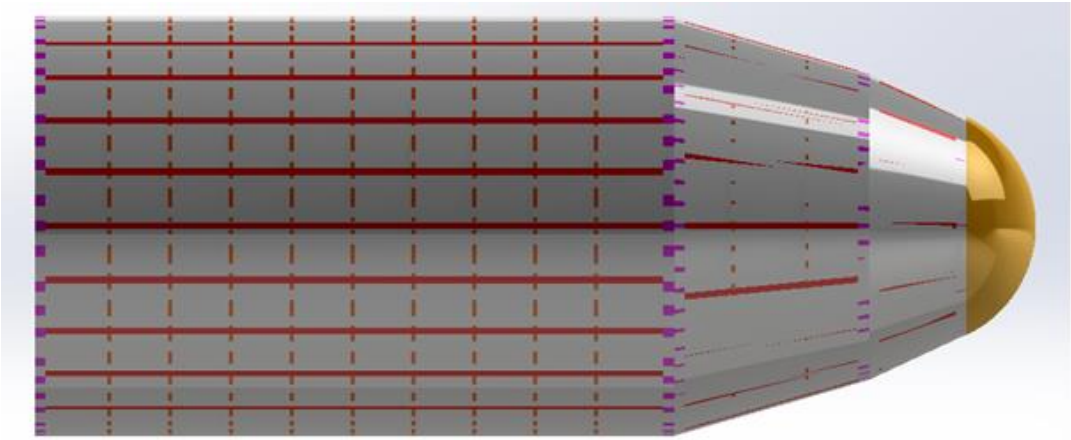

Fig 1. Payload Fairing (PLF)

TABLE I
DECISION VARIABLES OF PAYLOAD FAIRING STRUCTURAL DESIGN

No	Decision Variable	Definition
1	a	Number of transverse beam in Cylindrical Part of PLF
2	c	Number of transverse beam in conical part of PLF
3	materialType	Material type used in PLF (Aluminum, Magnesium, Steel)
4	shellThickness	Shell thickness of PLF
5	beamType	Beam type of PLF (I Beam, Z Beam, H Beam, R Beam, C Beam, T Beam, L Beam, W Beam)
6	beamLength	Beam length of PLF

TABLE II.
MATHEMATICAL MODEL PARAMETERS OF PAYLOAD FAIRING STRUCTURAL DESIGN

No	**Parameter**	**Definition**
1	$beamArea_i$	Beam section area for beam type i
2	beamLength_a	Beam length of beam used in cylindrical section
3	$beamLength\_c_l$	Beam length of beam used in conic section
4	$shellArea_j$	Section area of shell number j
5	$Smax_k$	Stress limit of material type k used in PLF
6	$Tmax_k$	Tip deflection limit of material type k used in PLF
7	yogunlukm	Density of material m used in PLF

TABLE III.
INITIAL VALUES AND LOWER-UPPER LIMIT OF VARIABLES

Variable	**Unit**	**Initial Value**	**Upper Limit**	**Lower Limit**
a	piece	10	1	15
c	piece	4	1	6
MaterialType	N/A	Al	N/A	N/A
ShellThickness	mm	2	1	2.5
BeamType	N/A	I	N/A	N/A
BeamLength	mm	20	10	25

N/A: Not Applicable

Mathematical model of the PLF structural optimization is given below;

Objective Function

$$\min \sum materialType_m * density_m * \left(\sum_i beamArea_i * beamLength_a * a * beamType_i + \sum_i \sum_l beamArea_i * beamLength\_c_l * c * beamType_i + \sum_j shellArea_j * shellThickness\right) \quad (1)$$

Constraints

$$S < \sum_m Smax_m * materialType_m \quad (2)$$

$$T < \sum_m Tmax_m \quad (3)$$

$$a > 1 \quad (4)$$

$$c > 1 \quad (5)$$

$$\text{shellThickness} \geq 1\ mm \quad (6)$$

$$\sum_m \text{materialType}_m = 1 \quad (7)$$

$$\sum_i \text{beamType}_i = 1 \quad (8)$$

$$\text{beamLength} \geq 10\ mm \quad (9)$$

$$\text{a, c integer} \quad (10)$$

Equation (1) is the objective function of the mathematical model. The aim of PLF structural design optimization problem is minimizing the mass, which is the summation of beam and shell masses. The mass values are obtained by multiplying the

densities and the volumes of the PLF cylindrical and conical section beams and PLF shell parts.

Equations (2), (3), (4), (5), (6), (7), (8), (9) and 10 are the constraints of mathematical model. Equation (2) constrains the stresses developed at the structural parts. This constraint is used to make the PLF structural design strong enough against to the stress emerged during flight. The 'S' value used in this term denotes the stress and it is obtained from PLF structural analysis. S_{max} value in Equation (2) is the maximum allowable stress of material represented by $materialType_m$.

Equation (3) constrains the deflections of the structural parts. This constraint is used to make the PLF structural design stiff enough. The 'T' value used in this term denotes the deflection is obtained from PLF structural analysis. T_{max} value in Equation (3) is the maximum allowable deflection of PLF.

Equation (4) constrains the number of transverse beam used in the cylindrical section of PLF. This constraint ensures the use of at least two transverse beams in cylindrical section. Equation (5) constraints the number of transverse beam used in the conical section of PLF. This constraint ensures the use of at least two transverse beams in conical section.

Equation (6) constrains the thickness of shell. The minimum value of this shell thickness is determined as 1 mm (due to manufacturing limits).

Equation (7) guarantees to choose at least and only one material type for PLF. There alternatives are evaluated during optimization. These alternatives are aluminum, steel and magnesium. Equation (8) guarantees to choose at least and only one beam type for PLF. The beam types evaluated in OS are 'Z' beam, 'C' beam, 'T' beam, 'L' beam, 'W' beam, 'I' beam and 'R' beam.

Equation (9) constrains the length of beam used for PLF design. The minimum value of this beam length is determined as 10 mm.

Equation (10) defines that variables 'a' and 'c' can take only integer values.

When the mathematical model is inspected, structural analysis program should integrated to the OS to obtain the stress 'S' and deflection 'T' values. Details of the OS is explained next.

i. Optimization System (OS)

PLF structural optimization study contains a multi-disciplinary engineering approach. The OS developed in this scope includes more than one subsystem that belongs to different engineering branches.

OS basically contains the following three subsystems;

- Heuristic Subsystem,
- Design Subsystem,
- Analysis Subsystem.

The flow chart explaining the working principle of OS is given in **Hata! Başvuru kaynağı bulunamadı.**.

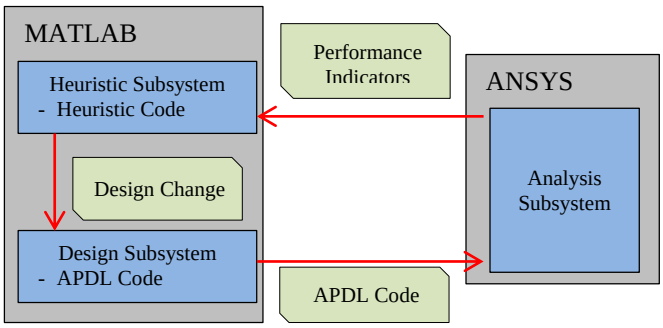

Fig 2. Flow Chart of Optimization System

Design, Analysis and Heuristic Subsystems work together and each subsystem gets the inputs, works over the inputs, creates the outputs and gives it to next subsystem. Each subsystem working principle is explained in the following sections.

a. Heuristic Subsystem

The inputs of Heuristic Subsystem are the existing PLF design and the performance indicators. The output of this subsystem is the design change of existing PLF design. This output is given to Design Subsystem to update the PLF design. All design variables describing the PLF design are evaluated as decision variables in Heuristic Subsystem. These decision variables are transformed into Heuristic Subsystem optimization moves and so objective function of PLF structural design is become optimized. Heuristic method used in Heuristic Subsystem is coded, and the whole logic and scanning operations of the heuristic method are realized using MATLAB.

Tabu Search is determined as a suitable heuristic method for PLF structural optimization. Tabu Search is coded in MATLAB to be integrated to OS. Initial values, neighbors and lower/upper limits of decision (design) variables used in Tabu Search are given in

.

TABLE IV.
NEIGHBORS AND STEPS OF VARIABLES

Variable	Step	Neighbors
a	Increasing and decreasing 1	a+1, a-1
c	Increasing and decreasing 1	c+1, c-1
materialType	Other all materials	
shellThickness	Increasing and decreasing 0,1	shellThickness+0.1, shellThickness -0.1
beamType	Other all beam types	
beamLength	Increasing and decreasing 1	beamLength+1, beamLength -1

In the first part of Tabu Search, the moves on the existing PLF design decision variables given in TABLE IV are realized and new PLF designs are obtained. The APDL codes of the new PLF designs are written to the text document. The text documents created for all neighbors are given to the ANSYS analysis program as an input. ANSYS analysis program conducts the structural analysis and gives the results of

performance indicators in the form of a text document to the Heuristic Subsystem to be evaluated.

If both maximum stress and maximum deflection values are smaller than the desired values, the PLF design is assessed as feasible and the move is realized on PLF design. The assessment process is completed for all neighbors. The objective function values are calculated for all feasible PLF neighbors and the neighbor having the best objective function value is determined as the selected neighbor.

The move of selected neighbor is controlled whether it is in Tabu list or not in the next phase. In the continuation of this phase;

- If the selected neighbor move is in the Tabu list, the selected neighbor is controlled whether it is better than the best solution or not.
  - If the selected neighbor has better objective function value than the best solution, the selected neighbor is accepted as the next solution and the best solution, and the iteration number is increased.
  - If the selected neighbor is not better than the best solution, the next better neighbor solution is accepted and this phase is repeated.
- If the selected neighbor move is not in the Tabu list, the selected neighbor is controlled whether it is better than the best solution or not.
  - If the selected neighbor is better than the best solution, the selected neighbor is accepted as the next solution and the best solution, and the iteration number is increased.
  - If the selected neighbor is not better than the best solution, the selected neighbor is accepted as the next solution, and the iteration number is increased.

Tabu list is updated in the next phase. The new move of the selected neighbor is added to Tabu list and the oldest move in the Tabu list is deleted. Neighbor moves are stored in the Tabu list to preserve repetition of the same move. Thus, different parts of the solution cluster can be searched and evaluated. This provides the diversification over the problem. In case the solution is better than the best solution despite it is in the Tabu list, this solution is set as next solution. This situation is called as aspiration criteria and this process provides intensification over the solution cluster.

The flowchart of the process described above is given in Fig 3.

b. Design Subsystem

This subsystem applies the design changes to the PLF structural design during the optimization iterations. Design changes include changing the dimensions of PLF mechanical components, the material of PLF and the configuration of PLF. These changes are reflected to the design by using ANSYS Parametric Design Language (APDL).

APDL is coded by using MATLAB and shared with ANSYS. In each iteration of the OS, the design is updated automatically with APDL parametric definition. Design changes, which are the output of Heuristic Subsystem, become inputs of the Design Subsystem to update the design. Updated APDL, which is the output of Design Subsystem, is given to Analysis Subsystem as an input.

c. Analysis Subsystem

PLF structural analysis is realized to determine the performance indicators (e.g., stresses and deflections) of the existing or the updated PLF design. Performance indicators show the effectiveness of the design and they are evaluated to determine whether the design is feasible or not.

PLF structural analysis is conducted using ANSYS. APDL code of the updated APDL design is transferred to the Analysis Subsystem from Design Subsystem. ANSYS computes the performance indicators of the updated design and these performance indicators are transferred to Heuristic Subsystem as an input.

III. Results and Discussion

The optimization runs are conducted by using the OS. The runs are executed by using a workstation with Intel Core i7 64bit processer and 8GB RAM. The results of the optimization runs are given in TABLE V. It is observed that the PLF mass can be reduced from 180.51 kg to 75.58 kg (reduced by 58.7%).

TABLE V
RUN RESULTS FOR DIFFERENT NUMBER OF ITERATIONS

Number of Iteration	a	c	Material Type	Shell Thickness	Beam Type	Beam Length (mm)	Objective Function Value(kg)
0	10	4	1	2	1	20	180,51
5	10	4	3	1,6	1	20	144,89
10	10	4	3	1,1	1	20	100,03
20	10	4	3	1	1	11	80,83
50	7	6	Mg	1	3	10	75,58

TABLE V also shows that the shell thickness is reduced to its lower limit of 1 mm. Another change observed for the PLF design is the material type. Magnesium is used instead of aluminum and this change decreases the PLF weight by 40%.

It can be seen that the decision variables a and c are also design critical in terms of PLF flight loads. It is found that the optimizer reduces the number of beams in the cylindrical part (a) and increases the number of beams in the conical part (c) to decrease the PLF weight while maintaining the stresses and deflections below the specified constraint values.

Another criteria that can be used to evaluate the performance of OS is the run time of the system. The run times are listed in TABLE VI, which shows that the run time increases exponentially with respect to the iteration number. Therefore, it is required to keep the iteration number as low as

possible. The evolution of the objective function value through iterations are depicted in Fig 4, which shows that 30 iterations are enough for OS to get near optimal solutions.

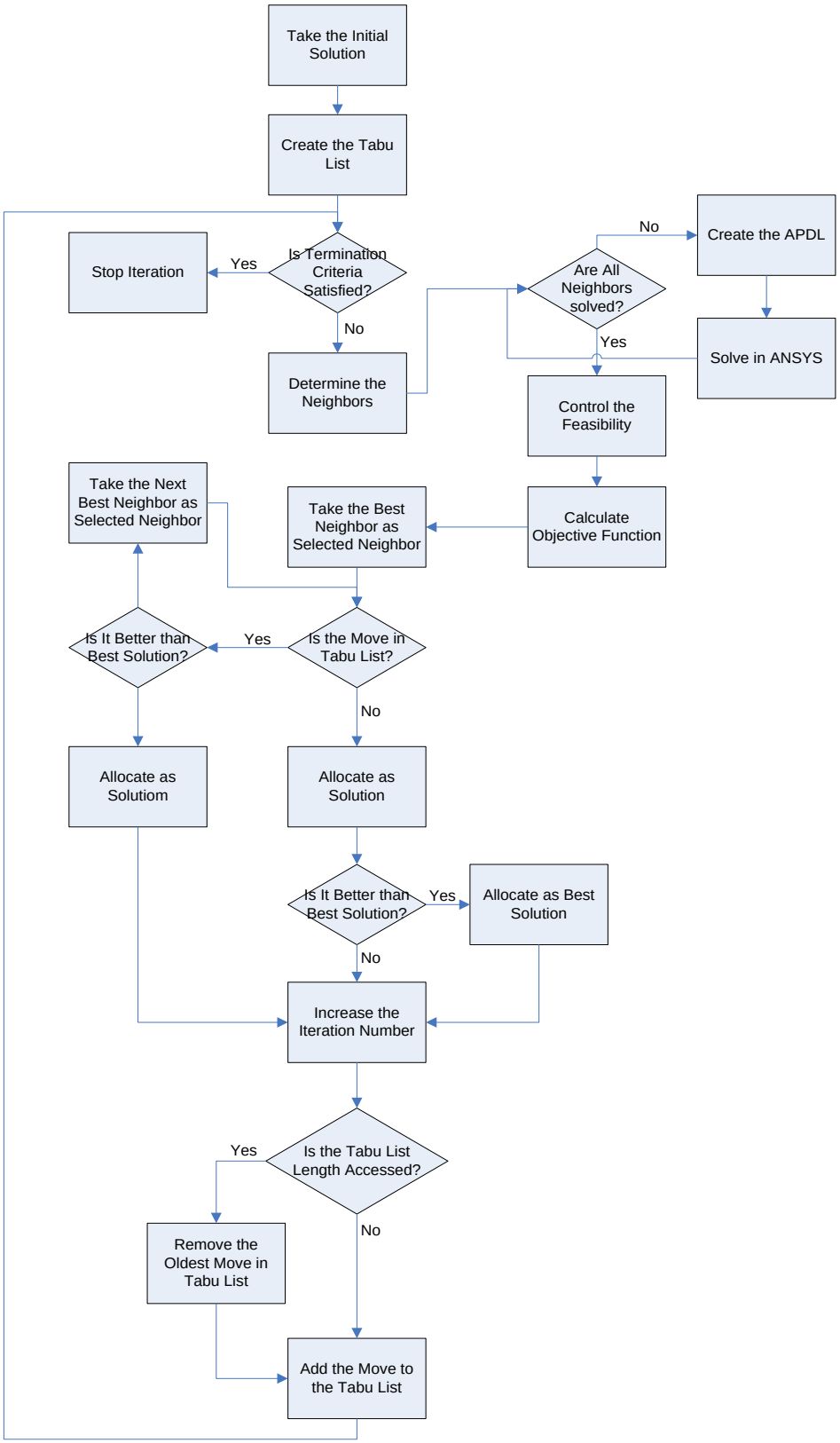

Fig 3. Optimization Subsystem Flow Chart

TABLE VI.
THE RUN TIMES FOR DİFFERENT ITERATION NUMBERS

Iteration Number	Run Time (second)
5	503
10	1086
20	3174
50	10573

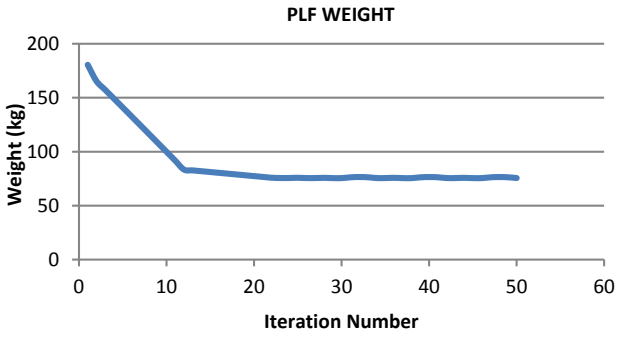

Fig 4. PLF Weight Change for Different Iteration Numbers

IV. CONCLUSION

In this study, Payload Fairing (PLF) used in Space Launch Vehicles was optimized using Tabu Search, which is a heuristic method. Optimization results showed that the optimum PLF design should have 1mm shell thickness, and that PLF material should be aluminum. PLF beam length should be 10 mm. The number of beams in the conical section should be six, and the number of beams in the cylindrical section should be seven. This design changes resulted in 58.7% weight reduction. It was also found that 30 iterations were enough for OS to get near optimal solutions and high performance from OS, and that Tabu Search can be used to optimize PLF design and to get the good solutions efficiently.

Future study could focus on using other heuristic methods (e.g., Genetic algorithm, simulated annealing, etc.) and the most suitable method for PLF design could be determined.

ACKNOWLEDGMENT

The study is selected from National Engineering Research Symposium 2015 (Ulusal Mühendislik Araştırmaları Sempozyumu) UMAS 2015 (Duzce University).

REFERENCES

[1] Krivanek T.M., Yount B.C. (2012), Composite Payload Fairing Structural Architecture Assessment and Selection, E-18094, NASA Glenn Research Center, Cleveland.

[2] Wenger P.M., Higgins J. E., VanWest B. P. (2002) Application of Advanced Grid-Stiffened Structures Technology to the Minotaur Payload Fairing, AIAA 2002-1336, 1061-1067.

[3] Irish Angelin S., Senthilkumar S. (2013) Aerodynamic Shaping of Payload Fairing for Launch Vehicle, Journal of Spacecraft and Rockets, Vol. 50, No. 6, pp. 1299-1304. doi: 10.2514/1.A32838.

[4] Reisenthel P. H. ,Childs R. E., Higgins J. E., (2007) Surrogate-Based Design Optimization of a Large Asymetric Launch Vehicle Payload Fairing, 46th Aerospace Sciences Meeting and Exhibit, 2007-0361, ISSN: 10877215

[5] Togan V., Seyhun M. O., Daloglu A. (2015) A Comparative Study For The Optimum Design of StructuresUsing GeneticAlgorithm, www.researchgate.bet, search on 15th of June.

[6] Kargahi, M. and Anderson, J. (2006) Structural Weight Optimization with Tabu Search. Earth & Space 2006: pp. 1-8. doi: 10.1061/40830(188)163.

[7] Connor, A.M., Seffen, K.A., Clarkson, P.J. & Parks, G.T. (1999) Efficient Optimisation Of Structures Using Tabu Search, Proceedings of the 1st ASMO/ISSMO Conference on Engineering Design Optimization, 127-134

[8] A. Gauchía, B.L. Boada, M.J.L. Boada and V. Díaz (2014). Integration of MATLAB and ANSYS for Advanced Analysis of Vehicle Structures, MATLAB Applications for the Practical Engineer, Mr Kelly Bennett (Ed.), ISBN: 978-953-51-1719-3

[9] Zafar N., Linshu H., (2010) Multidisciplinary Design Optimization of Solid Launch Vehicle Using Hybrid Algorithm, 51st AIAA/ASME/ASCE/AHS/ASC Structures, Structural Dynamics, andMaterials Conference, DOI: 10.2514/6.2010-3010

[10] Inc. PADT, Strain J.,"Introduction to the ANSYS Parametric Design Language (APDL): A Guide to the ANSYS Parametric Design", CreateSpace Independent Publishing Platform; 1 edition, ISSN: 146641135X

[11] Bayley D. J., Hartfield R J., Burkhalter J E., , Jenkins R M.(2008), Design Optimization of a Space Launch Vehicle Using a Genetic Algorithm, Journal of Spacecraftand Rockets, Vol. 45, No. 4 , pp. 733-740.doi: 10.2514/1.35318.

BIOGRAPHIES

Hakan ATAR was born in Aydın, Turkey in 1990. He received his BS in Industrial Engineering and double major BS in Mechanical Engineering at the TOBB University of Economics and Technology of Turkey where he is currently receiving his MS degree since 2013.
Since 2013 he is serving as System Engineering and Technology Management Engineer in Space Systems Company in Ankara. He is working as system engineering responsible of the projects and technology management engineer of Engineering Directorate. His research area includes design optimization of mechanical systems. His research on design optimization of mechanical system is focused on heuristic methods.

Erdem ACAR received his BS and MS degrees in Aerospace Engineering at the Middle East Technical University in 1999 and 2002, respectively, and his PhD degree in the same field at the University of Florida in 2006. He served as postdoctoral research associate at the Center for Advanced Vehicular Systems of the Mississippi State University from 2006 to 2008. He began his academic career in 2008 at the TOBB University of Economics and Technology of Turkey, where he is currently an Associate Professor at the Department of Mechanical Engineering. He is actively engaged in teaching and research. His primary areas of teaching include structural analysis and reliability assessment of mechanical systems. His research efforts are focused on design optimization of mechanical systems, with strong emphasis on reliability-based design optimization and surrogate-based design optimization. He has published around sixty refereed journal and conference papers in the above areas. He is an associate fellow of AIAA, and a member of the AIAA Non Deterministic Approaches Technical Committee.

Establishing the Potential Clients Using Artificial Neural Networks

Z. Pamuk, Y. Yurtay, and O.Yavuzyilmaz

***Abstract*—Today, technologies retrieving forward-looking information from the existing data are available. In this study, whether the clients would open a deposit account was estimated using the data in the marketing campaign of a bank in Portugal for its clients. The purpose of the study was to create a decision support system to determine the potential clients in future. The data set collected from 4.512 subjects consists of 16 input attributes (job, age, balance, etc.) and 1 output attribute (yes/no). In the study, the 6-fold cross validation method was used. The data obtained from 3.760 people were used for the training process and the data obtained from 752 people were used for the testing process. As classifiers; Feed Forward Neural Networks (FFNN), Probabilistic Neural Network (PNN) and k Nearest Neighbor (kNN) were used. At the end of the study, success ratios of different algorithms were compared by Receiver Operating Characteristics (ROC) analysis method. Feed forward neural network yielded the best result with an accuracy rate of 95.74%.**

***Index Terms*—Bank data, deposit, artificial neural network, k nearest neighbor algorithm.**

I. INTRODUCTION

TODAY, data can be digitally collected and stored due to the rapid development of computer systems. Together with the high increase of data and the need for obtaining significant extractions, the concept of data mining emerged. The main objective of data mining is to find out information such as relationships between data, patterns, changes, deviations and trends and certain structures with the combinations of mathematical theories and computer algorithms and obtain valuable information through the interpretation of this information.

Data mining is considered to consist of four main topics including classification, categorization, estimation and visualization. Marketing campaigns occupy an important place for banking institutions. In this study, the marketing campaign is based on telephone conversations.

Z.Pamuk, Electrical Electronic Engineering Department, University of Sakarya. 54100, Sakarya, Turkey, (e-mail: ziynet@sakarya.edu.tr).

Y.Yurtay, Computer Engineering Department, University of Sakarya, Sakarya, Turkey,(e-mail: yyurtay@sakarya.edu.tr)

O.Yavuzyilmaz, Kocaeli University, Gazanfer Bilge Vocational School, Department of Public Relations and Publicity, Kocaeli, Turkey, (e-mail:oguz.yavuzyilmaz@kocaeli.edu.tr)

Telephone conversations have a significant impact on the decision-making process of clients. A classification was made using the client information obtained in the telemarketing campaign the employees of the Portugal Bank carried out for its clients and whether they would be deposit account clients was tried to be determined.

In some studies carried out using bank data, whether the clients would be a deposit account subscriber or not was predicted using the information obtained from the clients and data mining techniques. For example; Moro et al. made analyses using data mining techniques in line with the information obtained as a result of telemarketing campaigns. They used support vector machine, decision tree and naive bayes classifier data mining models. In the study, the best results were obtained from the Support Vector Machine Model [1]. Moro et al. studied on the same topic in the study titled "A data mining approach for bank telemarketing using the rminer package and R tool" they carried out in 2013. They performed that study using the r tool extension of rapidMiner program [2]. In the study titled "Bank direct marketing based on neural network" carried out by Elsalamony Hany A. and Elsayad Alaa. M., the data obtained as a result of the marketing campaign were analyzed with MLPNN (Multi-Layer Perceptron Neural Network) and Decision Tree-DT models [3]. In the study titled "Evaluating marketing campaigns of banking using neural networks" carried out by Qeethara Kadhim Al-Shayea, the prediction about whether the clients would be a deposit account holder or not was made in line with the information obtained from them through ANN and DT techniques [4].

II. METHOD

In the first stage, the data were preprocessed. Thus, it was aimed to obtain accurate results from the study. At this stage, data cleaning and data integration steps were applied. The missing data were deleted and the data were tried to be made consistent. In order to find out the relationships between the data and obtain information through the interpretation of them, ANN and as a different classifier apart from ANN; k nearest neighbor algorithm, which is simple and frequently used in the literature, were used. *k* nearest neighbor algorithm is abbreviated as *kNN*. In the stage of evaluation of the results, Receiver Operating Characteristic –ROC Formulas were used.

A. *Pre-processing*

Pre-processing is quite important to obtain the most accurate result from the data. At this stage, first data cleaning, next data integration processes were carried out. In the final stage, data conversion process was performed.

B. *Data cleaning*

Approximately seventy thousand people were interviewed in the data recording process. However, not all these data were processable. In order to increase the usability of the data, the data including missing information and incorrect data were cleaned and 4.512 processable data were obtained.

C. *Data integration*

17 variables of the 4.512 data have different types such as symbolic, numeric and categorical. In the study, all variable types were digitized in order to facilitate the analyses on the data. The digitized values are indicated in Table 1 Input data and Table 2 Output data.

D. *Data Conversion*

The digitized data were normalized between -1 and +1 with the help of Matlab © code. Thus, the speed of processing increased while the data were trained.

E. *Data Set*

The data set was obtained from the telephone conversations between the employees of the Portuguese bank and the bank clients. The study was carried out using the client information obtained from the telemarketing campaign of the bank and whether the clients would be deposit account subscriber or not was tired to be determined with the help of the information given by the clients. The data belonging to a total of 4.512 clients are given in Table 1 and Table 2.

The data were divided into training and testing sets. The data were also divided into K=6 groups using the k fold cross validation technique. How the groups were determined is given in Table 4 in the Application section.

F. *Classification Methods*

ANN emerged as a result of the efforts to simulate the working system of human brain artificially. The first artificial neural network was realized by Warren McCulloch, a neurologist, and Walter Pitts, a mathematician, in 1943. McCulloch and Pitts modelled a simple neural network with electrical circuits being inspired by the computing capacity of human brain. They are information processing systems which generally simulate the working principles of human brain or central nervous system [5].

ANN has a simple structure and a directed graph format. Each node is an nth degree nonlinear circuit called “cell”. These nodes are defined as processing elements in ANN. There are links connecting the nodes to each other and each of them functions as a simplex communication path. A single output can feed several cells, in other words; each communication element can receive a desired number of input connections and a single output connection. The output of the processing element can be in a desired mathematical type. Continuously working input elements produce an output signal. The input signals carry information to ANN and the result can be obtained from the output signals. ANN is composed of three layers including Input Layer, Interlayers (Hidden Layers) and Output Layer [6].

Feed Forward Network (FFN) and Probabilistic Neural Network (PNN) were used in the application as available network types in ANN. The accuracy results of the data sets were analyzed giving different values to the variables of the number of neurons, the number of layers, goal and lr determined in FNN Network. Goal value is a value indicating how much of the error can be minimized. Generally a value near zero is given instead of giving zero. In this study, the value of 0.01 was given. It continues training till the network error value is 0.01 or the desired epoch, i.e. “cycle number” is reached. The LR value, i.e. learning rate should not be selected as a very high or very low value. If a very high value is selected, the network memorizes the data. On the contrary, if a very low value is selected, then the network either learns the data too slowly and causes loss of time or cannot learn it.

FFN includes a series of layers. The first layer has a connection from the network inputs. Each layer is connected with the previous layer. The final layer produces the network outputs. Feed Forward Networks can be used for output matching and any kind of input. A Feed Forward Network can be used in any finite input output matching problems with a hidden layer and sufficient neurons in the hidden layer [7].

PNN is a radial basis neural network. It is based on counselling learning. PNN is a neural network which uses Bayes Theorem in decision making. According to Bayes theorem, if an equality of vector x is accurate, it belongs to the 1^{st} class, if not, it belongs to the 2^{nd} class [8].

kNN method is one the learning methods which solves the classification problem. With this method, the similarities of the data to be classified to the data in the learning set is calculated, the average of the values of their k nearest neighbors is taken and they are assigned to a class according to their threshold value. In order to perform this assignment, the characteristics of each class should be clearly determined in advance.

TABLE 1.
INPUT DATA

id	Variables	Explanation	Type	Value (digitized value)
1	Age	Age when contacted	numeric	18 +
2	Occupation	Occupation of the contact person	categorical	unknown(1), administrator(2), unemployed(3), manager(4), servant(5), contractor(6) , student(7), worker(8), self-employed (9), retired(10), technician(11), service personnel(12)
3	Marital status	Marital status of the contact person	categorical	single(1) , divorced(0), married(-1)
4	Education	Educational status of the contact person	categorical	unknown(1),primary school(2), secondary school(3), undergraduate(4)
5	Non-performing loan	Does the client have a non-performing loan?	categorical	yes(1), no(-1)
6	Avg balance	Average annual balance of the client's current accounts in Euro currency	numeric	-3313euro < ; < 71188 euro
7	Mortgage loan	Does the client have a mortgage loan?	symbolic	yes(1), no(-1)
8	Personal loan	Does the client have a personal loan?	symbolic	yes(1), no(-1)
9	Communication type	What was used as a means of communication?	categorical	unknown(1), telephone(0), mobile phone(-1)
10	Last contact day	Last contact day when the clients were interviewed for the campaign	numeric	1<; <30
11	Last contact month	Last contact month of the year when the clients were interviewed for the campaign	categorical	January(1), February(2).....December(12)
12	Length of interview sec.	Length of the interview (in seconds)	numeric	4 sec < ; <3025 sec
13	Number of contacts established in the campaign	Number of contacts during the campaign	numeric	1 < ; <50
14	How many days after the last campaign the interview was made	How many days after the last campaign were the clients contacted?	numeric	1 < ; <871 ;
15	Number of pre-campaign contacts	Number of contacts before the campaign	numeric	0< ;<25
16	Previous campaign result	Result of the previous marketing campaign	categorical	unknown(1), imperfect(2), other(3), successful(4)

TABLE 2.
OUTPUT DATA

id	Variables	Explanation	Type	Value
1	Y	Has the client subscribed to a term deposit account?	symbolic	yes (1) , no (-1)

kNN is an instance-based learning algorithm and used for performing classifications over the available learning data when a new instance is encountered. The algorithm determines the class of the instance looking at its k nearest neighbor when a new instance is encountered [9]. Referring to the data whose classes are known, their distance to the data whose classes are unknown is calculated and it is based on the selection of k number of observations with the minimum distance.

In the example in Figure 1, the number of nearest neighbors was taken as 5 and in which class the unknown data would be included was determined. As the number of neighbors in Class A was higher than the number of neighbors in Class B, the unknown data was included in Class A. The k value in the figure is not the value in the application, which is 511.

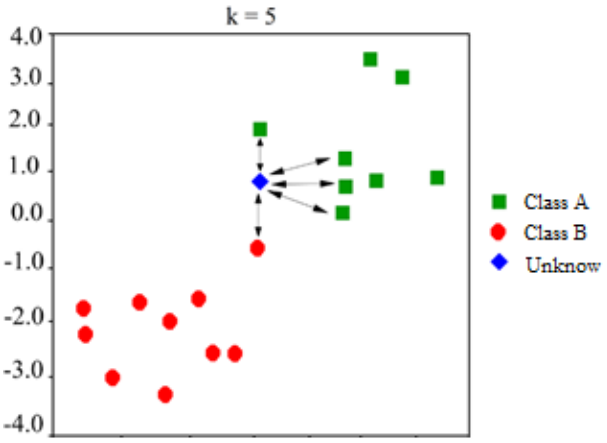

Fig 1. kNN representation

The steps of *kNN* algorithm are as follows.

1- The newcomer individual is added into the class.
2- *k* number of neighbors are looked at.
3- The distance is calculated using various distance function (Euclidean distance function).
4- The individual is assigned to the nearest place [10].

In equation 1, the Euclidean Distance Function formula, where d is the function of distance between two points, i and j are the indices of the points, x is the position of this point and the p value is 752, which is the test value, is given.

$$d(i,j)=\sqrt{(x_{i1}-x_{j1})^2+(x_{i2}-x_{j2})^2+\ldots+(x_{ip}-x_{jp})^2} \quad (1)$$

The distances of a point to all the other points are calculated separately, the rows are sorted and the smallest k number is selected. In which category the selected rows are is determined and the most repeated category is selected.

G. *Evaluation*

Receiver Operating Characteristic (ROC) was developed for the accurate identification of the signals detected on radar in Britain during the World War II and enabling the distinction between friend and foe. Lusted suggested the use of ROC analysis in decision making in medicine in 1967 and led to the use of it in medical imaging devices in 1969. In the following years, the use of ROC analysis in the evaluation of the performance of diagnostic tests in medicine gradually became widespread. The developments emerging with ROC analysis are a natural consequence of the need for the evaluation and comparison of statistical results [11].
ROC analysis is defined as "the receiver operating characteristic" or simply "ROC curve" in signal detection theory. The ROC curve is obtained with the ratio of sensitivity to specificity in cases where the distinction threshold value varies in binary classifier systems. In simpler terms, ROC can be expressed as the fraction of true positives to false positives [11].
While performing a ROC analysis, a classification should primarily be made. Meanwhile, the threshold values are determined and divided into two classes. These classes are positive (P) and negative (N) values according to the threshold value. When subjected to this classification, the estimated and actual values are divided into four different classes.

- If the estimated value is positive (P) and the actual value is also positive (P), it is called a true positive (TP).
- If the estimated value is positive (P) and the actual value is negative (N), it is called a false positive (FP).
- If the estimated value is negative (N) and the actual value is also negative (N), it is called a true negative (TN).
- If the estimated value is negative (N) and the actual value is positive (P), it is called a false negative (FN).

TABLE 3.
ERROR MATRIX FOR THE ANSWER "NO"

Error matrix		Classifier Outcomes	
		YES	NO
Actual Results	YES	TN	FP
	NO	FN	TP

Accuracy is the proximity of the measured value to the actual value. Error is the difference between the measured value and the actual value [12].

$$Accuracy=\frac{TP+TN}{(TP+TN+FP+FN)} \quad (2)$$

III. APPLICATION

All the data were divided into two groups as training and testing data to be given to the classifiers. While performing this division in the data set, the k-fold clustering algorithm was used. Firstly, a k value was selected to apply to the data set. For K=6, the data set including 4.512 data were divided into 6 equal parts (folds). The K-folds are illustrated in Table 4.

During fold partition, the numbers of "yes" and "no" belonging to the outcome variable were also taken into consideration. Thus, the state of excess of "yes" or "no" in any of the folds, which is possible in a random distribution, was eliminated. In case of such a situation, the outcomes of the model will also be affected negatively.

TABLE 4.
K-FOLDS

id	Yes	No	Total
Fold 1	86	666	752
Fold 2	86	666	752
Fold 3	86	666	752
Fold 4	86	666	752
Fold 5	86	666	752
Fold 6	86	666	752
Total	516	3996	4512

As illustrated in Table 5 randomly chosen 5 folds constitute the training data (3.760 pieces) and 1 fold constitutes the testing data (752 pieces). In Table 5, how the k-folds were formed is clearly expressed (k=6). In the k-fold technique, the data were named as A-B-C-D-E-F and 6 different data sets were created.

TABLE 3.
DATA SETS

Data set	Training Folds	Testing Folds
A	Fold1 - Fold 2 - Fold 3 - Fold 4 - Fold 5	Fold 6
B	Fold 1 - Fold 2 - Fold 3 – Fold 6 - Fold 5	Fold 4
C	Fold 2 – Fold 3 – Fold 4 – Fold 5 – Fold 6	Fold 1
D	Fold 1 – Fold 3 – Fold 4 – Fold 5 – Fold 6	Fold 2
E	Fold 1 – Fold 2 – Fold 4 – Fold 5 – Fold 6	Fold 3
F	Fold 1 - Fold 2 - Fold 3 - Fold 4 – Fold 6	Fold 5

The classification techniques applied in this study were realized using the data sets in Table 5. In the evaluation stage, the data set which gave the most accurate result to determine whether the client would be a deposit account subscriber in the future or not was found to be the data set B.

The numbers of the training and testing data sets used by ANN are shown in Table 6.

TABLE 6.
NUMBER OF DATA

	Yes	No	Total
Training	430	3330	3760
Testing	86	666	752
Total	516	3996	4512

The training set includes a total of 3.760 data records, whereas the testing set includes 752 data records. Each row in Table 1 corresponds to a record here.

The accuracy results of the data sets were examined by giving different values to the variables of the number of neurons, the number of layers, goal and lr determined in FFN network structure. The values which gave the best result were identified as follows; the number of neurons = 80, the number of layers = 1, goal = 0.01, lr = 0.005. With this identified network, the best accuracy result determined with ROC was found.

The vector state of the training output was found in PNN. The reason for the conversion of the training output into a vector matrix was that it would be used in creating a network. During the creation of the neural network, the training input, the training output vector and the distribution values were taken. Upon the creation of the network, the testing data were given to the network. As the training input values had been converted into the vector state initially, the results were produced in index format upon obtaining the testing output in vector state. The PNN model was experimented for the selected data set B, however the algorithm did not give a good result due to the excess number of data.

In the data set B, the data were classified using the kNN algorithm. The algorithm was implemented in the selected data set B. 3.760 data of the data set B were separated for training and 752 data for testing. The training input, training output and testing input data were given to the algorithm. The testing output was taken from the result of the algorithm. The classes of the data in the training input given to the algorithm were known, whereas the data whose classes were unknown belonged to the testing input data. The distance of each data in the set whose classes are known to the observation values whose classes are unknown is calculated according to the kNN algorithm. In the calculation of the distance, Manhattan distance function, Minkowski distance function and Euclidian distance function are used. K number of data with the minimum distance according to the calculation is selected. In this study, Euclidian distance function was used. K number was taken as 511. 511 data with the minimum distances calculated according to the algorithm were selected. To measure the reliability of the results, the obtained results were evaluated with ROC.

IV. CONCLUSIONS

In this study, the probability of people to open a deposit account in the bank was estimated for marketing campaigns. 3.760 of the 4.512 data were used as the training data and 752 as the testing data. The data were studied using ANN classification models; FFN and PNN networks and also kNN. As shown in Table 7. ROC Accuracy Results, the method which gave the best result was FNN. For bank marketing campaigns, the probability of people to open a deposit account was estimated with the accuracy rate of 94.22% and the probability not to open a deposit account with the accuracy rate of 94.10%.

TABLE 7.
ROC ACCURACY RESULTS

Model Name	YES (%)	NO (%)
FFN	94.22535	94.10071
PNN	69.9468	69.9468
KNN	88.56382	88.56382

As a result of the study, the training process was completed with the training set and processes were performed with the testing set where whether the client became a deposit account subscriber or not was not known. As a result of the testing set, the FFN classifier identified the outcome of "Yes" for "Has the client become a deposit account subscriber?" correctly with a rate of 94.22% and identified the outcome of "No" for "Has the client become a deposit account subscriber?" correctly with a rate of 94.10.

FNN achieved a better result compared to the other methods. This method is thought to be utilized by banks and all the institutions which conduct marketing activities.

ACKNOWLEDGMENT

The study is selected from National Engineering Research Symposium 2015 (Ulusal Mühendislik Araştırmaları Sempozyumu) UMAS 2015 (Duzce University).

REFERENCES

[1] Moro S. , Laureano R., Cortez P. (2011). Using data mining for bank direct marketing: an application of the crisp-dm methodology. European Simulation and Modelling Conference.
[2] Moro S.(2013). A data mining approach for bank telemarketing using the rminer package and R tool. Working Paper. ISCTE - Instituto Universitário de Lisboa.
[3] Elsalamony Hany A., Elsayad Alaa. (2013). M. Bank direct marketing based on neural network. International Journal of Engineering and Advanced Technology (IJEAT) ISSN: 2249 – 8958, Volume-2, Issue-6, August 2013.
[4] Qeethara Kadhim Al-Shayea. (2013). Evaluating Marketing Campaigns of Banking Using Neural Networks, Proceedings of the World Congress on Engineering 2013, Vol II.
[5] Oztemel E., Artificial Neural Networks, Papatya Publishing, İstanbul, 2003.
[6] Kayhan Gulez. www.yildiz.edu.tr/~gulez/3k1n.pdf. 2015.
[7] Beale, M.H., Hagan, M.T., Demuth, H.B. Neural Network Toolbox. 383, 2012.
[8] Specht, D. F.(1990). Probabilistic neural networks, Neural Networks, Vol. 3 (1), pp 109-118.
[9] Nearest Neighbors Tutorial people.revoledu.com/kardi/tutorial/KNN/HowTo_KNN.html. 2015.
[10] Özkan, Y., Data Mining Methods. Papatya Publishing, İstanbul, 2013.
[11] http://tr.wikipedia.org/wiki/ROC. 2015.
[12] Fawcett, T.(2006). An introduction to ROC analysis, Pattern Recognition Letters, 27, 861-874.

BIOGRAPHIES

Ziynet PAMUK was born in Zonguldak, Turkey, in 1980. She has received the bachelor's degree and master's degree from the Sakarya University, Sakarya, Turkey, in 2002 and 2008, respectively. She has graduated Ph.D. at Department of Electrical and Electronics Engineering in 2014. She has been working at Sakarya University since 2004. Her interests are Biomedical Engineering, Classification Algorithms, and Artificial Immune System and Artificial Neural Network.

Yüksel YURTAY was born in Eskişehir, Turkey, in 1968. He has received the bachelor's degree from Anadolu University, Turkey, in 1992. He has received the master's degree from the Sakarya University, Turkey, in 1997. He has been working at Sakarya University since 1993. His interests are Software Engineering, Data Mining, and Numerical Analysis.

Oğuz YAVUZYILMAZ was born in Kocaeli, Turkey, in 1980. He has received the bachelor's degree from Marmara University, in 2003 İstanbul and master's degree Kocaeli University in 2008, Kocaeli, Turkey. Since 2011; he is continuing his PhD studies at Production Management and Marketing of Science program in Sakarya University, Sakarya, Turkey. He has been studying; Marketing, Postmodern Marketing, Womm, Data Mining, Production and Marketing analysis techniques.

Time Series Analysis and Data Relationships

Y. Bicen, M. Kayikci, and F. Aras

***Abstract*—The time-series models which has an has an important place in the statistical forecasting methods are widely used in many disciplines such as economy, production management, and engineering in order to perform realistic estimates for the future. Produced results of these methods which are diversified in time, is variable for different data sets. A model that produces pretty good results for a dataset may not be realistic for the other dataset. The success of the time-series forecasting methods is directly related to the quantitative characteristic features of a dataset ranked through time. In this study, it is tried to identify the main principles for determining the correct method and suitably selecting the parameters within the framework of time-series forecasting models and quantitative characteristics of the data sets.**

Index Terms— **Exponential smoothing, forecasting methods, time series, statistics.**

I. Introduction

TODAY, forward-looking strategic planning is needed for a competitive free market economy. In this sense, monitoring of the balance between demands and manufactured products continually is critical to make accurate assessments. Time series methods which are classified in quantitative forecasting methods are used effectively quite a long time in particular to estimate short and medium-term data. Time-series forecasting models utilize historical data lined up at regular intervals. It is possible to encounter many different varieties such as simple moving averages, exponential smoothing methods, adaptive smoothing methods, and etc. Certainly, the reason for the emergence of many types of methods is due to the changing of success level according to different data characteristics. In this study, some of time-series forecasting models and the relationships among their performances with the series characteristics are examined.

Y. BICEN is with the DMYO, the Department of Electronics and Automation, Duzce University, Uzunmustafa, 81010, Duzce, Turkey. (e-mail: yunusbicen@duzce.edu.tr)

M. KAYIKCI is with the DMYO, the Department of Computer Technologies, Duzce University, Uzunmustafa, 81010, Duzce, Turkey. (e-mail: mustafakayikci@duzce.edu.tr).

F. ARAS is with the Department of Aircraft Electrical and Electronics, Kocaeli University, Turkey (e-mail: faruk.aras@kocaeli.edu.tr).

II. The Time Series Analysis

The preferred time series models are differ from each other according to the data sets in various sectors. In the literature, the time series characteristics are described in principle generally [1-4]. The characteristics changes shown in Fig. 1 may be involved individually or in combination in the time series. In such a case, the method to be used should be selected correctly in order to make accurate forecasts or time series analysis.

Trend:
It refers to the long term upward or downward changes. Linear, exponential or logarithmic may be.

Seasonal changes:
It refers to short-term and regular changes within a certain period.

Conjectural changes:
It refers to long-term and cyclical changes.

Deviations:
It refers to non-periodic unusual changes.

Random changes:
It refers to all changes except the other changes.

From simple to complex, there are many time-series analysis methods. One of the most successful methods following the characteristic of time series is exponential smoothing method [5]. Brown and Holt's (1950) exponential smoothing method has been developed and many additions have been made on original method during this time [1,5-7]. In the literature first time, exponential smoothing method has been classified by Pegels (1969) for different combinations of trends and seasonal changes. And then, this classification has been extended by Gardner, McKenzie and Taylor [2,8]. As is apparent from Table 1, trend and seasonal components are not a function of each other in additive model but these components varies in direct proportion to each other in the multiplicative model.

Three different parameters α, β, and δ used in the Extended exponential smoothing method, refer to the level, the trend, and the seasonal components respectively.

TABLE I
EXTENDED EXPONENTIAL SMOOTHING STATEMENTS

		Seasonality		
		None	*Additive*	*Multiplicative*
Trend	*None*	$S_t = \alpha X_t + (1-\alpha)S_{t-1}$ $\hat{X}_t(m) = S_t$	$S_t = \alpha(X_t - I_{t-p}) + (1-\alpha)S_{t-1}$ $I_t = \delta(X_t - S_t) + (1-\delta)I_{t-p}$ $\hat{X}_t(m) = S_t + I_{t-p+m}$	$S_t = \alpha(X_t/I_{t-p}) + (1-\alpha)S_{t-1}$ $I_t = \delta(X_t/S_t) + (1-\delta)I_{t-p}$ $\hat{X}_t(m) = S_t\, I_{t-p+m}$
	Additive	$S_t = \alpha X_t + (1-\alpha)(S_{t-1} + T_{t-1})$ $T_t = \beta(S_t - S_{t-1}) + (1-\beta)T_{t-1}$ $\hat{X}_t(m) = S_t + mT_t$	$S_t = \alpha(X_t - I_{t-p}) + (1-\alpha)(S_{t-1} + T_{t-1})$ $T_t = \beta(S_t - S_{t-1}) + (1-\beta)T_{t-1}$ $I_t = \delta(X_t - S_t) + (1-\delta)I_{t-p}$ $\hat{X}_t(m) = S_t + mT_t + I_{t-p+m}$	$S_t = \alpha(X_t/I_{t-p}) + (1-\alpha)(S_{t-1} + T_{t-1})$ $T_t = \beta(S_t - S_{t-1}) + (1-\beta)T_{t-1}$ $I_t = \delta(X_t/S_t) + (1-\delta)I_{t-p}$ $\hat{X}_t(m) = (S_t + mT_t)I_{t-p+m}$
	Multiplicative	$S_t = \alpha X_t + (1-\alpha)(S_{t-1}R_{t-1})$ $R_t = \beta(S_t/S_{t-1}) + (1-\beta)R_{t-1}$ $\hat{X}_t(m) = S_t\, R_t^m$	$S_t = \alpha(X_t - I_{t-p}) + (1-\alpha)(S_{t-1}R_{t-1})$ $R_t = \beta(S_t/S_{t-1}) + (1-\beta)R_{t-1}$ $I_t = \delta(X_t - S_t) + (1-\delta)I_{t-p}$ $\hat{X}_t(m) = S_t\, R_t^m + I_{t-p+m}$	$S_t = \alpha(X_t/I_{t-p}) + (1-\alpha)(S_{t-1}R_{t-1})$ $R_t = \beta(S_t/S_{t-1}) + (1-\beta)R_{t-1}$ $I_t = \delta(X_t/S_t) + (1-\delta)I_{t-p}$ $\hat{X}_t(m) = (S_t\, R_t^m)I_{t-p+m}$
	Additive damped	$S_t = \alpha X_t + (1-\alpha)(S_{t-1} + \emptyset T_{t-1})$ $T_t = \beta(S_t - S_{t-1}) + (1-\beta)\emptyset T_{t-1}$ $\hat{X}_t(m) = S_t + \sum_{i=1}^{m} \emptyset^i T_t$	$S_t = \alpha(X_t - I_{t-p}) + (1-\alpha)(S_{t-1} + \emptyset T_{t-1})$ $T_t = \beta(S_t - S_{t-1}) + (1-\beta)\emptyset T_{t-1}$ $I_t = \delta(X_t - S_t) + (1-\delta)I_{t-p}$ $\hat{X}_t(m) = S_t + \sum_{i=1}^{m} \emptyset^i T_t + I_{t-p+m}$	$S_t = \alpha(X_t/I_{t-p}) + (1-\alpha)(S_{t-1} + \emptyset T_{t-1})$ $T_t = \beta(S_t - S_{t-1}) + (1-\beta)\emptyset T_{t-1}$ $I_t = \delta(X_t/S_t) + (1-\delta)I_{t-p}$ $\hat{X}_t(m) = \left(S_t + \sum_{i=1}^{m} \emptyset^i T_t\right) I_{t-p+m}$
	Multiplicative damped	$S_t = \alpha X_t + (1-\alpha)(S_{t-1}R_{t-1}^{\emptyset})$ $R_t = \beta(S_t/S_{t-1}) + (1-\beta)R_{t-1}^{\emptyset}$ $\hat{X}_t(m) = S_t\, R_t^{\sum_{i=1}^{m}\emptyset^i}$	$S_t = \alpha(X_t - I_{t-p}) + (1-\alpha)(S_{t-1}R_{t-1}^{\emptyset})$ $R_t = \beta(S_t/S_{t-1}) + (1-\beta)R_{t-1}^{\emptyset}$ $I_t = \delta(X_t - S_t) + (1-\delta)I_{t-p}$ $\hat{X}_t(m) = S_t\, R_t^{\sum_{i=1}^{m}\emptyset^i} + I_{t-p+m}$	$S_t = \alpha(X_t/I_{t-p}) + (1-\alpha)(S_{t-1}R_{t-1}^{\emptyset})$ $R_t = \beta(S_t/S_{t-1}) + (1-\beta)R_{t-1}^{\emptyset}$ $I_t = \delta(X_t/S_t) + (1-\delta)I_{t-p}$ $\hat{X}_t(m) = \left(S_t\, R_t^{\sum_{i=1}^{m}\emptyset^i}\right) I_{t-p+m}$

α	*Smoothing parameter for the level of the series*
β	*Smoothing parameter for the trend*
δ	*Smoothing parameter for seasonal indices*
ϕ	*Damping parameter*
m	*Number forecast period*
p	*Number of periods in the seasonal cycle*
S_t	*Smoothed level of the series in period(t)*
X_t	*Observed value of the time series in period(t)*
$\hat{X}_t(m)$	*Forecast for m periods ahead from (t)*
T_t	*Smoothed additive trend in period(t)*
R_t	*Smoothed multiplicative trend in period(t)*
I_t	*Smoothed seasonal index in period(t)*

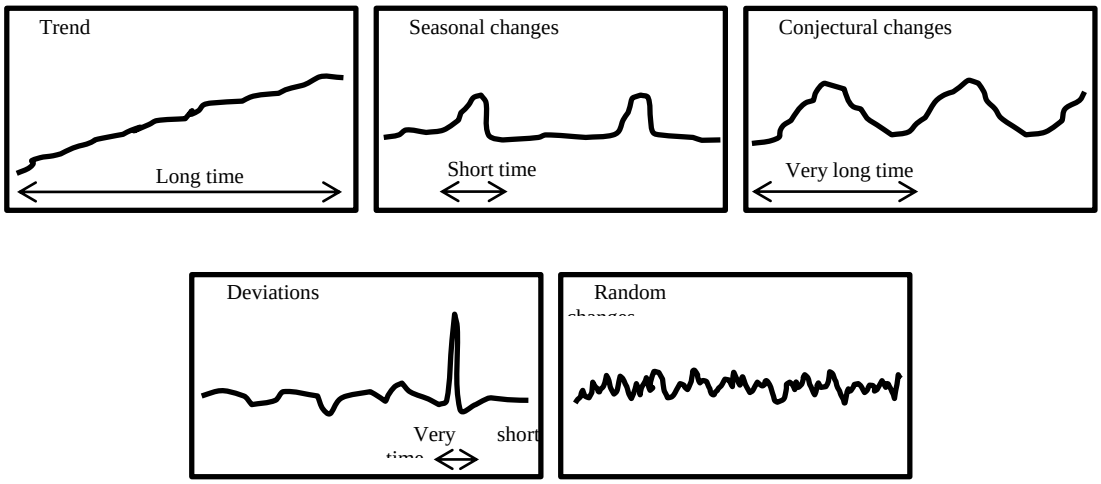

Fig. 1. The characteristics of the time series

Each one is selected independently according to the characteristics of the time series. Except for some studies, these parameters are chosen between 0 and +1 value as a general rule. Selecting of each parameter close to the value 0, it means reduced sensitivity to noise on the related components. But in this case, it becomes difficult to catch the changes of the related components. If the parameters are selected close to the value +1, the changes of the related components may be quickly caught. But in this case, noise will be effective on the estimates. If there are non-uniform or step changes of the time series, the error rates increase. Therefore, a different approach emerged that the smoothing factor should be changed sensitive to current changes of the time series. There are many methods introduced within the scope adaptive smoothing title but the most well-known method is Trigg and Leach version in the literature [5, 9]. This method is based on simple exponential smoothing method and only α parameter is adjusted.

$$S_{t+1} = \alpha_t X_t + (1 - \alpha_t) S_t \quad (1)$$

$$a_t = \left|\frac{E_t}{A_t}\right| \quad (2)$$

$$E_t = \gamma e_t + (1 - \gamma) E_{t-1} \quad (3)$$

$$A_t = \gamma |e_t| + (1 - \gamma) A_{t-1} \quad (4)$$

Where, α_t refers to the smoothing factor in period (t), E_t refers to the smoothed forecast error, At refers to the smoothed absolute error, γ refers to the arbitrarily selected constant, and et refers to the forecast error ($e_t = X_t - S_t$) in period (t). Although the Trigg and Leach method is one of the pioneer studies in adaptive smoothing methods, some cases it produces unstable forecast results [1,5]. Moreover, there are many studies used fixed smoothing factor that give better results than the adaptive version [1, 10, 11]. Regarding the adaptive smoothing approach, newly and promising studies continue for different time series characteristics [5, 12-17].

III. Quantitative Analysis

Simple Exponential smoothing (SES) and weighted moving average (WMA) methods are very similar mathematically. In both methods, it is important to choose right parameters according to the data set in order to reduce error rates. As shown in Fig. 2, the parameters are chosen (n=3; 0.5, 0.3, 0.2) for WMA method and (α=0.8) for ES method. ES method has two advantages compared to WMA method. The first, the forecast could start from the second iteration and secondly, the equation is simpler.

The objective function that minimizes the mean squared error can be used for the selection of the optimal smoothing factor. The changes of the time series are shown in Fig. 3 for large, small, and optimal values of the smoothing parameters. Mean square errors are found 1164 for α = 0.8, 1118 for α = 0.55, and 1215 for α = 0.2, respectively. Optimal value of α contained herein is calculated considering the whole time series. Therefore, using optimal factor will not be eligible for the next estimates, if there are the major changes that have occurred in the recent period of the series. In such cases, adaptive smoothing method is advisable.

The extended models of exponential smoothing, trends and seasonality components can be incorporated into the series; it enables to make more accurate estimates. Trends and seasonality components in the expanded exponential smoothing methodology presented in Table 1 can be analyzed as additive or multiplicative in the series. However, the choice of multiplicative model gives better results for the time series which includes linear and nonlinear trend. This situation may be understood from time series analysis in Fig. 4 and the rate of errors in Table 2. The time series including trend and seasonality, in the process of determination of the factors α, β and δ, it can be monitored which component is more effective

on the series. Here, the objective function that minimizes the mean squared error mentioned above can be used in determining the appropriate factors.

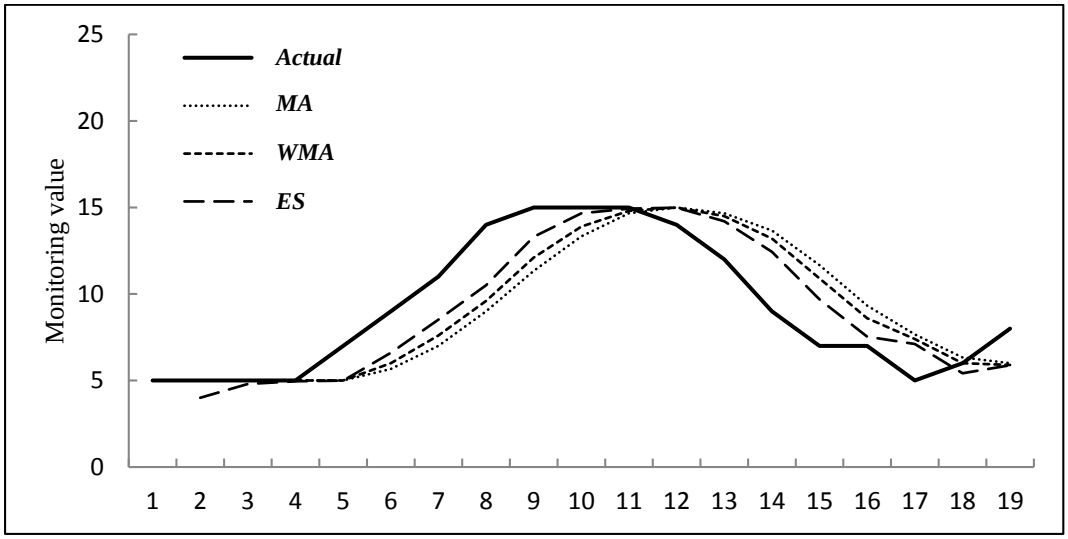

Fig. 2. The comparative forecast changes

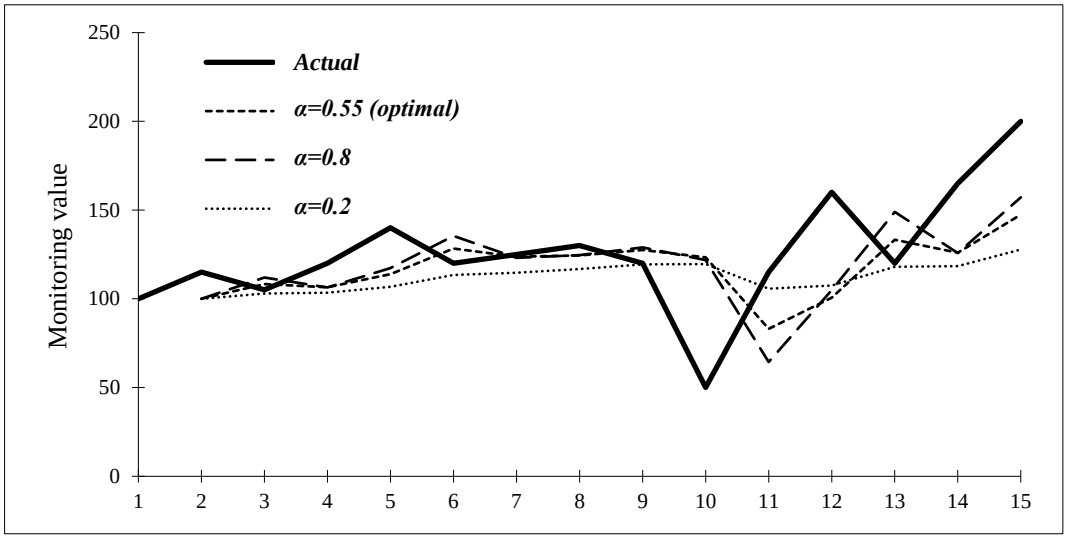

Fig. 3. The forecast changes for different α factors

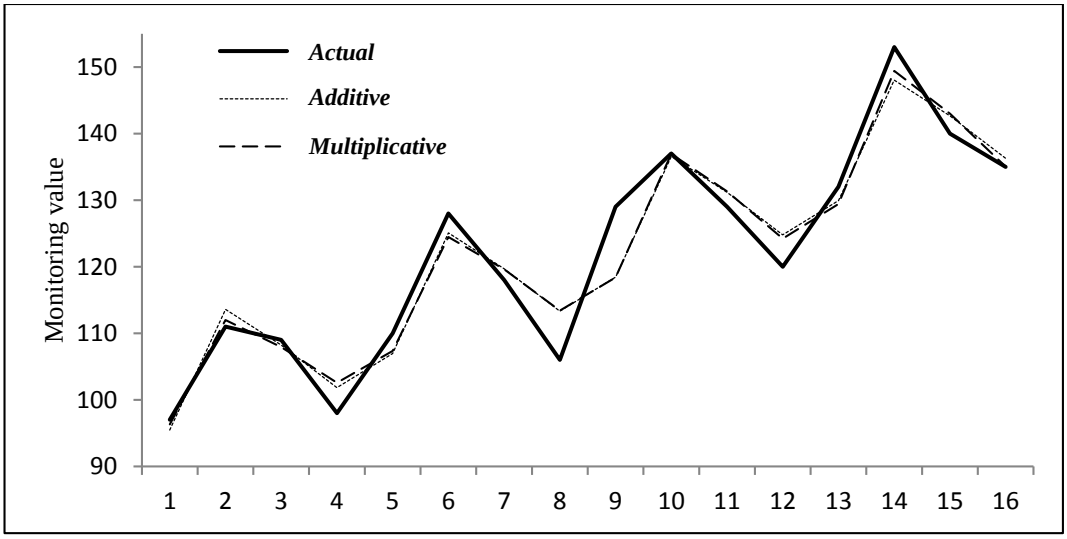

Fig. 4. The forecast changes for extended exponential smoothing methods

TABLE 2
STATISTICAL EVALUATION (FOR FIGURE 4)

Method	Errors		
	MAD	MSE	MAPE
Multiplicative (ES)	3.06	16.57	2.55%
Additive (ES)	3.29	17.24	2.74%

IV. RESULTS AND DISCUSSION

The characteristic of time series has a major importance to determine the methods and to select the smoothing factors used in the related method. Some suggestions should be considered in the choice of the factors for simple or expanded exponential smoothing methods:

For simple exponential smoothing;

- If the time series are unidirectional and stable, α can be selected close to 1,
- If the series changes character and continuous as the long-term stable, α can be selected close to 1,
- If there are short-term and continuing fluctuations in series, α can be selected close to 0,

For extended exponential smoothing;

- If the series contains a non-linear trend, in other words a change in the trend observed, the trend component β should be considered,
- The coefficient β can be determined in proportional to the trend changes rate in the real,
- If there are more or less repeated changes at regular intervals in the series, seasonality component δ should be considered,
- Some waveforms in the time series move by sliding in the periods and this situation should be kept out of the seasonality. Otherwise the error rate can increase depending on the width of the slide,

For adaptive smoothing;

- If major and permanent changes (steps, shifts, unidirectional and quick rises etc.) reveals on the series in non-periodic intervals, adaptive smoothing method may be preferred,
- If the changes happen on the very short-term as unstable fluctuations, using classic adaptive smoothing method may not be a solution. Because the error rates may increase. However, improved adaptive smoothing methods can offer solutions to this problem because it contains certain constraints.

ACKNOWLEDGMENT

The study is selected from National Engineering Research Symposium 2015 (Ulusal Mühendislik Araştırmaları Sempozyumu) UMAS 2015 (Duzce University).

REFERENCES

[1] E.S. Gardner, "Exponential smoothing: the state of the art", *Journal of Forecasting* vol. 4, no. 1, pp. 1–28, 1985.
[2] E.S. Gardner, "Exponential smoothing: the state of the art—part II", *International Journal of Forecasting*, vol. 22, pp. 637–666, 2006.
[3] J.T. Mentzer, M.A. Moon, "Sales Forecasting Management: A Demand Management Approach", Sage Puplications, UK, 2005.
[4] J.S. William, "*Operations Management*", McGraw-Hill Higher Education,USA, 2012.
[5] J.W. Taylor, Smooth Transition Exponential Smoothing, Journal of Forecasting, vol. 23, pp. 385–404, 2004.
[6] J.T. Mentzer, "Forecasting with adaptive extended exponential smoothing", *Journal of the Academy of Marketing Science*, vol. 16, no. 3-4, pp. 62-70, 1988.
[7] R.J. Hyndman, A.B. Koehler, R.D. Snyder, G. Simone , "A state space framework for automatic forecasting using exponential smoothing methods", *International Journal of Forecasting*, vol. 18, no.3, pp. 439–454, 2002.
[8] C.C. Pegels, "Exponential forecasting: some new variations", *Management Science*, vol. 12 pp. 311–315, 1969.
[9] D.W. Trigg, A.G. Leach, "Exponential smoothing with an adaptive response rate", *Operational Research Quarterly*, vol. 18, no. 1, pp. 53–59, 1967.
[10] S. Ekern, "Adaptive exponential smoothing revisited", *The Journal of the Operational Research Society*, vol. 32, no. 9 pp. 775-782, 1981.
[11] S. Makridakis, A. Andersen, R. Carbone, R. Fildes, M. Hibon, R. Lewandowski, J. Newton, E. Parzen, R. Winkler, "The accuracy of extrapolation (time series) methods: Results of a forecasting competition", *Journal of Forecasting*, vol. 1, pp. 111-153, 1982.
[12] D.C. Whybark, "Comparison of adaptive forecasting techniques", *Logistics Transportation Review*, vol. 8, pp. 13–26, 1973.
[13] D.W. Bunn, "Adaptive forecasting using the Kalman filter", *Omega*, vol. 9, pp. 323–324, 1981.
[14] P.C. Young, "Nonstationary time series analysis and forecasting", *Progress in Environmental Science*, vol. 1, pp. 3–48, 1999.
[15] J.T. Mentzer, R. Gomes, "Further extensions of adaptive extended exponential smoothing and comparison with the M-Competition", *Journal of the Academy of Marketing Science*, vol. 22, pp. 372–382, 1994.
[16] S.N. Pantazopoulos, C.P. Pappis, "A new adaptive method for extrapolative forecasting algorithms", *European Journal of Operational Research*, vol. 94, pp. 106–111, 1996.
[17] C.W.J. Granger, T. Teräsvirta, "*Modelling nonlinear economic relationships, advanced texts in econometrics*", Oxford University Press: New York, 1993.

BIOGRAPHIES

Yunus BICEN received the MSc. degree in Electrical Education from the University of Kocaeli in 2006 and the PhD degree in 2012 at the same university. He is presently working as Assist. Prof. at the Department of Electronics and Automation in the University of Duzce. His research interests are in power system condition monitoring, service lifetimes, transformers and cables.

Mustafa KAYIKCI received the MSc. degree in Faculty of Arts and Sciences Mathematics from the University of Sakarya in 2003 and the PhD degree in 2010 at the same university. He is presently working as Assist. Prof. at the Department of Computer Technologies in the University of Duzce. His research interests are in double-dimensional arrays spaces, Riesz difference sequence spaces.

Faruk ARAS received the B.Sc. degree from Marmara University, Electrical Education Department, Istanbul, Turkey in 1994, the MSc and PhD degrees from Kocaeli University, Kocaeli, Turkey in 1996 and 2001, respectively. He is a Professor at the Department of Aircraft Electrical and Electronics in Kocaeli University. His current research interests are in the area of power system, aging, cables and transformers.

Wind Speed Potential Analysis Based on Weibull Distribution

E. Dokur, and M. Kurban

***Abstract*— Weibull probability density function used to determine the wind energy potential commonly. In this paper, wind energy potential of Bilecik region is analyzed statistically by using the Turkish State Meteorological Service's hourly wind speed data between 2010-2014 measured in Bilecik meteorological station. It is used the two- parameter Weibull to determine wind energy potential of the region. The parameters of the Weibull distributions used for finding the estimation of average speed, standard deviation, and power density is found by using the Maximum likelihood method. All analysis is carried out by Matrix Laboratory (MATLAB) programming language. Monthly and yearly wind speeds are modeled by Weibull distribution statistically. Accuracy of the modeling is evaluated in terms of Root Mean Square Error (RMSE).**

***Index Terms*— Weibull Distribution, Wind Speed, Energy.**

I. INTRODUCTION

GLOBALLY fossil resources have very wide application area. The reason that fossil fuels used for meeting the energy need shall run short together with the fact that they are harmful for the environment leaded the path for a search of new energy sources worldwide and renewable energy sources have gained importance in this respect.

One of the renewable energy resources is wind energy. Actually wind energy which is the oldest source has been used since BC 2800 by humankind. Until recent year this energy has been used for water pumping and power generation in rural areas. Today it is used as an alternative source of energy production. Wind energy systems operate depend on wind regime, wind shaft position and size of power generation system [1,2].

Wind energy conversion systems are chosen based on wind speed potential analysis of a region. Frequency distribution of wind speed can be displayed different distributions such as Gamma, lognormal, Rayleigh and Weibull. Two parameter Weibull distribution is used to model of many regions of the world wind speed in recent year. The reason of using this method is very good fit wind distribution [3].

E. Dokur, Electrical and Electronics Engineering Department , Bilecik S.E. University, Bilecik, Turkey, (e-mail: emrah.dokur@bilecik.edu.tr).

M. Kurban, Electrical and Electronics Engineering Department , Bilecik S.E. University, Bilecik, Turkey, (e-mail: mehmet.kurban@bilecik.edu.tr)

Two Weibull parameters are estimated using both the graphical and maximum likelihood methods. Genc et al [4]. Wind energy potential of Nigde region is studied statistically by using the Turkish State Meteorological Service's hourly wind speed data between 2008 and 2009 measured in Nigde meteorological station by Yıldırım et al [5]. On the side, there is novel method about Weibull distribution in literature [6].

In this paper, wind energy potential is modelled based on two parameter Weibull distribution statistically for Bilecik ,city in Turkey, by using the Turkish State Meteorological Service's hourly wind speed data between 2010 and 2014 measured. Scale and shape parameters are determined by maximum likelihood method. Matlab © (Matrix Laboratory) software is used for all analyses. Performance criteria of model is shown that RMSE (Root Mean Square Error).

II. WEIBULL DISTRIBUTION

There are different methods for determining the wind speed distributions. In the literature, the two parameters Weibull distribution is often used in the statistical analysis of data. The Weibull distribution function is given by formula (1) :

$$f(\mathrm{v}) = \frac{k}{c}\left(\frac{v}{c}\right)^{k-1} e^{-\left(\frac{v}{c}\right)^{k}} \qquad (1)$$

Where $f(v)$ is the frequency or probability of occurrence of wind speed V, c is the Weibull scale parameter with unit equals to the wind speed unit and k is the unitless Weibull shape parameter. The higher value of *c* indicates that the wind speed is higher, while the value of k shows the wind stability. *k* shape parameters are between 1.2 and 2.75 in the literature. The cumulative Weibull distribution function F(V) gives the probability of the wind speed exceeding the value V. It is expressed by formula (2):

$$\mathrm{F(v)} = 1 - e^{-\left(\frac{v}{c}\right)^{k}} \qquad (2)$$

Maximum frequency of wind speed is determined by formula (3):

$$v_{\mathrm{mod}} = c\left(1 - \frac{1}{k}\right)^{1/k} \qquad (3)$$

Maximum wind speed can be calculated formula (4) [7] :

$$v_{maks} = c\left(\frac{k+2}{k}\right)^{1/k} \quad (4)$$

Wind power is found commonly by formula (5) :

$$P = \frac{1}{2}\rho A v^3 \quad (5)$$

Where ρ (kg/m^3) is air density, A (m^2) is swept area. Mean power density for Weibull distribution is given by formula (6):

$$P_w = \frac{1}{2}\rho c^3 \Gamma\left(1+\frac{3}{k}\right) \quad (6)$$

Where Γ is gamma function. Here, taking into account, the density of the air at sea level, 1 atmosphere pressure and 16.6. Celsius degree ρ_0 =1.225 kg/m^3 value; the corrected air density in reference to the height of the sea level (H_m) and other location information can be found according to formula (7) [8].

$$\rho = \rho_0 - 1.194.10^{-4} H_m \quad (7)$$

As is seen that the most important input is wind speed data for determining of power potential. Wind direction is important for position of installation wind energy conversion systems.

III. Maximum Likelihood Method

Several methods are available in order to determine the two parameters of Weibull distribution. One of these methods is maximum likelihood method that is proposed by Steven and Smulders [9]. Maximum likelihood method requires large scale numerical iterations. Shape parameter and scale parameter are calculated by formula (8) and formula (9):

$$k = \left(\frac{\sum_{i=1}^{n} v_i^k \ln(v_i)}{\sum_{i=1}^{n} v_i^k} - \frac{\sum_{i=1}^{n} \ln(v_i)}{n}\right)^{-1} \quad (8)$$

$$c = \left(\frac{\sum_{i=1}^{n} (v_i)^k}{\sum_{i=1}^{n} v_i^k}\right)^{\frac{1}{k}} \quad (9)$$

Where v_i is wind speed and n is number of wind speeds.

Performance criteria of analysis is shown Root Mean Square Error (RMSE) by formula (10).

$$RMSE = \sqrt{\frac{1}{n}\sum_{i=1}^{n} (y_i - x_i)^2} \quad (10)$$

Where, y_i is the actual wind speed probability value, x_i is the probability value calculated from Weibull distribution and n is the number of observations.

IV. Wind Speed Potential Analysis

Future and available wind potential is very important to build of wind energy conversion system. For this reason estimation parameter results of distribution are studied monthly. Optimum model can be chosen according to performance criteria. In this paper, estimation of monthly and annual parameters for Bilecik region are implemented in table 1 by using hourly wind speed data between 2010 and 2014. The maximum likelihood method was used for determining Weibull parameters.

It can be seen from the Figure 1 that Weibull distribution function and cumulative distribution function of sample data, April 2010, was shown.

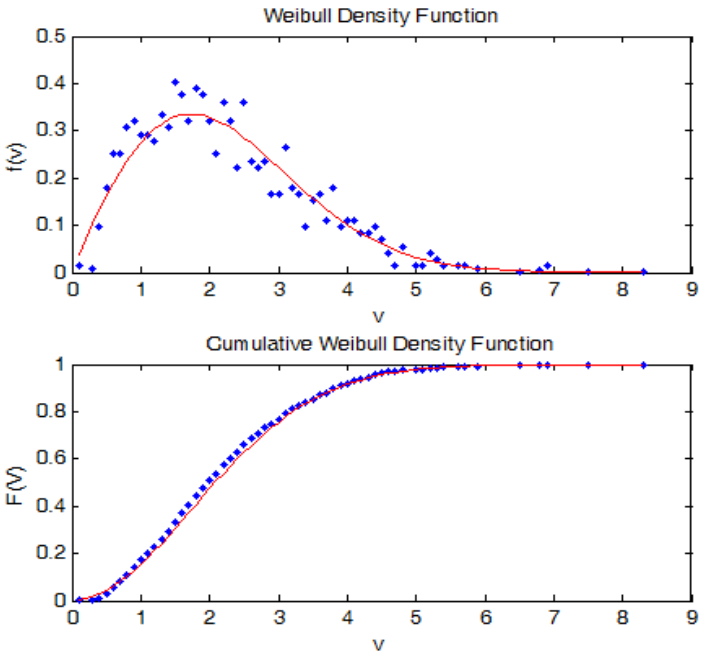

Fig.1. Probability density and cumulative probability density function for sample months

TABLE 1
WEIBULL PARAMETERS AND ERROR VALUES

	2010			2011			2012			2013			2014		
Months	**k**	**c**	**RMSE**	**k**	**c**	**RMSE**	**k**	**c**	**RMSE**	**k**	**c**	**RMSE**	**k**	**c**	**RMSE**
January	1.8139	2.4980	0.0254	2.0186	2.1777	0.0232	1.8901	2.4506	0.0367	2.2400	2.4860	0.0284	2.1885	2.0545	0.0328
February	1.8435	2.4785	0.0250	2.0939	2.0817	0.0281	1.9126	3.1130	0.0338	2.1236	2.2914	0.0387	1.9435	1.8455	0.0406
March	1.8592	2.4059	0.0228	1.8042	2.4342	0.0311	1.8626	2.2839	0.0304	2.0730	1.2524	0.0364	2.2748	2.1660	0.0261
April	1.9416	2.5110	0.0172	1.7541	2.4472	0.0301	1.7668	2.6074	0.0318	2.3111	2.3331	0.0267	2.0241	2.0614	0.0320
May	1.7574	2.3265	0.0292	2.0714	2.2945	0.0197	1.9938	2.1983	0.0317	1.9387	2.3502	0.0322	2.0202	2.0965	0.0258
June	1.9759	2.5162	0.0267	2.1847	2.3154	0.0177	1.9064	2.4906	0.0287	1.9435	2.6441	0.0322	2.1401	2.3132	0.0294
July	2.2358	2.9342	0.0158	2.1570	2.6608	0.0220	2.1363	2.9130	0.0231	2.3567	3.1580	0.0247	2.2348	2.5420	0.0301
August	1.9625	2.7771	0.0177	2.2373	2.9908	0.0246	2.0782	2.8532	0.0287	2.1287	2.8553	0.0362	2.0093	2.5030	0.0324
September	2.0343	2.4339	0.0204	2.2018	2.4763	0.0186	1.9479	2.3917	0.0280	2.0093	2.3163	0.0291	2.1629	2.1439	0.0353
October	1.7729	2.0780	0.0393	2.1314	2.1950	0.0222	2.1143	2.0224	0.0353	1.8692	2.0347	0.0367	2.2758	1.8371	0.0390
November	1.7828	2.1033	0.0341	2.2821	1.9283	0.0297	2.3329	2.1829	0.0259	2.2285	1.7290	0.0391	2.1381	1.8864	0.0371
December	1.9091	2.4441	0.0339	1.8086	2.2769	0.0437	1.8765	2.2167	0.0413	2.1275	2.2904	0.0321	1.9591	1.7732	0.0347
Yearly	1.8535	2.4775	0.0204	2.0053	2.3580	0.0203	1.8976	2.4743	0.0263	1.9156	2.3089	0.0268	2.0466	2.1061	0.0284

Wind data, consisting of hourly wind speed records over a 5-year period, 2010-2014, were measured in the Turkish State Meteorological Service in Bilecik. In Bilecik region by using wind speed measured for 4 years between 2010 and 2014, the conformity of wind speed blowing hours with Weibull function has been examined. Distribution of Wind speed is shown by Weibull functions. Scale and shape parameters are calculated 1.8535,2.0053,1.8976,1.9156,2.0466 and 2.4775, 2.3580, 2.4743, 2.3089, 2.1061 (m/s) for years, respectively.

Table 1 shows scale and shape parameters for each months of five years and error values.

Other values of 2013 and 2014 years are illustrated in Table 2. σ is standard deviation of wind speed in formula (11). Other formulas of wind speed parameters were given in section 2.

$$\sigma = \sqrt{c^2[\Gamma(1+\frac{2}{k}) - \Gamma^2(1+\frac{2}{k})]} \qquad (11)$$

Probability density and cumulative probability density functions of wind speed are illustrated in Figure 2 and 3, respectively for 2010-2014 years.

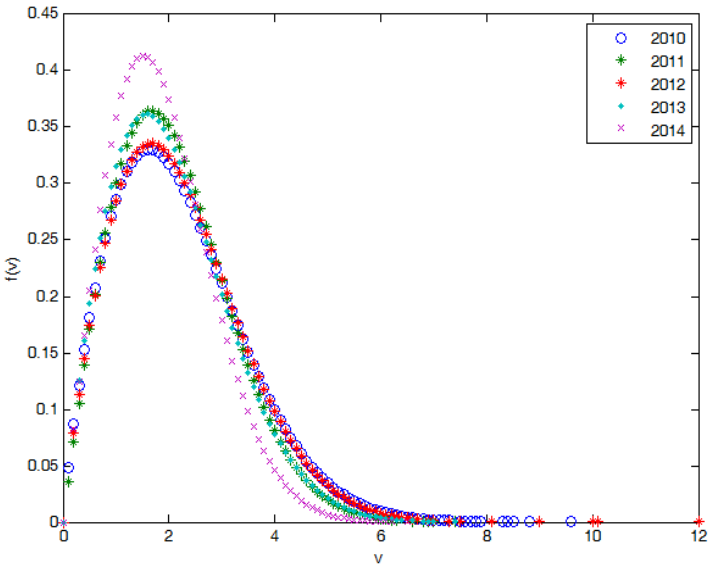

Fig.2. Probability density functions of Weibull distributions

TABLE II
WIND VALUES AND POWER DENSITY

Months	2013					2014				
	v_m	σ	v_{mod}	v_{maks}	P_w	v_m	σ	v_{mod}	v_{maks}	P_w
January	2.2018	1.0396	1.9091	3.3053	10.31	1.8195	0.8772	1.5544	2.7639	5.93
February	2.0294	1.0051	1.6980	3.1320	8.46	1.6365	0.8778	1.2724	2.6559	4.84
March	1.1094	0.5615	0.9115	1.7348	1.41	1.9186	0.8934	1.6791	2.8582	6.73
April	2.0671	0.9490	1.8256	3.0557	8.31	1.8265	0.9445	1.4723	2.8948	6.46
May	2.0842	1.1225	1.6167	3.3876	10.02	1.9368	1.0050	1.8425	3.1246	8.50
June	2.3448	1.2577	1.8230	3.8054	14.24	2.0486	1.0076	1.7236	3.1487	8.64
July	2.7986	1.2625	2.4983	4.0986	20.31	2.2514	1.0652	1.9494	3.3837	11.04
August	2.5287	1.2497	2.1194	3.8976	16.34	2.2180	1.1546	1.7768	3.5300	11.65
September	2.0526	1.0685	1.6443	3.2668	9.23	1.8987	0.9250	1.6092	2.9019	6.81
October	1.8065	1.0037	1.3508	3.0029	6.79	1.6273	0.7575	1.4246	2.4237	4.10
November	1.5313	0.7263	1.3235	2.3047	3.48	1.6706	0.8224	1.4046	2.5690	4.69
December	2.0285	1.0030	1.6994	3.1275	8.43	1.5722	0.8373	1.2315	2.5394	4.25
Yearly	2.0483	1.1131	1.5705	3.3535	9.63	1.8658	0.9553	1.5177	2.9396	6.81

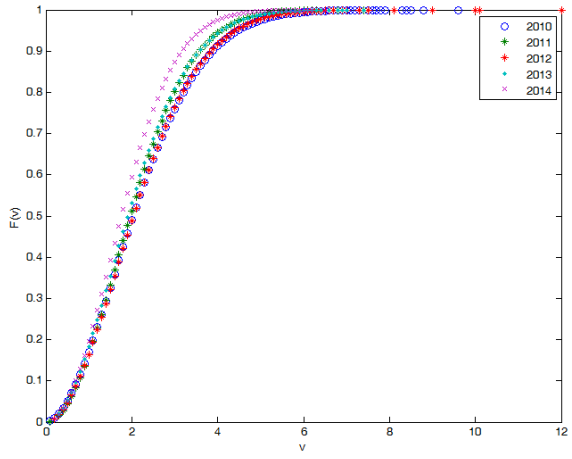

Fig.3. Cumulative probability density function

V. CONCLUSIONS

It is necessary to establish determine wind speed distribution for establishing a region of wind energy potential. Wind power density distribution is determined according to the definition of wind speed.

The wind energy potential in Bilecik is statistically analyzed based on wind speed data which measured hourly in 2010-2014.

It is used the Weibull distribution to determine wind energy potential of the region. Determination of Weibull parameters was used maximum likelihood method. Weibul shape parameter, k and scale parameter, c are found yearly, 1.8535,2.0053,1.8976,1.9156, 2.0466 and 2.4775, 2.3580, 2.4743, 2.3089, 2.1061 (m/s) , respectively.

The lowest power density is observed in winter and autumn for Bilecik region in 2010-2014. Generally, average wind speed and power density values are high in summer. However average wind speed and power density is not only important but also data distribution is significant for energy production.

The studies should continue and the measurements should be done in different regions and at different heights and for long periods of time. The whole region should be examined thoroughly, the characteristics of the region should be identified and cost analysis should be carried out. As a result it is possible to make more accurate and true assessments. Our work about identification and evaluation of renewable energy potential of this region will be continued.

Such studies which are determined to speed up the use of these energy sources and its production in our country is very important for our future.

ACKNOWLEDGMENT

The study is selected from National Engineering Research Symposium 2015 (Ulusal Mühendislik Araştırmaları Sempozyumu) UMAS 2015 (Duzce University).

REFERENCES

[1] Kurban, M., Kantar, Y. M., & Hocaoğlu, F. O. (2006). Rüzgar Enerjisi Potansiyelinin Araştırılmasında Weıbull Ve Rayleıgh Dağılımının Kullanılması. Sakarya Üniversitesi Fen Bilimleri Enstitüsü Dergisi, 10(1), 14-21.

[2] Kurban, M., Hocaoğlu, F. O., & Kantar, Y. M. (2011). Rüzgar Enerjisi Potansiyelinin Tahmininde Kullanılan İki Farklı İstatistiksel Dağılımın Karşılaştırmalı Analizi. Pamukkale University Journal Of Engineering Sciences, 13(1).

[3] Akdağ, S. A., & Güler, Ö. (2008) Weibull Dağılım Parametrelerini Belirleme Metodlarının Karşılaştırılması. VII. Ulusal Temiz Enerji Sempozyumu, UTES'2008 17-19 Aralık 2008, İstanbul,707-714.

[4] Genc, A., Erisoglu, M., Pekgor, A., Oturanc, G., Hepbasli, A., & Ulgen, K. (2005). Estimation of wind power potential using Weibull distribution. Energy Sources, 27(9), 809-822.

[5] Yıldırım, U., Gazibey, Y., & Güngör, A. (2012). Niğde İli Rüzgar Enerjisi Potansiyeli. Mühendislik Bilimleri Dergisi, 1(2), 37-47.

[6] Akdağ, S. A., & Dinler, A. (2009). A New Method To Estimate Weibull Parameters For Wind Energy Applications. Energy Conversion And Management, 50(7), 1761-1766.

[7] Cheng, R. C. H., & Amin, N. A. K. (1983). Estimating parameters in continuous univariate distributions with a shifted origin. Journal of the Royal Statistical Society. Series B (Methodological), 394-403.

[8] Patel, M. R. (2005). Wind and solar power systems: design, analysis, and operation. CRC press.

[9] Stevens, M. J. M., & Smulders, P. T. (1979). The estimation of the parameters of the Weibull wind speed distribution for wind energy utilization purposes. Wind engineering, 3, 132-145

BIOGRAPHIES

Emrah DOKUR was born in Istanbul, Turkey in 1987. He received the B.Sc. in Electrical and Electronics Engineering from Faculty of Engineering, Istanbul University, Turkey in 2010 and M.Sc. degrees in Electrical Engineering, Istanbul Technical University, Turkey in 2013. He is a Ph.D. student Department of Energy System Engineering in Bilecik S.E. University. Since 2011, he has been research assistance in the same university. His research areas include high voltage engineering, renewable energy systems, power system analysis.

Mehmet KURBAN was born in Istanbul, Turkey. He graduated from Istanbul Technical University (ITU) in Turkey as an Electrical Engineer from Faculty of Electrical and Electronics Engineering in 1991. He got M. Sc. and Ph. D degree from ITU in 1994 and 2001, respectively. Since 2011, he has been professor in the same Bilecik S.E. University. His special fields of interest included renewable energy, power system cost analysis and optimization.

The Investigation of Channel Selection Effects on Epileptic Analysis of EEG Signals

M. Yıldız, and E. Bergil

***Abstract*—A great number of methods are used in order to increase the speed of decision units in epileptic analysis of the multi-channel EEG signals. Channel selection is one of the main methods used for the reduction of the processing load. By eliminating the non-distinct channels, the performance of the system can be improved. In this study, the seizure detection performances of EEG signals obtained by 21 different channels were evaluated. This study was carried out patient-specifically for each six patients. The feature set is generated via calculating 26 features from EEG signals. The dimension of feature set for each channel is reduced using Principal Component Analysis. The reduced feature sets were divided as training and testing data using cross-validation method. With Linear Discriminant Analysis, the classification was done for each channel and performances of channel were compared. Depending on the channel selection, almost 9% differences in the classification accuracies have been observed.**

***Index Terms*—Epilepsy, seizure detection, channel selection, classification.**

I. INTRODUCTION

EPILEPSY is a disease that is characterized by recurrent seizures. It occurs without impulse and causes disturbance in the nervous system. Seizures, can be detected with clinical symptoms, are the temporary anomalies of the electrical activities caused by a group cell in brain. EEG signal has been widely used in the study and diagnosis of epilepsy. The EEG signals can be obtained by placing necessary electrode from different centers and direct measures [1,2,3]. Electrode placement, used the most widely for Multi-channel EEG measurement, is the 10-20 system. Electrode placement for extended 10-20 system is shown in the Figure 1.

Getting started to use the high-performance processors has caused to raise the interest to the issues such as the emergence of seizure phase, detection, and prediction [4]. For the purpose of getting the most meaningful performance in EEG analysis, it is necessary to get the desired signal among multi-channel measurements. In addition, the signals containing unnecessary information and noise have decrease the performance. Moreover, they cause to lower the reaction speed of the system [5].

M. Yıldız, Electrical-Electronics Engineering Department, Faculty of Engineering,Sakarya University, , P.O. Box 54187 , Sakarya, Turkey, (e-mail: myildiz@sakarya.edu.tr).

E. Bergil, The Program ofControl and Automation Technology,Electronics and Automation Department, Technical Sciences Vocational School, Amasya University, P.O. Box 05100, Amasya, Turkey, (e-mail: erhan.bergil@amasya.edu.tr).

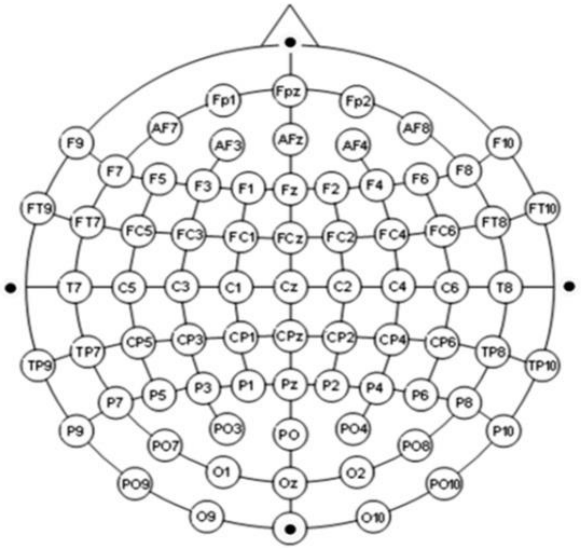

Fig.1. Extended 10/20 system on the cap

Qaraqe et al., have suggested a new architecture to develop the performance of seizure detector. In their studies carried out for patient-specific, they have improved the system sensitivity at 7 % higher than the current ones by utilizing channel selection and feature enhancement. They also have decreased the number of the fault detection appeared per hour [6].

Duun-Henriksen et al., have examined the effects of different channel selection methods on the performance of seizure detection. In their study where they extracted features by using wavelet transform, they used support vector machines as classifier. They reached to the best achievement by the method of maximum variance based channel selection instead of focal channels used extensively. Using only 3 channels, they performed seizure detection without performance reduction [7].

Faul and Marnane have developed dynamic electrode selection method to decrease power consumption in seizure detection. They have provided power saving at 47 % without any decrease in detection performance in the study where they evaluated power consumption and detector performance by using different number of electrodes [8].

Tekgul et al., have performed seizure detection via EEG records taken from newborns with the 10-20 electrode system.

As a result of the classification performed by using all the electrodes, they have detected the all 31 seizures. They repeated the all processes by using only 9 electrodes. Although they couldn't detect only one patient's seizure for the reduced montage, they reached 100 % specificity and 96,8 % sensitivity respectively comparing with the results taken by using all electrodes [9].

Channel selection process was frequently used to decrease the load of the processor especially in real time applications. With the channel selection process, it was aimed to eliminate the channels not including distinguishing information. By this way, it is possible to design high-speed detectors without losing performance in the process of seizure detection. In this study, the effects of EEG signals taken from different channels on epileptic analysis have been evaluated. The multi-channel EEG signals taken from 6 epilepsy patients have been analyzed. Since the characteristics of epilepsy differs patient specifically, the analysis have been done in accordance to the patient specifically. At the beginning, feature sets from normal and seizure stage EEG signals for each channel have been generated. In the following step, the dimension of these feature sets has been decreased via Principal Component Analysis (PCA). 26 features were reduced to 8 features. The feature set for each channel has been divided into 2 parts as testing and training data by the method of cross-validation. Via Linear Discriminant Analysis (LDA), classification process has been carried out for 21 different channels and their classification accuracies have been compared. In consequences of the analysis, it is aimed to contribute to the design and production studies of portable seizure detection systems by determining the effects of channel on epileptic analysis.

II. MATERIAL AND METHOD

In this study, the process consists of pre-processing, feature extraction, dimension reduction, PCA distribution and classification stages. First of all, pre-processing where the EEG signals taken from normal and seizure phases divided into 5 second parts has been performed. In the second stage, feature set has been obtained by calculating 26 features for each EEG period. Feature set has been calculated for different 21 channels. Then, the number of the features has been decreased to 8 by PCA method. With cross-validation method, testing and training data have been obtained and by this way the classification process has been performed. LDA method has been used for classifier. The classification process has been performed by using 1000 different testing and training data. The classification results and data of testing and training have been registered for the highest classification performance. In order to observe the effect of channels on classification performance, PCA projection has been used. The testing data of channels having the highest and lowest accuracy which belongs to the patient 4 has been reflected to the plane consisting of the highest weight first two principal components and the principal component distribution has been obtained. The block schema of this process has been illustrated in the Figure 2.

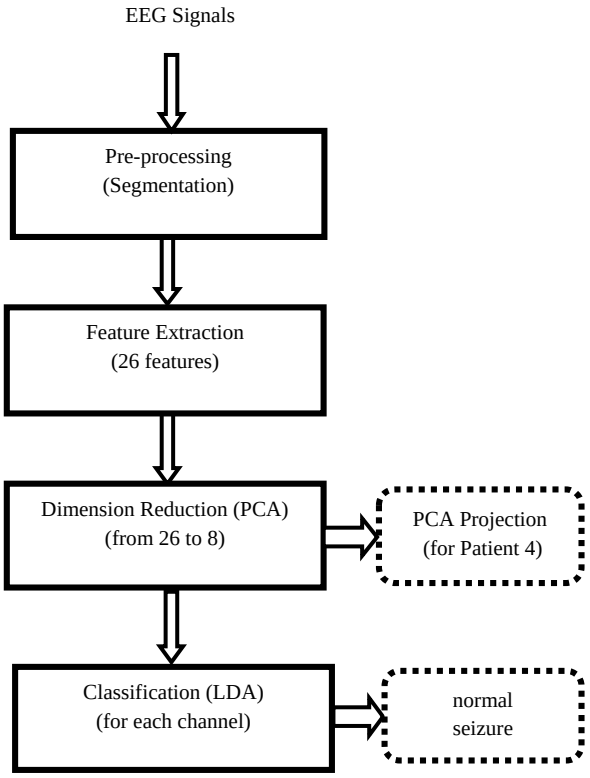

Fig.2. Block diagram of the process

EEG signals were taken from PhysioNet database [10]. The scalp EEG signals were obtained using 10-20 electrode system and sampled in 256 Hz. The starting points and total durations of seizures in EEG records were remarked by the specialists. Data, taken from seizure and seizure-free stages, were divided into 5 second periods. This study was done for 6 epilepsy patients. The demographic information of patients is given in the Table I.

TABLE I
DEMOGRAPHIC INFORMATION

Patient	Sex	Age
Patient 1	Female	11
Patient 2	Female	14
Patient 3	Female	15
Patient 4	Male	3.5
Patient 5	Male	3
Patient 6	Female	6

The numbers of sample belong to normal and seizure stage for all patient are given in the Table II.

TABLE II
THE SAMPLE NUMBERS FOR EACH PATIENT

Patient	Normal Stage	Seizure Stage
Patient 1	192	88
Patient 2	192	78
Patient 3	192	108
Patient 4	192	182
Patient 5	192	88
Patient 6	192	84

Feature Extraction: 26 features widely used in epilepsy studies are selected. These features, based on time-domain, frequency-domain and power spectrum, are given in the Table III.

TABLE III
FEATURES

No	Feature	No	Feature
1	Mean	11	Hjorth Activity
2	Standard Deviation	12	Hjhort Mobility
3	Variance	13	Hjhort Complexity
4	Total Power	14	Renyi Entropy
5	Power of Delta Band (0.5-2 Hz)	15	Entropy
6	Power of Delta Band (2-4 Hz)	16	Maximum
7	Power of Theta Band	17	Minimum
8	Power of Alpha Band	18	Zero Cross Rate
9	Power of Beta Band	19-26	Auto-Regressive Coefficients (Burg Method)
10	Mod		

*Dimension Reduction:*26 features generated from EEG signals have been decreased to 8 with the method of Principal Component Analysis. The studies of principal component analysis started with Karl Pearson in 1901 were developed by Hotelling in 1933. It is a transform technique which uses to convert a data set of correlated variables into a set of linearly uncorrelated variables. This method can be used for dimension reduction. The variables after the transformation are called as principal components of first variables. The first principal component has the highest variance value and the other principal components are in the decreasing variance values order. Low sensitivity towards noise, the decrease of the memory and capacity needs can be mentioned among its main advantages [11,12].

Classification: In classification stage of this study, Linear Discrimination Analysis has been performed. The feature set has been divided into testing and training data by cross-validation method for each patient. At the end of this classification process, it was aimed to detect the normal and seizure stage of the testing data.

Linear Discriminant Analysis is one of the classification methods that is commonly used in the fields of machine learning and statistics. LDA is a method of which features can be used as linear classifiers to separate the samples of two or more classes and which tries to find the linear combination. In other words, LDA is a method, tries in order to get vectors belong to the space, which are able to separate each classes [13-17].

This approach generates a new variable which is the combination of the available data. This variable closers to data points in the same class each other, and pushes apart the data points belonging to different classes [14,16,17].

III. RESULTS OBTAINED AND DISCUSSION

The all feature sets have been divided into training and testing data with the cross-validation method. Afterwards, classification has been performed by using LDA. This process was repeated 1000 times for 21 channels, the training and testing data that have the highest accuracy classification performance was registered. As a result of this processes, the best classification performances belonging to 6 patients for 21 different channels have been shown in the tables IV,V,VI,VII,VIII and IX. In the tables, the channels showing the worst classification performances have been highlighted.

TABLE IV
THE CLASSIFICATION RESULTS FOR PATIENT 1

Channel	normal stage		seizure stage		Accuracy
	normal	seizure	normal	seizure	
Fp1-F7	64	0	0	29	100
F7-T7	64	0	0	29	100
T7-P7	64	0	0	30	100
P7-O1	64	0	0	29	100
Fp1-F3	64	0	0	29	100
F3-C3	64	0	0	30	100
C3-P3	64	0	0	29	100
P3-O1	64	0	0	29	100
Fp2-F4	64	0	0	29	100
F4-C4	64	0	0	29	100
C4-P4	64	0	0	29	100
P4-O2	64	0	0	30	100
Fp2-F8	64	0	0	29	100
F8-T8	64	0	0	30	100
T8-P8	64	0	0	29	100
P8-O2	**64**	**0**	**1**	**28**	**98,92**
Fz-Cz	64	0	0	30	100
Cz-Pz	64	0	0	29	100
T7-Ft9	64	0	0	30	100
Ft9-Ft10	64	0	0	29	100
Ft10-T8	**63**	**1**	**0**	**29**	**98,92**

TABLE V
THE CLASSIFICATION RESULTS FOR PATIENT 2

Channel	normal stage		seizure stage		Accuracy
	normal	seizure	normal	seizure	
Fp1-F7	64	0	0	26	100
F7-T7	64	0	0	26	100
T7-P7	64	0	0	26	100
P7-O1	64	0	0	26	100
Fp1-F3	64	0	0	26	100
F3-C3	64	0	0	26	100
C3-P3	64	0	0	26	100
P3-O1	64	0	0	26	100
Fp2-F4	64	0	0	26	100
F4-C4	64	0	0	26	100
C4-P4	64	0	0	26	100
P4-O2	64	0	0	26	100
Fp2-F8	64	0	0	26	100
F8-T8	**63**	**1**	**0**	**26**	**98,89**
T8-P8	64	0	0	26	100
P8-O2	64	0	0	26	100
Fz-Cz	64	0	0	26	100
Cz-Pz	64	0	0	26	100
T7-Ft9	64	0	0	26	100
Ft9-Ft10	64	0	0	26	100
Ft10-T8	64	0	0	26	100

TABLE VI
THE CLASSIFICATION RESULTS FOR PATIENT 3

Channel	normal stage		seizure stage		Accuracy
	normal	seizure	normal	seizure	
Fp1-F7	62	2	0	36	98
F7-T7	63	1	2	34	97
T7-P7	**63**	**1**	**3**	**33**	**96**
P7-O1	64	0	2	34	98
Fp1-F3	63	1	2	34	97
F3-C3	64	0	0	36	100
C3-P3	64	0	0	36	100
P3-O1	64	0	0	36	100
Fp2-F4	63	1	2	34	97
F4-C4	64	0	1	35	99
C4-P4	64	0	0	36	100
P4-O2	64	0	0	36	100
Fp2-F8	64	0	0	36	100
F8-T8	64	0	3	33	97
T8-P8	61	3	0	36	97
P8-O2	63	1	0	36	99
Fz-Cz	64	0	0	36	100
Cz-Pz	64	0	0	36	100
T7-Ft9	64	0	2	34	98
Ft9-Ft10	64	0	0	36	100
Ft10-T8	64	0	2	34	98

TABLE VII
THE CLASSIFICATION RESULTS FOR PATIENT 4

Channel	normal stage		seizure stage		Accuracy
	normal	seizure	normal	seizure	
Fp1-F7	61	3	3	58	95,2
F7-T7	61	3	0	61	97,6
T7-P7	62	2	1	60	97,6
P7-O1	64	0	1	60	99,2
Fp1-F3	**60**	**4**	**7**	**54**	**91,2**
F3-C3	61	3	7	53	91,94
C3-P3	63	1	6	55	94,4
P3-O1	61	3	0	61	97,6
Fp2-F4	63	1	4	57	96
F4-C4	63	1	0	61	99,2
C4-P4	61	3	0	61	97,6
P4-O2	64	0	0	61	100
Fp2-F8	60	4	0	61	96,8
F8-T8	64	0	0	60	100
T8-P8	64	0	0	60	100
P8-O2	63	1	0	60	99,19
Fz-Cz	63	1	1	59	98,39
Cz-Pz	64	0	2	59	98,4
T7-Ft9	64	0	3	58	97,6
Ft9-Ft10	61	3	2	59	96
Ft10-T8	64	0	2	59	98,4

TABLE VIII
THE CLASSIFICATION RESULTS FOR PATIENT 5

Channel	normal stage		seizure stage		Accuracy
	normal	seizure	normal	seizure	
Fp1-F7	64	0	2	27	97,85
F7-T7	64	0	1	29	98,94
T7-P7	64	0	0	29	100
P7-O1	64	0	0	29	100
Fp1-F3	63	1	1	28	97,85
F3-C3	64	0	3	27	96,81
C3-P3	64	0	1	29	98,94
P3-O1	64	0	0	30	100
Fp2-F4	64	0	3	26	96,77
F4-C4	64	0	1	28	98,92
C4-P4	64	0	0	29	100
P4-O2	64	0	0	30	100
Fp2-F8	63	1	3	27	95,74
F8-T8	64	0	0	29	100
T8-P8	64	0	2	28	97,87
P8-O2	64	0	0	29	100
Fz-Cz	63	1	1	29	97,87
Cz-Pz	64	0	2	28	97,87
T7-Ft9	62	2	1	28	96,77
Ft9-Ft10	**61**	**3**	**3**	**27**	**93,62**
Ft10-T8	63	1	2	27	96,77

TABLE IX
THE CLASSIFICATION RESULTS FOR PATIENT 6

Channel	normal stage		seizure stage		Accuracy
	normal	seizure	normal	seizure	
Fp1-F7	64	0	0	28	100
F7-T7	64	0	0	28	100
T7-P7	64	0	0	28	100
P7-O1	64	0	0	28	100
Fp1-F3	64	0	0	28	100
F3-C3	64	0	0	28	100
C3-P3	64	0	0	28	100
P3-O1	64	0	0	28	100
Fp2-F4	63	1	1	27	97,83
F4-C4	64	0	0	28	100
C4-P4	64	0	0	28	100
P4-O2	64	0	0	28	100
Fp2-F8	62	2	0	28	97,83
F8-T8	62	2	0	28	97,83
T8-P8	63	1	1	27	97,83
P8-O2	64	0	0	28	100
Fz-Cz	63	1	2	26	96,74
Cz-Pz	64	0	2	26	97,83
T7-Ft9	64	0	0	28	100
Ft9-Ft10	64	0	0	28	100
Ft10-T8	**61**	**3**	**1**	**27**	**95,65**

The classification results show that The LDA classifier was able to perform seizure detection with error-free at least three channels for each patient. Especially for the first two patients, the classification process has been implemented without error in almost all channels. The seizure detection process affected at least level for these patients. According to the classification accuracy for patient 4 the worst performance was obtained at Fp1-F3 channel. For patient 4, the difference between accuracy of channels reached the highest level.

The first two major principal components were used to visualize the variation in performances of the classifier. In this stage, for patient 4 who would be able to affected mostly from the channel selection, P4-O2 channel's testing data with highest classification performance has been reflected to the plane which consist of first two major principal components. The PCA projection of this channel has been illustrated in the Figure 3.

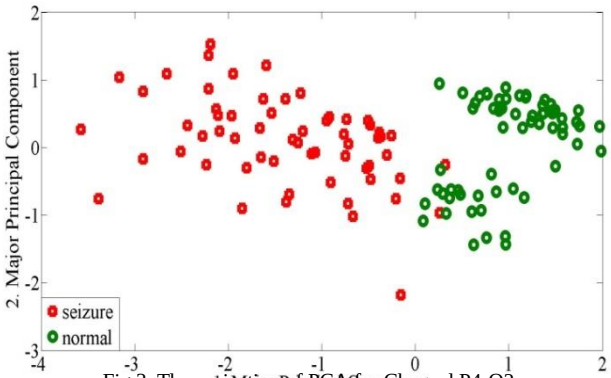

Fig.3. The projection of PCA for Channel P4-O2

These processes has been repeated for the Fp1-F3 channel that has the lowest classification accuracy. The PCA projection for this channel has been illustrated in the Figure 4.

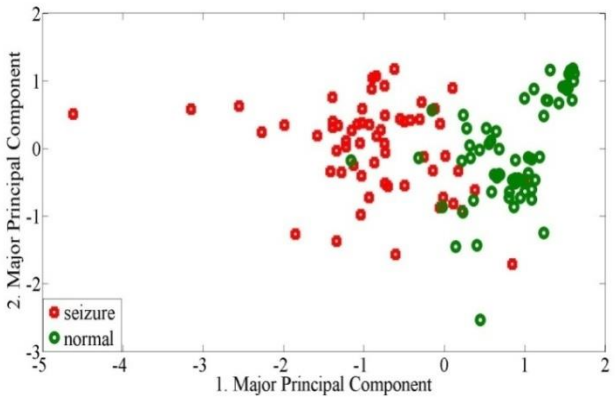

Fig.4. The projection of PCA for Channel Fp1-F3

According to Figure 3 and Figure 4, it is seen that normal and seizure stages largely separated from each other in the reflection for P4-O2 channel. Classification results also support the PCA projection. For this channel classification process has been performed without error. For Fp1-F3 channel, it is also seen that normal and seizure stages didn't separate clearly. These stages interfered each other. In the classification result for this channel, four normal samples detected as seizure and seven seizure samples detected as normal. Receiver Operating Characteristic curves of the classification process for these two channels are shown in the Figure 5.

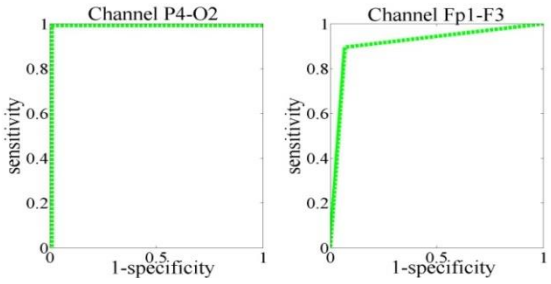

Fig.5. ROC curves for Patient 4

The area values under the ROC curve (Area Under the Curve: AUC), respectively, are calculated as 1 and 0.9133.

IV. CONCLUSIONS

Developments in computer, electronics, and signal processing methods began to be used widely in the medical electronics field recently. Researchers propose systems which capable of analyzing of EEG effectively. Designers have been developing portable seizure detection prototypes. A lot of processing load in the real time applications affects negatively the response speed of the seizure detector. Designers use various methods to reduce the process load to a reasonable level. In this study, it is aimed to evaluate channel selection effects on seizure detector performance by analyzing effects of EEG signals obtained from different channel on seizure detection process.

Analysis have been implemented patient-specifically for six patient. The differences between the best and worst channel

accuracies and number of channel, is able to detect seizure with error-free, in the classification process using 21 channels for each patient are given in the Table X.

TABLE X
THE MAXIMUM RIPPLE OF CHANNEL CLASSIFICATION ACCURACIES AND THE NUMBER OF CHANNEL WHICH IS CAPABLE OF THE ERROR-FREE CLASSIFICATION FOR EACH PATIENT

	P1	P2	P3	P4	P5	P6
Maximum ripple of Channel Accuracies	1,08	1,11	4,00	8,80	6,38	4,35
Number of channel capable of seizure detection error-free	19	20	9	3	7	14

Table V shows that channel selection can affect the classification results up to % 8.80 level. Patient 1 and Patient 2 are the most immune to channel selection. For these patients, it can be said that channel selection hasn't affected scarcely in seizure detection process. The most affected patient by channel selection was patient 4. For this patient, classification process was performed error-free for only three channels. According to the analysis results, depending on the channel selection, a ripple at the classifier accuracy can occur about 9%. These results show that Designers must choose more distinctive channels to obtain the most useful data in the channel selection processes.

ACKNOWLEDGEMENT

This research was supported by Sakarya University Scientific Research Projects Commission (Project Number: 2013-50-02-010).

The study is selected from National Engineering Research Symposium 2015 (Ulusal Mühendislik Araştırmaları Sempozyumu) UMAS 2015 (Duzce University).

REFERENCES

[1] N. Sivasankari, K. Thanushkodi, "Automated Epileptic Seizure Detection in EEG Signals Using FastICA and Neural Network", Int. J. Advance, Soft Comput. Appl., Vol. 1, No. 2, pp. 1-14, 2009.

[2] A. Shoeb, J. Guttag, "Application of Machine Learning To Epileptic Seizure Detection", The 27th International Conference on Machine Learning ICML 2010, 21-24 June 2010, Haifa-Israel.

[3] H. Vavadi, A. Ayatollahi, A. Mirzaei, "A wavelet-approximate entropy method for epileptic activity detection from EEG and its sub-bands", J. Biomedical Science and Engineering, Vol. 3, No. 2010, pp. 1182-1189,2010.

[4] G. Ouyang, X. Li, Y. Li, X. Guan, "Application of wavelet-based similarity analysis to epileptic seizures prediction", Computers in Biology and Medicine, Vol. 37, No. 2007, pp. 430-437, 2007.

[5] M. Arvaneh, C. Guan, K.K. Ang, H.C. Quek, "Optimizing the channel selection and classification accuracy in EEG-Based BCI", IEEE Transactions on Biomedical Engineering, Vol. 58, No. 6, pp. 1865-1873, 2011.

[6] M. Qaraqe, M. Ismail, Q. Abbasi, E. Serpedin, "Channel Selection and Feature Enhancement for Improved Epileptic Seizure Onset Detector", 4th International Conference on Wireless Mobile Communication and Healthcare MOBIHEALTH 2014, 03-05 November 2014, Athens, Greece.

[7] J. Duun-Henriksen, T.W. Kjaer, R.E. Madsen, L.S. Remvig, C.E. Thomsen, H.B.D. Sorensen, "Channel selection for automatic seizure detection", Clinical Neurophysiology, Vol. 123 No. 2012, pp. 84–92,2012.

[8] S. Faul, W. Marnane, "Dynamic, location-based channel selection for power consumption reduction in EEG analysis", Computer Methods and Programs in Biomedicine, Vol. 108, No. 3, pp. 1206-1215,2012.

[9] H. Tekgul, B.F.D. Bourgeois, K. Gauvreau, A.M. Bergin, "Electroencephalography in neonatal seizures: Comparison of reduced and a full 10-20 montage", Pediatric Neurology, Vol. 32, No. 3, pp. 155-161, 2005.

[10] PhysioNet International database, 6.12.2011 http://www.physionet.org/physiobank/database/chbmit/

[11] Meyer-Baese, Pattern Recognition for Medical Imaging, Elsevier Academic Pres, California, 2004.

[12] R.O. Duda, P.E. Hart, D.G. Stork, Pattern Classification, Wiley-Interscience, New York, 2001.

[13] A.K. Junoh, M.N. Mansor, "Safety System Based on Linear Discriminant Analysis", 2012 International Symposium on Instrumentation & Measurement, Sensor Network and Automation (IMSNA), 25-28 Augost 2012, Sanya, China.

[14] N.Panahi, M.G. Shayesteh, S. Mihandoost, B.Z. Varghahan, "Recognition of Different Datasets Using PCA, LDA, and Various Classifiers", 5th International Conference on Application of Information and Communication Technologies (AICT), 12-14 October 2011, Baku, Azerbaijan.

[15] A. ÜNSAL, "Diskriminant analizi ve uygulaması üzerine bir örnek", Gazi Üniversitesi İktisadi ve İdari Bilimler Fakültesi (G.Ü.İ.İ.B.F.) Dergisi, Vol.2, No. 3, pp. 19-35, 2000.

[16] A. Fielding, "Cluster and Classification Techniques for the Biosciences", Cambridge University Press, New York, 2000.

[17] M.M. Fraz, P. Remagnino, A. Hoppe, S.A. Barman, "Retinal image analysis aimed at extraction of vascular structure using linear discriminant analysis", 2013 International Conference on Computer Medical Applications (ICCMA), 20-22 January 2013, Sousse, Tunisia.

BIOGRAPHIES

Murat YILDIZ was born in Siirt, Turkey in 1977. He received the B.Sc., M.Sc. and Ph.D. degrees in Electrical-Electronics Engineering from Faculty of Engineering, Sakarya University, Turkey in 1999, 2003 and 2009 respectively. He worked in the Dept. of Electrical-Electronics Engineering as a Research Assistant in 2000-2009, and he has been an Assist. Professor since 2009.His research areas include renewable energy (solar energy, hydrogen energy and hybrid systems), electrical and electronic systems, biomedical signal processing, biomedical engineering and optimization.

Erhan BERGİL was born in Sivas, Turkey in 1980. He received the B.Sc. and M.Sc. degrees in Electrical-Electronics Engineering from Faculty of Engineering, Ondokuz Mayıs University, Turkey in 2001 and 2009 respectively. He continues his Ph.D. degree in Electrical-Electronics Engineering, Sakarya University, Turkey. Between 2002-2006, he worked in the Control and Automation Program in the Vocational High School, Ondokuz Mayıs University, Turkey as a lecturer. Since 2006, he has been working in the Control and Automation Technology Program, Department of Electronics and Automation, Technical Sciences Vocational School, Amasya University, Turkey, as a lecturer. His research areas include biomedical signal processing, electrical and electronic systems, control systems.

Open Source Mobile Robot with Raspberry Pi

E. Küçükkülahlı, and R.Güler

***Abstract*—The term of single board computer is used for computers which has built on a single circuit board with microprocessor, memory, input/output and other required units. In this study, control of a mobile robot in real time using Raspberry Pi which is a type of single board computer is performed via internet. In the developed system, all of the units in the mobile robot are controlled directly by Raspberry Pi, an additional microcontroller system is not used. Thus, without additional control equipment, a low cost and open source mobile robot design has been carried out.**

***Index Terms*—raspberry pi, mobile robot, remote control, websocket**

INTRODUCTION

Robots are considered as an essential part of modern life. Besides having been used in industry for a long time, they have become a part of end users' lives as a consequence of technological developments and cost reductions. In conjunction with increased use of mobile devices, remotely controlled implications have found a broader scope for themselves, which have enabled easy and fast control of such electronic devices remotely through mobile phone, tablet, or computer over internet.

There is a broad literature in remote device control, which might be distinguished according to control board and communication protocol used. Şahin and Yalvaç developed a wireless mobile robot prototype in their research [1]. Control board of the robot was designed using PIC16F877A, for the wireless control ARX-34S receiver and ATX-34S transmitter were used. Moreover, movements of the mobile robot was recorded by a wireless camera and transferred to a computer. Çayıroğlu and Şimşir controlled a camera installed-mobile robot car remotely using radio frequency signals [2]. Fong and Yusoff conducted research on a monitoring robot using Wi-Fi to control it real-time [3]. Robot's direction control was performed through internet connection with a wireless router on the mobile robot, taking the commands through Arduino and ethernet shield linked to it. Din and Lim suggested home automation system with a computer-controlled mobile robot [4]. Mobile robot is controlled through computer with XBee modules, and image transfer is done with a wireless camera. There is also wireless keys by 433MHz radio frequency modules, controlled by mobile robot. Kuo et al gave a cleaning robot wireless features with Arduino [5]. Wang et al introduced a feasible and affordable mobile vehicle [6]. Abid Al-Sahib and Azeez in their research created a mobile robot with a robotic arm and camera on it [7]. The robot can be controlled through internet. Raspberry Pi was used to get internet connection, while Arduino Mega board was used for direction control or the robot, and the movements of robotic arm. Espeset al. developed an affordable, web-controlled mobile robot for home monitoring [8]. Internet connection was attained through an Android smart phone on the mobile robot, while the information gathered was transferred to Arduino board over bluetooth, which control the robot. Prabha et al. recorded in a cloud system environmental factors such as heat and moisture with the Raspberry Pi-based mobile robot they developed [9].

In this research, an internet controlled-open source mobile robot design and application has been created. Mobile robot can be controlled through a web page, and immediate image transfer can be done by a camera on the robot. All these operations are controlled by Raspberry Pi, which is installed on the mobile robot. Second chapter will focus on hardware and software features of the mobile robot, while third chapter is a general review and suggestions about the research.

METHOD

A. Raspberry Pi

Various affordable computers have been developed in recent years, to expand the market. These computers mainly contain a processor, RAM, and input-output units, which are generally called single board computers. Received a great attention with their cheap prices from the users, these computers are mostly used at schools for computer learning.

The first of this trend, which became very popular was Mini2440'dır. Produced by Friendly ARM Company, this computer contains ARM9-based 400MHz Samsung processor, 64MB RAM, 1GB FLASH memory, and 34-pin GPIO [10]. Another board in this spectrum is BeagleBone, produced BeagleBoard.org establishment. BeagleBone computer contains 720MHz ARM Cortex-A8 processor, 256MB RAM, 2x46-pin GPIO [11].

E. Küçükkülahlı, Duzce Vocational School, Duzce University, 81010, Duzce, Turkey, (e-mail: enverkucukkulahli@duzce.edu.tr).

R. Güler, Duzce Vocational School, Duzce University, 81010, Duzce, Turkey, (e-mail: recepguler@duzce.edu.tr).

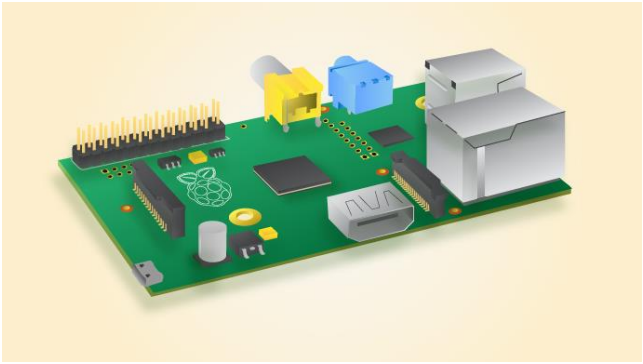

Fig. 1. Raspberry Pi Model B

Raspberry Pi board was introduced by Raspberry Pi establishment in 2011 [12]. Came out as the first model, Raspberry Pi Model B landed a sale over 2 million. Raspberry Pi Model B computer has 700MHz ARM-based Broadcom processor, 512MB RAM, 2 USB2.0 ports, 26-pin GPIO. 35$ price is the greatest factor in this computer's sale chart.

Many researchers conducted their research with the tendency to make more use of the advantages of Raspberry Pi computer. Dave Akerman and his friends connected Raspberry Pi to a meteorology balloon, and took Earth pictures up from 40 km. Prof. Simon Cox and his team composed 64 Raspberry Pi boards in order to create an experimental super computer [13].

Despite being a strong computer considering its price, Raspberry Pi also has limits. It can be used as a desktop, whereas its performance is almost the same as a mobile device (such as a tablet). Raspberry Pi establishment stated that the general performance of Model B is as much as the performance of a 300MHz Pentium 2 processor PC. Although its graphical performance is better, it is equal to the first version of Xbox game console [13].

Raspberry Pi's operating system is Linux. There is various Linux distribution is available for Raspberry Pi, which might be downloaded on www.raspberrypi.org webpage. The official and suggested distribution is Raspbian, which was developed by Mike Thompson and Peter Green. Operating system should be copied on an SD card after downloading. Raspberry Pi does not have an embedded memory, which only works through an SD card [13].

It is possible to use Raspberry Pi as a desktop when it is connected with peripherals such as screen, keyboard, and mouse, however, what distinguishes Raspberry Pi from other desktops is its GPIO, namely its general-purpose input/output pins which can be controlled by software (Figure 2). Therefore, units such as buttons, LED, engine might be controlled using Raspberry Pi board as in a micro controller, nevertheless it should be considered that Raspberry Pi's operating voltage is 3.3V [13].

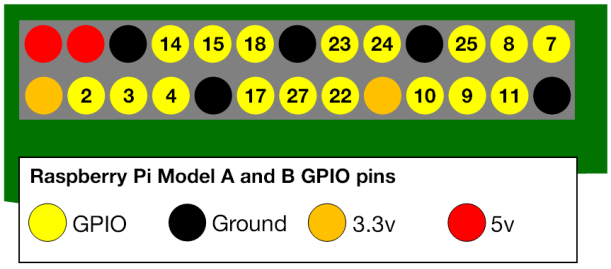

Fig. 2. Raspberry Pi GPIO pin outs

There are different methods to control Raspberry Pi's GPIO pins. In this research, input/output pins have been controlled using *node.jsrpi-gpio* library. Primarily, the library for software updating mode was downloaded. *setup()* method is used to read or write a pin [14].

```
var gpio = require('rpi-gpio');
gpio.setup(7, gpio.DIR_IN, readInput);
function readInput() {
    gpio.read(7, function(err, value) {
        console.log('The value is ' + value);
    });
}
```

A pin was set as input in the sample codes given above, and the output value was recorded [14]. "*gpio.setup(7, gpio.DIR_IN, readInput);*" code line with GPIO pin number 7 was set as input. Afterwards a function was created with the name "*readInput()*" and the pin was recorded by using "*gpio.read()*" command.

B. Motor Controller

Gear set-assembled DC engine kit was used to mobilize the designed mobile robot. L293D H-bridge drive was preferred in order to control DC engines' back-and-forth direction (Figure 3).

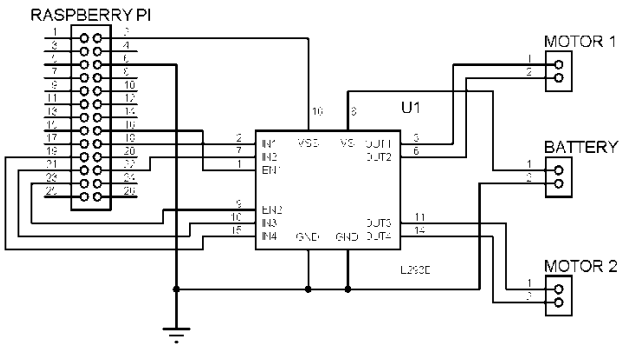

Figure 3. L293D motor driver circuit

Integrated L293D has a wide feed pitch (4.5V – 36V). Inputs of the integrated L293D are TTL-structured, and maximum output current is 600mA. Input of the circuit is controlled with GPIO pins number 19, 21, 23 and 16, 18, 22.

C. Camera

There are special camera modules that use GPIO pins for Raspberry Pi board, however, an oem webcam to work over USB port was preferred in order to reduce the cost (Figure 4). Camera uses 1.3MP CMOS sensor. A PanTilt module including two servo engines was added to make the camera move right-left and up-down. Direction control is possible directly through Raspberry Pi on the webpage.

Fig. 4. USB camera and Wi-Fi adapter

D. Wireless Adapter

Raspberry Pi might also be connected to wireless networks through its Ethernet input. The simplest and cheapest way to connect to wireless networks is to use a proper USB Wi-Fi adaptor (Figure 4). After the wireless adaptor is connected to Raspberry Pi, the system needs to be restarted in order for the system to recognize the new hardware, followed by network adjustment over operating system.

E. WebSocket and HTTP

Using an interface that works over web browser to control the mobile robot over cloud, without any other configuration enables the system to be available from everywhere. Connection between the server on the robot and a remote client over HTTP protocol might be a solution, however, some problems need to be solved in order to use HTTP protocol. HTTP was developed as a protocol to display constant HTML pages, but with technological developments it gained an expandable structure along with sessions and cookie software on the server side. Moreover, the connection was secured by the security features of HTTPS protocol [8].

HTTP protocol is based on a client starting a session on server, making a request, server replying, and ending the session. In this case, if HTTP protocol is used with a server working on robot, a secure connection is not possible, and the outcome will be a system which works independently from client. This is the reason why WebSocket technology is needed [8].

WebSocket protocol became standard in 2011 [15]. Connection in WebSocket is possible using servers and port 80. This sort of client is responsible for providing connection through URL.

The reason for using WebSocket in this research is a more secure and fast connection than HTTP protocol only by a single connection. At the same time a standard web browser is considered to be enough to monitor status of the robot, and to have an intercommunication.

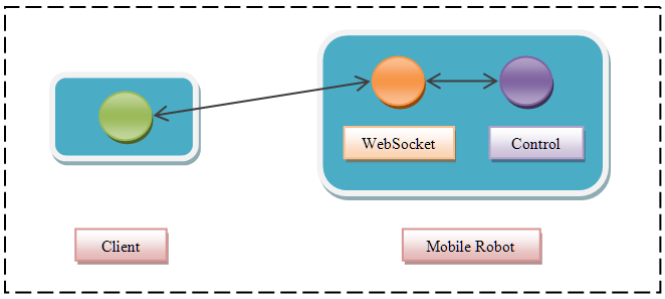

Fig. 5. Client – Mobil Robot connection

After having the connection as in the structure in Figure 5, client sends a request to WebSocket which works on the robot, and WebSocket transfers the request to robot controllers without waiting. In the meanwhile it returns the feedback from robot to client. WebSocket transfers cookies periodically from server to client and vice versa which allows the connection open during all the operations performed by robot, which prevents unintentional verbs in case of a disconnection between server and client by stopping all the operations, or by waiting for reconnection after putting all the operations on hold [8].

F. Mobile Robot Implementation

There are DC engines, a USB camera to extract footage, a wireless adaptor enabling connection, and two servo engine PanTilt unit controlling the direction of camera on the designed mobile robot (Figure 6). DC engines used on the robot are standard engines that work with 3-4.5V voltage, and they are fed by a separate resource not to influence the working of Raspberry Pi. All the other units are fed by Raspberry Pi.

In this research, NodeJs structure was used in order to manage both WebSocket protocol and engines through Raspberry Pi [16]. On the server side web service connection, DC and servo engines control, and webcam adjustments were made. To arrange these adjustments, necessary libraries were downloaded on server side, pre-adjustments were made and also GPIO pins were adjusted. Afterwards server application started recording pre-specified port of WebSocket, and waited for a client connection.

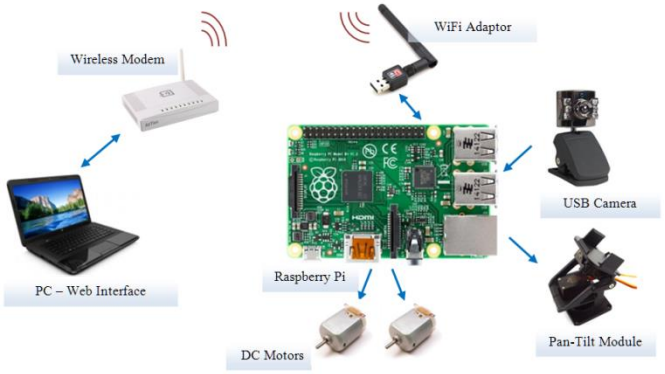

Fig. 6. Block diagram of the Mobil Robot

In the sample codes given below, the information is given that WebSocket to be working through port 8085 and the port number is specified, needed libraries are downloaded, and GPIO pins are adjusted as output port to be used by Raspberry Pi over initpins command. In conclusion, a function for run was identified, and preparations were concluded to make all the commands work on Raspberry Pi's console side.

```
vario = equire('socket.io').listen(8085)
var sys = require('sys'),
exec = require('child_process').exec
var path = '/sys/class/gpio/',
pins = [23, 24, 25, 10, 9, 11];
initPins()
functioncalistir(command) {
   exec(command, function (error, stdout, stderr)
   {
      if (error !== null)
         console.log('exec error: ' + error)
    })
}
```

After getting pre-adjustments done, a client was expected to connect to server. When a client sends a socket with the name of 'connection' to port 8085 of server, the function below runs and connection occurs.

```
io.sockets.on('connection', function (socket) {
   console.log('connection established');
})
```

After this step, connection starts working, and getting commands that would be sent from server client. In case of any data response, the command would be turned into an operation. Webpage designed to remotely control the mobile robot is seen in Figure 7. Control bars on right and left sides of the page enable controlling the right and left engines of the mobile robot separately, so robot's back and forth movements as well as its turning to right and left can be controlled. In the middle section of the page, snapshot from the camera can be displayed. Right below camera footage, there is a control bar enabling to change the direction of camera. Webpage also enables touch control on mobile devices.

Below there are some of the codes that are received when user moves the left bar.

```
socket.on('leftThrottle', function (data) {
   if (data < 0.5) {
      command = 'echo 1 > ' + path + 'gpio23/value';
      calistir(command);
      command = 'echo 1 > ' + path + 'gpio24/value';
      calistir(command);
   }
   else if (data > 0.5)
   {
      command = 'echo 1 > ' + path + 'gpio23/value';
      calistir(command);
      command = 'echo 1 > ' + path + 'gpio25/value';
      calistir(command);
   }
   else
   {
      command = 'echo 0 > ' + path + 'gpio23/value';
      calistir(command);
      command = 'echo 0 > ' + path + 'gpio24/value';
      calistir(command);
      command = 'echo 0 > ' + path + 'gpio25/value';
      calistir(command);
   }
});
```

leftThrottle information transfers information between [0-1] range. If the incoming information is less than 0.5 value, left engine will work backwards, if it is more than 0.5 value it will work forward, and if it is equal to 0.5 left engine will stop sensing that control bar was released. Same operation was written as *rightThrottle* for the right engine.

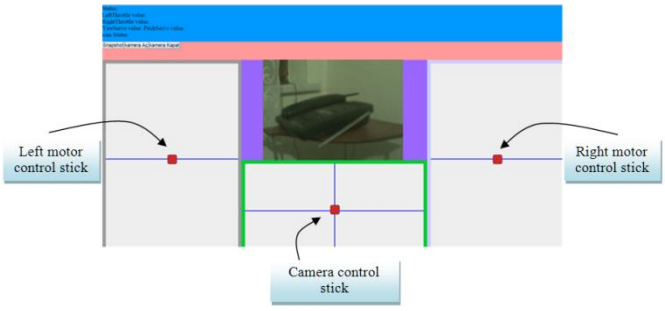

Fig. 7. Snapshot of the web site

There are two servo engines to move camera to right-left and up-down. Horizontal servo (yawServo) moves through information entered by '*servoblaster*' application [17]. The information for vertical servo is written as "*pitchServo*". "*mjpg_streamer*" application was used to get footage from camera. [18].

```
// yaw servo movement
socket.on('yawServo', function (data) {
   // data is normalized in 60-240
   var sonuc = (servoBuyuk - servoKucuk) * data +
   servoKucuk;
   command= 'echo 0=' + sonuc + ' >
   /dev/servoblaster';
   calistir(command);
});
```

On client side, a JavaScript supported HTML page was created to connect to server and get the required data from user, and at the same time transfer camera footage coming from server to user. To execute these operations, *jquery* library and open source joystick library for the user to control robot easily [19,20]. Below there are sample codes used to connect to server.

```
try {
   var socket =
   io.connect('http://192.168.2.6:8085')
}
catch (error) { }
$(document).ready(function () {
   try {
      socket.on('connect', function ()
      {
      $("#statusValue").html(connection
      established);
      })
   }
   catch (error) {
      $("#statusValue").html('can't connect to
      robot!');
   }
});
```

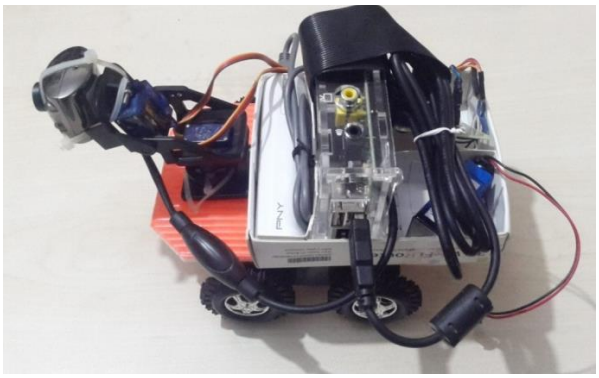

Fig. 8. Designed mobile robot

CONCULUSION AND PROPOSALS

In this research, a mobile robot design is offered using Raspberry Pi (Figure 8). Peripheral monitoring was performed by USB camera on the mobile robot. Mobile robot can be controlled real-time over a webpage, and can be monitored using a camera. During design process, all of the units on the robot were checked directly by Raspberry Pi, so an additional microcontroller system was not used, which enabled an affordable and open source mobile robot design without additional control hardware.

This study is a step to improve mobile robots especially on rough fields, using tracked system instead of wheel system. Various sensors installed on robot might be used to receive and process information. Moreover, this design might be improved more by adding a robot arm system.

ACKNOWLEDGMENT

The study is selected from National Engineering Research Symposium 2015 (Ulusal Mühendislik Araştırmaları Sempozyumu) UMAS 2015 (Duzce University).

REFERENCES

[1] Şahin, İ., Yalvaç, M. (2012). Myrobot: Kablosuz Kontrol Edilebilen Mobil Araştırma Robotu, e-Journal of New World Science Academy NWSA-Education Sciences, 7(1), 340-347.

[2] Çayıroğlu, İ., Şimşir, M. (2008). PIC ve Step Motorla Sürülen Bir Mobil Robotun Uzaktan Kamera Sistemi ile Kontrolü, *Erciyes Üniversitesi Fen Bilimleri Enstitüsü Dergisi*, 24(1-2), 1-16.

[3] Fong, P. E., Yusoff, M. A. (2011). Real-Time Control of Wi-Fi Surveillance Robot, *Proceeding of the International Conference on Advanced Science Engineering and Information Technology*, Malasia.

[4] Ud Din, Z., Lim, W. (2013). Home Automation with Smart Robot Featuring Live Video Feed and Remotely Controlled Switches, *IEEE Conference on Sustainable Utilization and Development in Engineering and Technology*

[5] Kuo, G., Cheng, C., Wu, C. (2014). Design and Implementation of a Remote Monitoring Cleaning Robot, *International Automatic Control Conference*, Taiwan

[6] Wang, Z., Lim, E. G., Wang, W., Leach, M., Man, K. L. (2014). Design of an Arduino–based Smart Car, *International SoC Design Conference*, Korea

[7] Al-Sahib, N. K. A., Azeez, M. Z. (2015). Build and Interface Internet Mobile Robot using Raspberry Pi and Arduino, Innovative System Design and Engineering, 6(1)

[8] Espes, D., Autret, Y., Vareille, J., Le Parc, P. (2014). Designing a Low-Cost Web-Controlled Mobile Robot for Home Monitoring, *The Eighth International Conference on Mobile Ubiquitous Computing, Systems, Services and Technologies*, Italy

[9] Prabha, S. S., Antony, A. J. P., Meena, M. J., Pandian, S. R. (2014). Smart Cloud Robot using Raspberry Pi, *International Conference on Recent Trends in Information Technology*, India

[10] http://www.friendlyarm.net/products/mini2440 (July '15)

[11] http://beagleboard.org (July '15)

[12] https://www.raspberrypi.org (July '15)

[13] McManus, S., Cook, M., *Raspberry Pi for Dummies*, John Wiley & Sons (2013)

[14] https://www.npmjs.com/package/rpi-gpio (July '15)

[15] The WebSocket Protocol. Internet Engineering Task Force (IETF). http://tools.ietf.org/html/rfc6455 (July '15)

[16] https://nodejs.org/ (July '15)

[17] https://github.com/richardghirst/PiBits/tree/master/ServoBlaster (July '15)

[18] https://github.com/jacksonliam/mjpg-streamer (July '15)

[19] https://jquery.com/ (July '15)

[20] https://github.com/mifi/jquery-joystick (July '15)

BIOGRAPHIES

Enver KÜÇÜKKÜLAHLI was born in Tosya, Turkiye in 1983. He received the B.Sc. degree in Computer Education and Instructional Technology from Faulty of Education, Ondokuz Mayıs University and M.Sc. degrees in Teacher Training in Electrical Works from Faulty of Technical Education, Duzce University, in 2006 and 2011. From 2007 he worked in Computer Technologies, Duzce Vocational School, Duzce University as a Lecturer. His research areas include optimization, image segmentation.

Recep GÜLER was born in Bursa, Turkiye in 1985. He received the B.Sc. and M.Sc. degrees in Electronic & Computer Education from Faulty of Technical Education, Gazi University, in 2008 and 2011. From 2008 to 2011 he worked in Electronic & Computer Education, Faulty of Technical Education, Gazi University as an Assistant Student and also work in BELTEK Educational Course as a Lecturer. His research areas include microcontroller systems, communication systems.

Performance Analysis of Slotted Aloha Protocol in Wireless Cognitive Radio Networks

M. E. Bayrakdar, and A. Calhan

***Abstract*—With the growing use of frequency based services and devices, the cognitive radio network has become an important technology for the future of wireless networks. However, the number of frequency based network applications for fixed and mobile devices both in licensed, and unlicensed networks also shows a significant increase. In addition to frequency based applications; for efficient use of spectrum in cognitive radio networks, characteristics of medium access techniques is utilized. Among these medium access techniques, slotted Aloha technique is among the most preferred. In our study, simulation of a cognitive radio network environment that consists of primary and secondary users utilizing slotted Aloha medium access technique is performed. The simulation of designed network environment is carried out by using Riverbed software. Upon making end to end delay analysis of the designed network, the results of maximum number of users that could be supported in cognitive radio networks utilizing slotted Aloha technique is observed.**

***Index Terms*—Cognitive radio, delay analysis, slotted Aloha.**

I. INTRODUCTION

COGNITIVE radio network is an important technology for the future of wireless networks [1-2]. The use of frequency based services and devices is increasing day by day. However, the number of frequency based applications on licensed and unlicensed networks for both fixed and mobile devices are increasing [2-3]. Similarly, there is growing need for the ISM (Industrial Science Medical) band. Despite constantly growing number of wireless services and devices, the provision of frequency spectrum is known to be a limited resource. Therefore, it is necessary to use the available spectrum band in a flexible and efficient manner [4]. According to the researches, it is seen that the majority of frequency spectrum is allocated to the primary users as fixed. In addition, a small portion of the spectrum is used for urgent applications. However, although some parts of the spectrum at given time intervals is used by primary users, there is some available part of the spectrum that is used partly and rarely [5]. One way to reduce these restrictions is to update the existing license allocation methods. By providing flexible access to frequency bands without harming primary users, spectrum access can be provided to secondary users in an opportunistic way. Thus, productivity and efficiency of the frequency spectrum can be well increased [2].

M. E. Bayrakdar, Computer Engineering Department, Duzce University, 81620, Duzce, Turkey, (e-mail: muhammedbayrakdar@duzce.edu.tr).

A. Calhan, Computer Engineering Department, Duzce University, 81620, Duzce, Turkey, (e-mail: alicalhan@duzce.edu.tr).

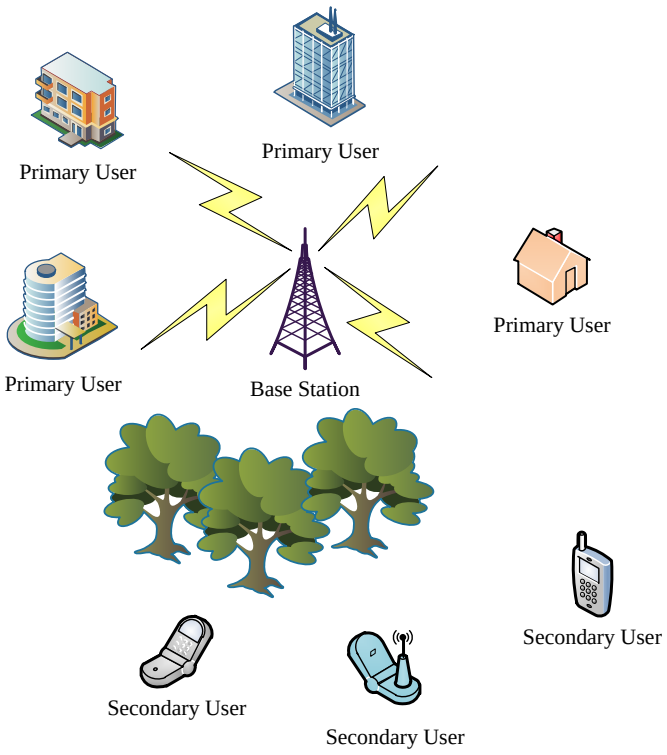

Fig.1. Cognitive radio environment

According to the current communication system policies, there are no flexibility advantages of frequency channels because they work in an allocated way. In contrast, flexible use of frequency channels is provided with cognitive radio technology [3]. Cognitive radio technology is a new technology which aims to be the solution for the future wireless communication technology by ensuring use of the spectrum more efficiently. Cognitive radio is a radio technology that can change the transmission parameters by interacting with its environment. The main tasks of cognitive radio are spectrum detection, spectrum management spectrum mobility and spectrum sharing [2]. The main goal of cognitive radio is to provide the flexibility of the wireless transmission systems with dynamic spectrum access in order to increase spectral efficiency and to optimize transmission performance. The components of the architecture of cognitive radio networks are divided into two separate groups, namely primary and

secondary networks [5]. Primary networks are licensed networks and they are authorized to use a particular frequency spectrum band. Secondary networks are unlicensed networks, so they can access to the spectrum only through access points opportunistically. Fig. 1 shows a network structure of the primary and secondary users that are located in the same environment.

In our study, a cognitive radio network environment where the primary and secondary users use slotted Aloha technique is considered. Simulation of the designed network environment was carried out using Riverbed software. Delay analysis of the designed network is expressed analytically with mathematical terms and analytical results are seen to be consistent with the simulation results.

II. System Model of The Network

In this study, end to end delay analysis of slotted Aloha medium access technique in cognitive radio networks is performed. End to end delay analysis is carried out with simulation scenarios involving different number of primary and secondary users. In the network environment scenarios developed; primary users, secondary users and access points that are serving to these users are existed together.

In Equation (1), analytical model of Slotted Aloha expected delay, D is given [1-3].

$$D = 1 + \frac{1-(1-\frac{G}{M})^{M-1}}{\frac{G}{M}(1-\frac{G}{M})^{M-1}}, \qquad (1)$$

where G is total load, and M is number of users [1-3].

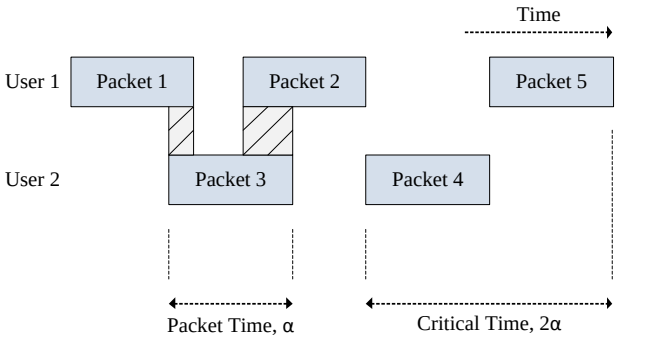

Fig.2. Aloha and slotted Aloha techniques

Slotted Aloha medium access technique is a kind of Aloha protocol that is divided into time periods to reduce the possibility of collisions [6-7]. In the Aloha protocol, direct packet transmission is performed regardless of whether another transmission is present in the environment. The worst part of this protocol is that the collision probability is much higher [8-9]. In Slotted Aloha medium access technique, when a packet is ready to be transmitted, the process of transmission is performed at the beginning of time periods after waiting until the beginning of the time periods. In this way, packet collisions that may be in the middle of the packet transmissions in Aloha protocol are prevented [10-11]. End to end delay of Slotted Aloha protocol is equal to the elapsed time from the time a packet is produced until reaching the destination.

In Fig. 2, packet transmission of Aloha and slotted Aloha techniques is observed. Here; packet collisions of packets 1, 2, and 3 in Aloha technique is seen. The packets 4, and 5 are transmitted at the beginning of the time period for which they are transmitted according to the characteristics of slotted Aloha techniques.

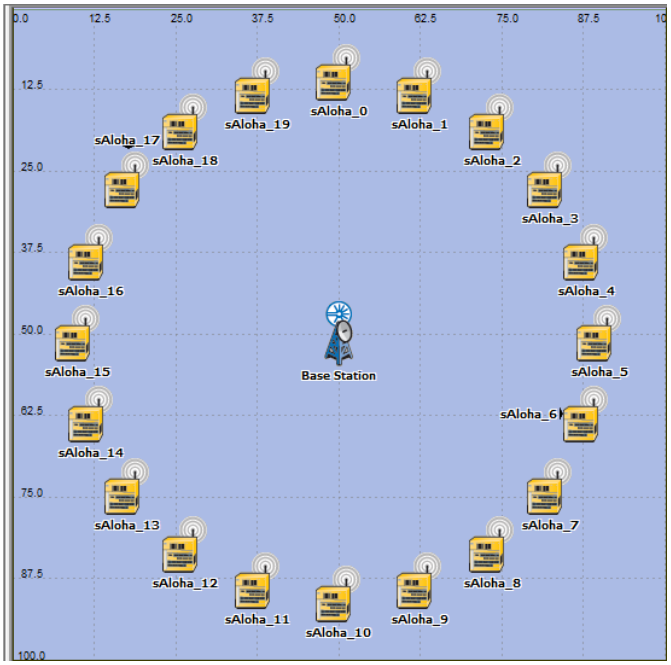

Fig.3. Primary network simulation environment

Fig. 3 shows simulation scenarios designed for primary users performed on Riverbed software. In Fig. 4, combination of cognitive radio network environment where primary and secondary users exist together is seen. Code of each designed node and access point are written in Riverbed simulation software.

Our network model consists of secondary users and base stations in the same communication area with the primary users. Slotted Aloha is exploited as random access scheme by the secondary users. The process of a secondary user in our network is as follows. Each secondary user makes a decision about the time slot usage at the beginning of each time slot. If the time slot is utilized by a primary user, then the secondary user waits for the availability of next time slots. If the time slot is idle, then the secondary user transmits its packet.

In our secondary network model, it is presumed that each secondary user generates packets according to Poisson process. Moreover, the packet length of secondary users is shorter than packet length of primary users because of the spectrum sensing time.

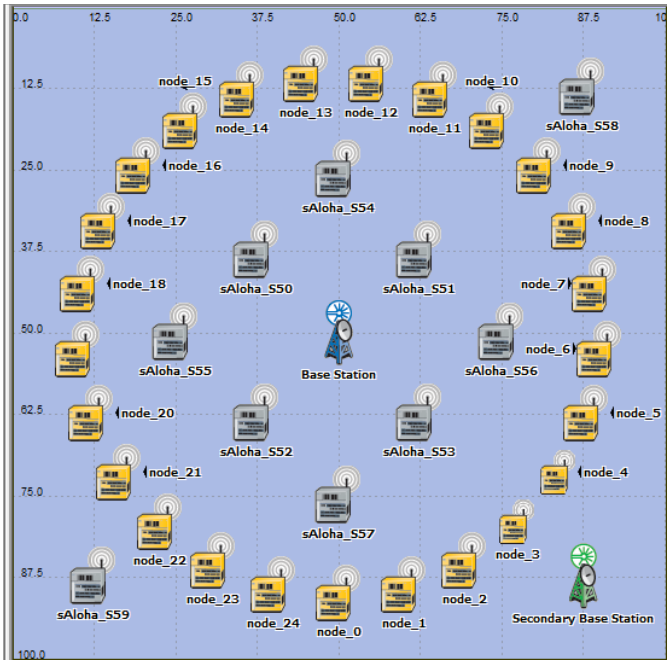

Fig.4. Secondary network simulation environment

III. Simulation Results of Primary and Secondary Networks

This section is devoted to the results obtained concerning the end to end delay and graphics. The obtained numerical results were obtained with the scenarios including different number of users.

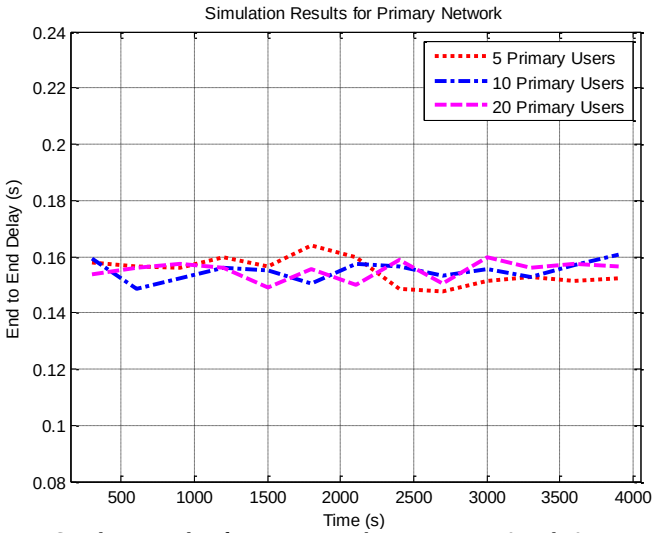

Fig.5. Simulation results of primary network containing 5, 10, and 20 primary users

Fig. 5, and Fig. 6 shows the simulation results for primary networks including only different number of primary users. As seen from the results in Fig. 5, end to end delay results of the primary network including 5, 10 or 20 users are pretty close to each other. Here, slotted Aloha technique appears to give very good results up to 20 users. However, the results for the scenarios with 50, and 100 users in Figure 6 is seen to be rather inconsistent. This shows that slotted Aloha technique is not suitable for network environments containing more than 25 users. Besides, overall network performance rather decreases when number of users exceeds 25 because of the collisions.

The Riverbed Modeler software offers some tools such as designing, simulation, and data aggregation [12]. Riverbed Modeler simulation software supports an extensive development environment containing the design of wireless communication networks, and distributed network systems as well [12]. In Riverbed Modeler, performance analysis of a simulation model is evaluated by means of discrete event simulations [12]. Configuration of the network is made in three stage; i.e. network level, node level, and process level. In the network stage, topology of the network is produced. The node stage defines the actions of the node and controls the data flowing in different part of the node. The process stage is characterized by state machines that are formed with states and transitions among them. The source code of Riverbed Modeler simulation software is written on C programming language [12].

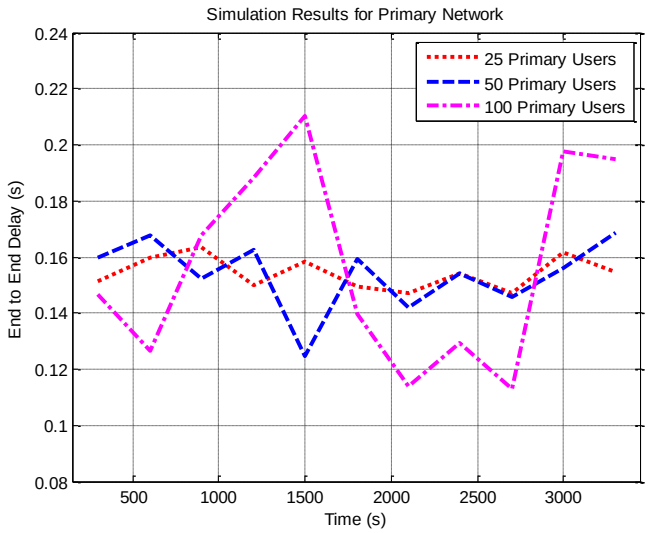

Fig.6. Simulation results of primary network containing 25, 50, and 100 primary users

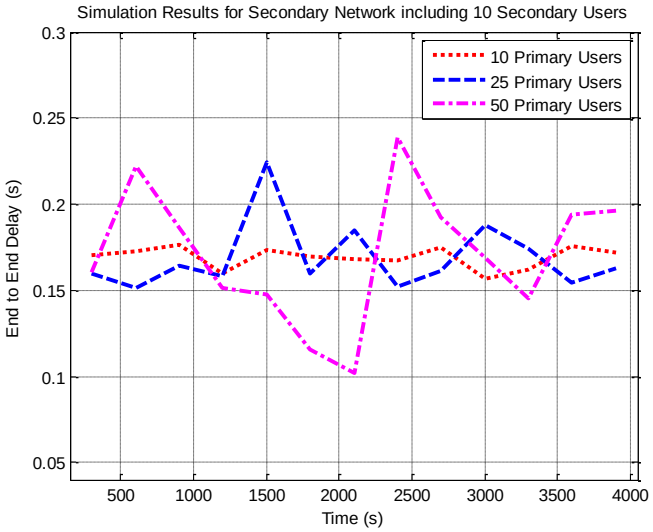

Fig.7. Simulation results of 10 users' secondary network containing 25, 50, and 100 primary users

In Fig. 7, the simulation results of the secondary network with 10 primary users for different number of secondary users is seen. The graph gives consistent end to end delay results when there are 10 primary users and 10 secondary users in the network structure. End to end delay results of the primary networks including 25, and 50 users are found to be inconsistent. Here, it is seen that cognitive radio networks utilizing slotted Aloha technique with maximum number of 10 primary users and 10 secondary users give appropriate results.

IV. Conclusions

In this study, simulation of a cognitive radio network environment which primary and secondary users use slotted Aloha medium access technique that is optimized format of Aloha protocol is carried out. Riverbed software is utilized to perform a simulation of the designed network. Making end to end delay analysis of the designed network, maximum number of users utilizing slotted Aloha technique that is supported in cognitive radio networks has been observed. According to the obtained results, a network structure consisting of the primary users that utilize slotted Aloha technique has been shown to give good results for up to 20 users. In cognitive radio network environment, network infrastructure that includes 10 primary users and 10 secondary users give good results. In subsequent studies, the performance of the secondary users in cognitive radio networks using different medium access techniques are expected to be analyzed.

Acknowledgment

This work is supported by the Duzce University Scientific Research Projects Office with project number 2015.07.02.329.

The study is selected from National Engineering Research Symposium 2015 (Ulusal Mühendislik Araştırmaları Sempozyumu) UMAS 2015 (Duzce University).

References

[1] A.J. Faria, J. M. C. Brito, "Average Delay in Cognitive Radio Networks using Slotted Aloha", IEEE International Conference on Communications, Computers and Applications, Istanbul, Turkey, 2012.

[2] S. Choe, "Throughput and Delay of Slotted-Aloha based Cognitive Packet Radio Network", IEEE International Conference on Communication Systems, Guangzhou, China, 2008.

[3] H. Takagi, L. Kleinrock, "Throughput-Delay Characteristics of some Slotted-Aloha Multihop Packet Radio Networks", IEEE Transactions on Communications, Vol. COM-33, No. 11, pp. 1200-1207, 1985.

[4] W. Yue, "Output and Delay Processes in a Slotted Aloha Multichannel Packet Radio Network with Capture", IEEE International Phoenix Conference on Computers and Communications, Scottsdale, Arizona, United States of America, 1991.

[5] C. Çiflikçi, A. T. Tuncer, A. T. Özşahin, S. M. Yesbek, "Bilişsel Radyo ve Ortam Erişim Kontrol Katmanı Protokolleri", Uluslararası İleri Teknolojiler Sempozyumu, Karabuk, Turkey, 2009.

[6] V. Naware, G. Mergen, L. Tong, "Stability and Delay of Finite-User Slotted Aloha with Multi Packet Reception", IEEE Transactions on Information Theory, Vol. 51, No. 7, pp. 2636-2656, 2005.

[7] Y. Yang, T. S. P. Yum, "Delay Distributions of Slotted Aloha and CSMA", IEEE Transactions on Communications, Vol. 51, No. 11, pp. 1846-1857, 2003.

[8] G. A. Cunningham, "Delay versus Throughput Comparisons for Stabilized Slotted Aloha", IEEE Transactions on Communications, Vol. 38, No. 11, pp. 1932-1934, 1990.

[9] F. L. Lo, T. S. Ng, T. I. Yuk, "Delay-Throughput Comparison of Single and Multi-Channel Slotted Aloha Networks", IEEE International Conference on Communication Technology, Beijing, China, 1996.

[10] A. Tremeau, N. Borel, "Throughput and Delay Analysis of Two-Tier Slotted Aloha", IEEE Wireless and Optical Communications Conference, Newark, New Jersey, United States of America, 2009.

[11] S. Solak, "Kablosuz Algılayıcı Ağlarda kullanılan MAC Protokollerinin Karşılaştırmalı Başarım Analizi", Yuksek Lisans Tezi, Kocaeli University, Graduate School Of Natural And Applied Sciences, 2008.

[12] Riverbed Modeler Software, 2015. http://www.riverbed.com/products/steelcentral/opnet.html.

Biographies

Muhammed Enes BAYRAKDAR was born in Izmit, Turkey in 1988. He received the M.Sc. degree from University of Kocaeli, Turkey in 2013. He studies for Ph.D. degree at Duzce University. His research interests are cognitive radio networks, queuing theory, medium access techniques, wireless communications, and artificial intelligence.

Ali ÇALHAN received the M.Sc. and Ph.D. degrees from University of Kocaeli, Turkey in 2006 and 2011, respectively. His research interests are cognitive radio, wireless heterogeneous networks, wireless communications, and artificial intelligence.

The Performance Analysis of Artificial Neural Network Based Shimizu-Morioka Chaotic System with Respect to Sample Numbers

M. Alçın, I. Pehlivan, and I. Koyuncu

***Abstract*— In this paper, Shimizu-Morioka Chaotic System (SMCS) is modelled using Feed Forward Artificial Neural Network. In the realized network model, Log-Sigmoid and Purelin transfer functions have been used for hidden and output layer, respectively. 3-10-3 network structure is created using MATLAB. The model inputs are the state variables of SMCS. Outputs represent not only the outputs of SMCS but also iterative versions of these inputs. For the equations' numeric solutions of describing SMCS, Runge Kutta 5 Butcher (RK-5-B) algorithm which is one of the differential equation solution methods, is used. Samples in the structure of described network, the created different numbers of samples using RK-5-B have been used as input data and performance analysis have been performed for these data. As a result, the paper shows that when the sample data numbers increase, network modeling performance gives more successful results.**

***Index Terms*—Artificial Neural Networks, Chaotic System, Numerical Algorithm, Modeling.**

I. Introduction

CHAOS has attracted the attention of scientists who work on nonlinear systems in recent years. Communication systems have become one of the most commonly used areas of chaos in engineering applications. Chaotic oscillators have frequently been used for the construction of such systems. There has been many researches exploiting chaotic oscillators in the areas of control, prediction, optimization, energy, cryptology and nanotechnology.

Artificial Neural Network (ANN) is a complex system in Artificial Intelligence (AI) that simulates human brain capabilities such as learning and generalization. It is possible to use ANN in function estimation, classification, pattern recognition, signal processing and system modeling.

M. Alçın is with Anadolu University, Porsuk Vocational School, Department of Electrical-Energy, Eskişehir, 26470, Turkey, (e-mail: muratalcin@anadolu.edu.tr).

I. Pehlivan is with Sakarya University, Department of Electrical and Electronics Engineering, Sakarya 54187, Turkey, (e-mail: ipehlivan@sakarya.edu.tr).

I. Koyuncu is with Duzce University, Duzce Vocational School, Department of Electronics and Automation, Duzce, 81100, Turkey, (e-mail: ismailkoyuncu@duzce.edu.tr).

ANN have recently been used in many fields like prediction [1, 2], classification [3, 4], control [5, 6], optimization [7, 8], the analysis of complex problems and modeling of nonlinear systems [9, 10]. The usage of ANN in modeling of nonlinear systems has an important role in modeling chaotic oscillators using ANN. In the present work, the modeling of Shimizu-Morioka Chaotic System (SMCS) using Feed Forward Neural Network (FFNN) is presented [11-13]. For the numeric solution of the system, Runge Kutta 5 Butcher (RK-5-B) algorithm which is one of the differential equation solution methods is used [14]. A detailed analysis of the modeling related to sample number is carried out and obtained results have been explained.

II. Background Information

A. Artificial Neural Networks

Nowadays, Fuzzy-Logic, Genetic Algorithms and ANN are among the AI technics that have been used in various areas [10, 15]. ANN can be used not only in system identification but also in modeling of system. Artificial Neuron system can be performed in modeling and analyzing of chaotic systems with a great success [9]. Model structure of feed-forward ANN for SMCS was shown in Fig. 1.

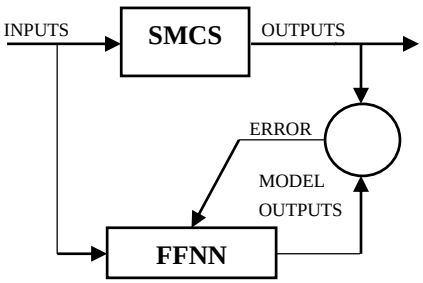

Fig. 1. Model structure of Feed-Forward ANN for SMCS.

ANN consists of inter-connected neurons which are organized in the form of layers [9]. The basic processing element of ANN is called artificial neuron (AN) as shown in Fig. 2. The ANN given in this figure has an input, denoted as p. The line connecting this input to the neuron is assigned a weight, denoted as *w*.

The neuron also includes an externally applied bias, denoted by b_k. The activation, *f*, determines whether the neuron is to be fired or not [16].

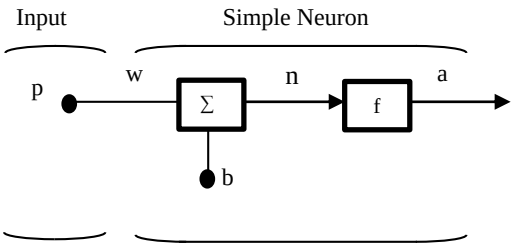

Fig. 2. Simple Neuron Structure [15].

This neuron has 3 functional operations. Firstly, p is multiplied with w to produce weighted input, denoted as wp in (1).

$$wp=w.p \tag{1}$$

Then, weighted input is summed with bias, denoted by *b* to produce net input, denoted by *n* in (2).

$$n=w.p+b \tag{2}$$

Finally, the net output, denoted by *a* is obtained by applying transfer function to *n*. These three steps are called weight function, net input function and transfer function [10, 17]. There are various transfer functions used in neuron structure in literature [18]. The neuron output, *a* is given in (3)

$$a=f(wp+b) \tag{3}$$

B. Shimizu-Morioka Chaotic System

Shimizu-Morioka Chaotic System is defined by the simple three-dimensional autonomous system in (4) [11]. T. Shimizu and N. Morioka have found out this system by computer simulations in 1980.

$$\begin{aligned} \dot{x} &= y \\ \dot{y} &= x - a \cdot y - x \cdot z \\ z &= - b \cdot z + x^2 \end{aligned} \tag{4}$$

$a = 0.85$ and $b = 0.5$ are the system pparameters of the SMCS. x_0=0.1, y_0=0.1, and z_0=0.1 are the initial conditions of SMCS. The chaotic attractors obtained from these conditions using MATLAB software were given in Fig. 3.

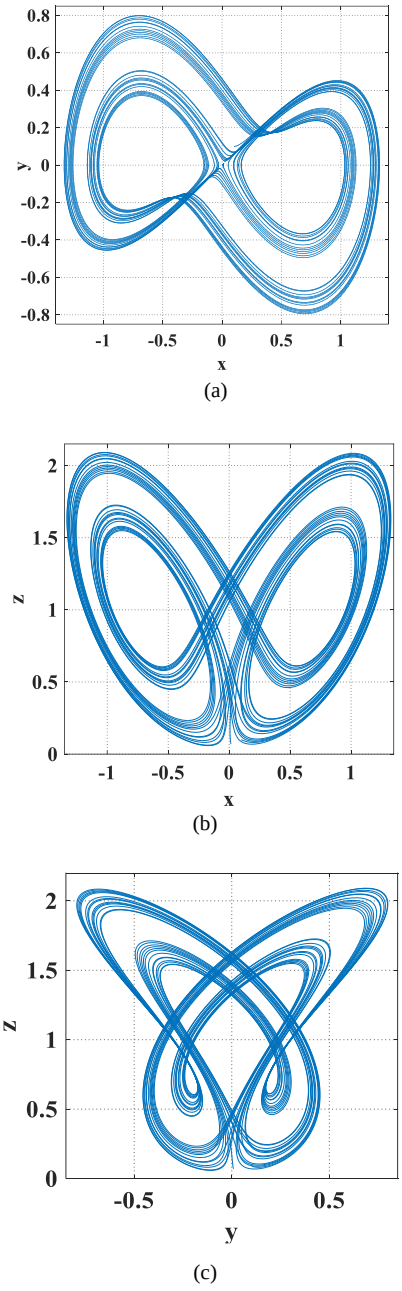

Fig. 3. The chaotic attractors of the Shimizu-Morioka Chaotic System for initial conditions x_0=0.1, y_0=0.1, z_0=0.1 and system parameters a=085 and b=0.5, a) x-y chaotic attractors, b) x-z chaotic attractors and c) y-z chaotic attractor.

III. MODELING OF THE SHIMIZU-MORIOKA CHAOTIC SYSTEM

In this paper, Shimizu-Morioka Chaotic System has been modeled using FFNN having different data sets of 100, 1000 and 10000 sample numbers. In the structure of modeled network, inputs represent the state variables and outputs represent the iterative versions of these inputs. As can be seen in Fig. 4, input layer has 3 inputs and output layer has 3 outputs. There are 10 neurons in hidden layer. LoSig (Logistic Sigmoid) transfer function has been used in hidden layer and Purelin transfer function has been used in output layer.

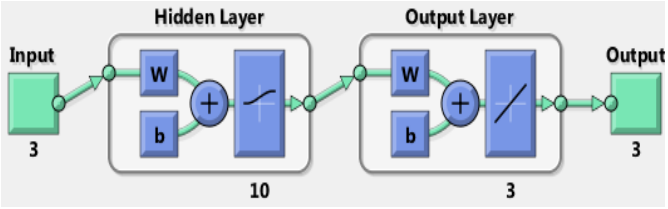

Fig. 4. View of ANN-based Shimizu-Morioka Chaotic System in MATLAB.

The parameters related to ANN-based Shimizu-Morioka Chaotic System has been given in Table I.

TABLE I
MODEL PARAMETERS

FFNN Model Structure	
Number of layers	3
Number of neurons in layers	Input: 3 Hidden:10 Output:3
Initial weights and bias values	Random
Transfer Function	Hidden:Log-Sigmoid Output:Linear
Learning Rule	Levenberg-Margquard Back Propogation

IV. PERFORMANCE RESULTS OF FFNN BASED SMCS

In this work, it is clear to see that the SMCS has been successfully modeled for three different data sets. The performance results related to training have been presented in Fig. 5, Fig. 6 and Fig. 7.

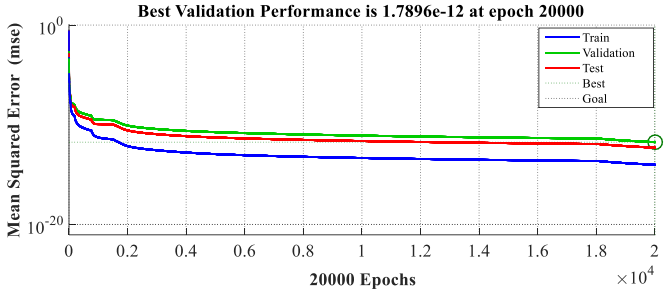

Fig. 5. Network performance results for data set of 100 samples.

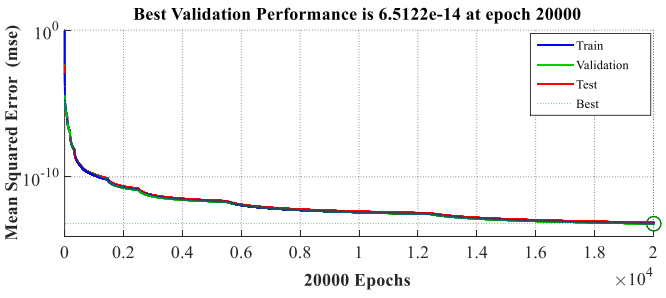

Fig. 6. Network performance results for data set of 1000 samples.

TABLE II
ANALYSIS OF MEAN SQUARE ERROR

	100 sample	1000 sample	10000 sample
Mean Square Error (MSE)	1.7896e-12	6.5122e-14	1.2622e-14

Mean Square Error (MSE) has been decreasing collaterally for each of training, validation and test data. Furthermore, the analysis results of MSE has been given in Table II.

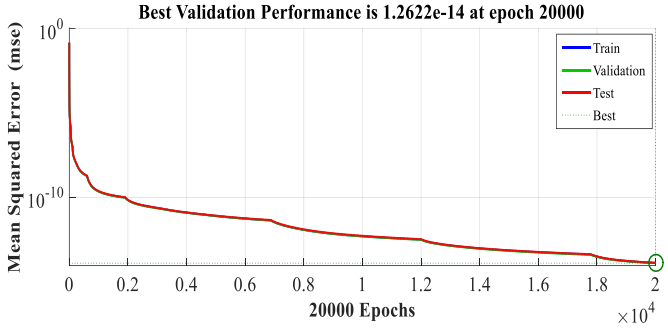

Fig. 7. Network performance results for data set of 10000 samples.

V. CONCLUSIONS

This paper presents the analysis of modeling performance effect of the network with respect to ANN model and sample data number to be used for modeling the dynamics of Shimizu-Morioka Chaotic System. The numeric solutions of the equations describing the SMCS have been performed with RK-5-B algorithm. The obtained data sets having sample numbers of 100, 1000 and 10000 have been modeled by FFNN separately for the network parameters. The performance results have been presented for each of the data sets. As a result, it is seen that the increment of sample number has a positive effect on the modelling performance. In other words, when the sample number increases, the Mean Square Error will decrease.

ACKNOWLEDGMENT

The study is selected from National Engineering Research Symposium 2015 (Ulusal Mühendislik Araştırmaları Sempozyumu) UMAS 2015 (Duzce University).

REFERENCES

[1] R. Adhikari, "A neural network based linear ensemble framework for time series forecasting", Neurocomputing, Elsevier, vol. 157, pp. 231–242, 2015.

[2] C. U. Vila, A. C. Z. Souza, J. W. M. Lima, and P. P. Balestrassi, "Electricity demand and spot price forecasting using evolutionary computation combined with chaotic nonlinear dynamic model", Electrical Power and Energy Systems, vol. 32, pp. 108–116, 2010.

[3] Q. Nie, L. Jin, S. Fei, and J. Ma, "Neural network for multi-classclassification by boosting composite stumps", Neurocomputing, vol. 149, pp. 949–956, 2015.

[4] A. J. Hussain, P. Fergus, H. Al-Askar, D. Al-Jumeily, and F. Jager, "Dynamic neural network architecture inspired by the immune algorithm to predict preterm deliveries in pregnant women", Neurocomputing, vol. 151, pp. 963–974, 2015.

[5] V. Kumar, P. Gaur, and A. P. Mittal, "ANN based self tuned PID like adaptive controller design for high performance PMSM position control", Expert Systems with Applications, vol. 41, pp. 7995–8002, 2014.

[6] M. M. Noel, and B. J. Pandian, "Control of a nonlinear liquid level system using a new artificial neural network based reinforcement learning approach", Applied Soft Computing, vol. 23, pp. 444–451, 2014.

[7] G. Das, P. K. Pattnaik, and S. K. Padhy, “Artificial Neural Network trained by Particle Swarm Optimization for non-linear channel equalization”, Expert Systems with Applications, vol. 41, pp. 3491–3496, 2014.
[8] J. D. Pintér, “Calibrating artificial neural networks by global optimization”, Expert Systems with Applications, vol. 39, pp. 25–32, 2012.
[9] R. Archana, A. Unnikrishnan, and R. Gopikakumari, “An Improved EKF based neural network training algorithm for the identification of chaotic systems driven by time series”, 2012 IEEE International Conference on Power, Signals, Controls and Computation (EPSCICON), 2012.
[10] H. Altınkaya, İ. M. Orak, and İ. Esen, “Artificial neural network application for modeling the rail rolling process”, Expert Systems with Applications, vol. 41, pp. 7135–7146, 2014.
[11] M. M. El-Dessoky, M. T. Yassen, and E. S. Aly, “Bifurcation analysis and chaos control in Shimizu–Morioka chaotic system with delayed feedback, Applied Mathematics and Computation”, vol. 243, pp. 283–297, 2014
[12] X. Liao, F. Xu, P. Wang, and P. Yu, “Chaos control and synchronization for a special generalized Lorenz canonical system – The SM system”, Chaos, Solitons and Fractals, vol. 39, pp. 2491–2508, 2009.
[13] S. Yu, W. K. S. Tang, J. Lü, and G. Chen, “Generation of nxm-Wing Lorenz-Like Attractors From a Modified Shimizu–Morioka Model”, IEEE Transactıons On Circuits And Systems—II: Express Briefs, vol. 55(11), 2008.
[14] C. Tsitouras, Runge–Kutta pairs of order 5(4) satisfying only the first column simplifying assumption, Computers and Mathematics with Applications, vol. 62, pp. 770–775, 2011.
[15] M. Tuna, C. B. Fidan, S. Kocabey, and S. Görgülü, “Effective and Reliable Speed Control of Permanent Magnet DC (PMDC) Motor under Variable Loads”, Journal of Electrical Engineering & Technology, vol. 10(5), pp. 2170–2178, 2015.
[16] M. H. Beale, M. T. Hagan, and H. B. Demuth, “The Neural Network Toolbox User’s Guide R2014b”, The MathWorks, 2015.
[17] Mohammed, E.Z., and Ali, H.K. “Hardware Implementation of Artificial Neural Network Using Field Programmable Gate Array”, International Journal of Computer Theory and Engineering, 5(5), 780-783, 2013.
[18] Sahin, I., and I. Koyuncu. “Design and Implementation of Neural Networks Neurons with RadBas, LogSig, and TanSig Activation Functions on FPGA”, Electronics and Electrical Engineering, vol. 120(4), pp. 51-54, 2012.

BIOGRAPHIES

Murat ALCIN was born in Esence Village, Eskisehir, in 1982. He received the B.S. and M.S. degrees in Electronic-Computer Teaching from the University of Marmara, Turkey, in 2006 and in 2009, respectively. Receiving his doctoral research in the Department of Electrical and Electronics Engineering at Sakarya University, in Sakarya-Turkey. He is a research assistant in Anadolu University Electric-Energy Department in Porsuk Vocational School, Eskisehir-Turkey. From 2006 to 2008, he was a teacher in Simav Anatolian Vocational High School in Kutahya. From 2008 to 2012, he was an instructor in Abant İzzet Baysal University Electronic Technology Program at Bolu Vocational School, Bolu-Turkey. From 2012 to 2014, he was an instructor in Osmangazi University Compter Programming Program at Sivrihisar Vocational School, Eskisehir-Turkey. Since 2014, he has been a Research Assistant with the Electric-Energy Department, Eskisehir Anadolu University. His research interests include Neural Networks, Chaotic Systems and FPGA-based digital system design.

Ihsan PEHLIVAN received the B.S. from Istanbul Technical University in 1997, M.S. and PhD degrees in 2001 and 2007 respectively in Electrical-Electronic Engineering from Sakarya University, Sakarya-Turkey. He is an Associated Professor in the Department of Electrical and Electronics Engineering at Sakarya University, in Sakarya-Turkey. He is the author of a book, more than 30 articles. His research interests include chaos, electric circuits and signals-system.

Ismail KOYUNCU has an M.S. from Abant Izzet Baysal University, Bolu-Turkey. He is currently conducting his doctoral research in the Department of Electrical and Electronics Engineering at Sakarya University, Sakarya-Turkey. He is an instructor in Duzce University Control and Automation Technology Program at Duzce Vocational High School, Duzce-Turkey. His main research interests are FPGA-based digital system design, neural networks, and reconfigurable computing. He is also interested in chaos and computer graphics.

Balkan Journal of Electrical & Computer Engineering
BAJECE
An International Peer Reviewed, Indexed and Open Access Journal

ISSN: 2147- 284X
Vol: 3
No: 4
Year: December 2015

CONTENTS

BALKAN JOURNAL OF
ELECTRICAL & COMPUTER ENGINEERING
(An International Peer Reviewed, Indexed and Open Access Journal)

Contact
Istanbul Technical University
Department of Electrical Engineering,
Ayazaga Campus, Maslak, Istanbul-Turkey

Web: https://www.bajece.com
http://dergipark.ulakbim.gov.tr/bajece/
e-mail: editor@bajece.com
bajece.editor@gmail.com